

This work was performed for the Jet Propulsion Laboratory,  
California Institute of Technology, sponsored by the  
National Aeronautics and Space Administration under  
Contract NAS7-100.

ANALYSIS OF POTENTIAL SECONDARY EXPERIMENTS  
FOR A SOLAR-THERMIONIC FLIGHT TEST VEHICLE

Prepared for  
California Institute of Technology  
Jet Propulsion Laboratory  
4800 Oak Grove Drive  
Pasadena, California  
Attention: Mr. J. L. Flatley

Contract No. 951162

EOS Report 6961-Final

19 November 1968

VOLUME III - ENGINEERING EXPERIMENTS CATALOG

Prepared by Staff  
Program Management and Systems Engineering

Approved by

J. Neustein, Manager  
PROGRAM MANAGEMENT AND SYSTEMS ENGINEERING

ELECTRO-OPTICAL SYSTEMS, INC. - PASADENA, CALIFORNIA  
A Subsidiary of Xerox Corporation

## CONTENTS

I	POWER	
I-A	Solar Cell Angle of Incidence Experiment	4
I-B	Optical Transmittance Test	9
I-C	Measurement of Reflective Surface Degradation	14
I-D	Heat Pipe Experiment	21
I-E	Concentrator Temperature and Strain Measurements	29
I-F	Concentrator Reflectance and Angular Error Measurements	34
I-G	Solar Cell Calibration Test	39
I-H	Solar Constant of the Sun	42
I-I	Measurement of Spectral Distribution of Space Sunlight	49
I-J	Evaluation of Conventional Batteries in Zero Gravity	58
I-K	Evaluation of Regenerative Hydrogen-Oxygen Fuel Cell in Zero Gravity	69
I-L	Radiation Effects on Solar Cells	71
I-M	Vee-Ridge (G.E. Experiment)	79
I-N	Thin-Film Solar Cells (G.E. Experiment)	79
I-O	Solar Thermoelectrics (G.E. Experiment)	78
I-P	Pyrometer Experiment	82
II	ATTITUDE CONTROL	
II-A	Flight Qualification of a Brushless DC Torquer-Reaction Wheel	86
II-B	Attitude Control by Electric Thrusters	90
III	THERMAL CONTROL	
III-A	Thermal Control with Phase Change Materials	98
III-B	Thermal Coatings (G.E. Experiment)	102

## CONTENTS (contd)

### IV MECHANICAL

IV-A	Cold Welding in Integrated Space Environment	105
IV-B	Sublimation of Materials in Space	108
IV-C	Meteoroid Armor Test	112

### V TELECOMMUNICATIONS

V-A	Laser Experiment	116
-----	------------------	-----

### VI OPTICAL

VI-A	Optical Transmittance Test	118
------	----------------------------	-----

### VII SUPPORTING SCIENCE

VII-A	Solar Ultraviolet	120
VII-B	Solar Lyman-Alpha Experiment	121
VII-C	Proton and Electron Spectra and Direction	124
VII-D	Solar Gamma Rays	127
VII-E	Solar X-Ray	129
VII-F	Micrometeoroids	131
VII-G	Magnetic Field	132
VII-H	Local Pressure	133

## 1. INTRODUCTION

This volume contains a description of representative engineering experiments which are applicable to a spacecraft of the type under consideration by JPL. By necessity, a study of this type is limited in the number of experiments that can be considered and the depth to which each experiment can be studied.

The engineering experiments were selected primarily on scoring well in the following areas:

1. The need for exposure to integrated space
2. Supplies information unavailable by ground simulation techniques
3. Compatibility with the specified spacecraft

The selected engineering experiments have been divided into engineering technologies and are listed in Table 1.

Due to several factors, such as

1. Accurate sun orientation of the spacecraft
2. Presence of the solar thermionic experiment
3. Ability of the spacecraft to accommodate a large number of solar-oriented experiments

the engineering experiments are mainly concentrated in the power technology area. The experiments in this area are relatively simple, yet supply valuable information.

The experiments considered in the telecommunications area were relatively complex and only a "laser experiment" was acceptable.

Several secondary engineering experiments considered in the General Electric Final Report for Contract No. 950852 for JPL are summarized in this volume. For additional information and engineering experiments, the reader is referred to the General Electric Final Report.

The results of this portion of the study are illustrative of the types of engineering experiments which can be included on the specified spacecraft.



TABLE 1. ENGINEERING EXPERIMENTS

<u>Technology</u>	<u>Experiment</u>
I Power	I-A Solar Cell Angle of Incidence Experiment
	I-B Optical Transmittance Test
	I-C Measurement of Reflective Surface Degradation
	I-D Heat Pipe Experiment
	I-E Concentrator Temperature and Strain Measurements
	I-F Concentrator Reflectance and Angular Error Measurement
	I-G Solar Cell Calibration Test
	I-H Solar Constant of the Sun
	I-I Measurement of Spectral Distribution of Space Sunlight
	I-J Evaluation of Conventional Batteries in Zero Gravity
	I-K Evaluation of Regenerative Hydrogen-Oxygen Fuel Cell in Zero Gravity
	I-L Radiation Effects on Solar Cells*
	I-M Vee-Ridge Photovoltaics*
	I-N Thin Film Solar Cells*
	I-O Solar Thermionics*
	I-P Pyrometer
II Attitude Control	II-A Brushless dc Torquer - Reaction Wheel
	II-B Attitude Control by Electric Thrusters
III Thermal Control	III-A Thermal Control Phase Change Materials
	III-B Thermal Coatings*

---

\* GE Final Report

EXPERIMENT I-A  
SOLAR CELL ANGLE OF INCIDENCE EXPERIMENT

1. BACKGROUND

Solar photovoltaic arrays that are not oriented to give normal incidence sunlight or arrays that are mounted on curved surfaces incur losses in power output due to the angle of incidence of the impinging illumination. For small angles of incidence, a cosine law deviation from the power output at normal incidence can be used. For large angles of incidence (greater than 30 degrees) there is a deviation from the cosine law which causes the power output to decrease more rapidly than would normally be expected. The deviation from the cosine law is also markedly affected by the type and thickness of coverglasses and filters used to protect the solar cell. The adhesive between the solar cell and coverglass may also cause a deviation from the cosine law at high angles of incidence. The deviation from the cosine law can probably be ascribed to polarization of the incident illumination by the coverglass and adhesive and defraction of the incident of illumination by the coverglass and adhesive and defraction of the incident of illumination by the coverglass adhesive. It may also be possible that the surface of the silicon solar cell may have some effect on the deviation from the cosine law at large angles of incidences. Since all of these items are affected by the space environment, it is entirely possible that ground test results will be different from space performance.

This experiment is designed to accomplish the following objectives:

1. Determine the deviation from the cosine law for angles of incidences from 0 to 90 degrees
2. Determine the effect of various coverglass thicknesses on the deviation of the cosine law

TABLE 1. ENGINEERING EXPERIMENTS (contd)

<u>Technology</u>	<u>Experiment</u>
IV Mechanical	IV-A Cold Welding in Integrated Space Environment
	IV-B Sublimation of Materials in Space
	IV-C Meteoroid Armor Test
V Telecommunications	V-A Laser Experiment*
VI Optical	VI-A Transmittance Test
VII Supporting Science	VII-A Solar Ultraviolet
	VII-B Solar Lyman Alphas
	VII-C Proton-Electron
	VII-D Solar Gamma Ray
	VII-E Solar X-Ray
	VII-F Micrometeoroids Pressure
	VII-G Magnetic Field
	VII-H Local Pressure

\* GE Final Report

3. Determine the effect of different types of adhesives on the deviation from the cosine law.
4. Determine if the silicon surface of the solar cell affects the deviation from the cosine law.

## 2. EXPERIMENT DEFINITION

A spacecraft designed to test a solar thermionic system also makes a suitable test platform for a sun angle experiment. The overall spacecraft will be sun-oriented in order to keep the primary thermionic experiment normally incident to the sun's illumination. All that would be necessary for the sun angle experiment is a secondary orientable array that incorporated cells at 0 to 90° illumination angles of incidence and the necessary telemetry and measuring devices to determine the effect of varying angle of incidence on the test specimens. The primary experiment would provide measurements of the solar intensity radiation ;environment, orientation (of the overall spacecraft), and micrometeoroid density.

The experiment would consist of one secondary orientable array, approximately 1 ft x 1 ft x 0.25 inches.

The test specimens will consist of ten groups of 10 cells for a total 100 cells. Each group will be as follows:

1. Bare n-on-p 2 x 2 cm solar cell with no surface preparation other than grid lines
2. 2 x 2 cm n-on-p solar cell with a mechanically-clamped 3-mil coverslide
3. 2 x 2 cm n-on-p solar cell with mechanically-clamped 12-mil coverslide
4. 2 x 2 cm n-on-p solar cell with mechanically-clamped 30-mil coverslide
5. 2 x 2 cm n-on-p solar cell with mechanically-clamped 60-mil coverslide

6. 2 x 2 cm n-on-p solar cell with LTV-602 adhesive and 3-mil coverslide
7. 2 x 2 cm n-on-p solar cell with LTV-602 adhesive and 12-mil coverslide
8. 2 x 2 cm n-on-p solar cell with LTV-602 adhesive and 30-mil coverslide
9. 2 x 2 cm n-on-p solar cell with LTV-602 adhesive and 60-mil coverslide
10. Bare 2 x 2 cm n-on-p solar cell with antireflective coating

Within each group, every 2 cells could be placed at a different angle.

Each of the test solar cells will be pre-irradiated with 1 mev electron to a total integrated flux of  $1 \times 10^{15}$  electrons/cm<sup>2</sup>. This will minimize the effect of space radiation on the performance of the solar cells during the test period. The temperature of the secondary array and test specimens will be monitored with thermistors as indicated in Fig. 1.

The measured parameters would be short-circuit current and temperature. Approximately 100 channels of information are required with slow sampling rates.

### 3. EXPERIMENT SPECIFICATION

The interface requirements for the sun angle experiment are summarized below (see Fig. 2):

Electrical power required:	1.5 watts for operation of thermistors
Weight:	Less than 3.5 lb (including electronics)
Size:	1 ft x 1 ft x 1.5 inches plus 3 in x 6 in x 6 in electronics
Telemetry accuracy required:	1 percent of full scale reading
Data rate:	~ 1 bit/sec
Thermal:	-20°C to +70°C

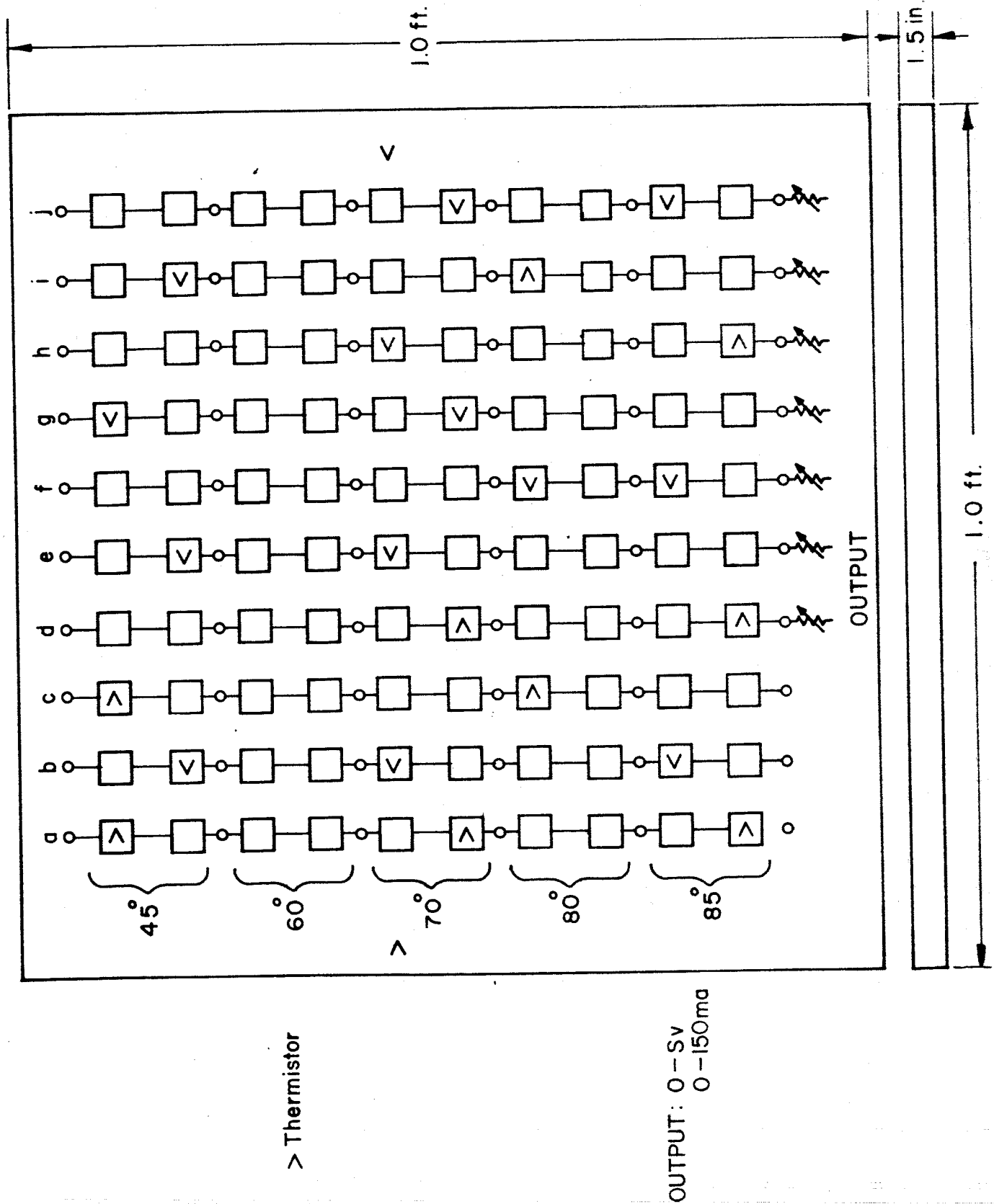


FIG. 1 SIN-ANGLE EXPONENT SCHEMATIC

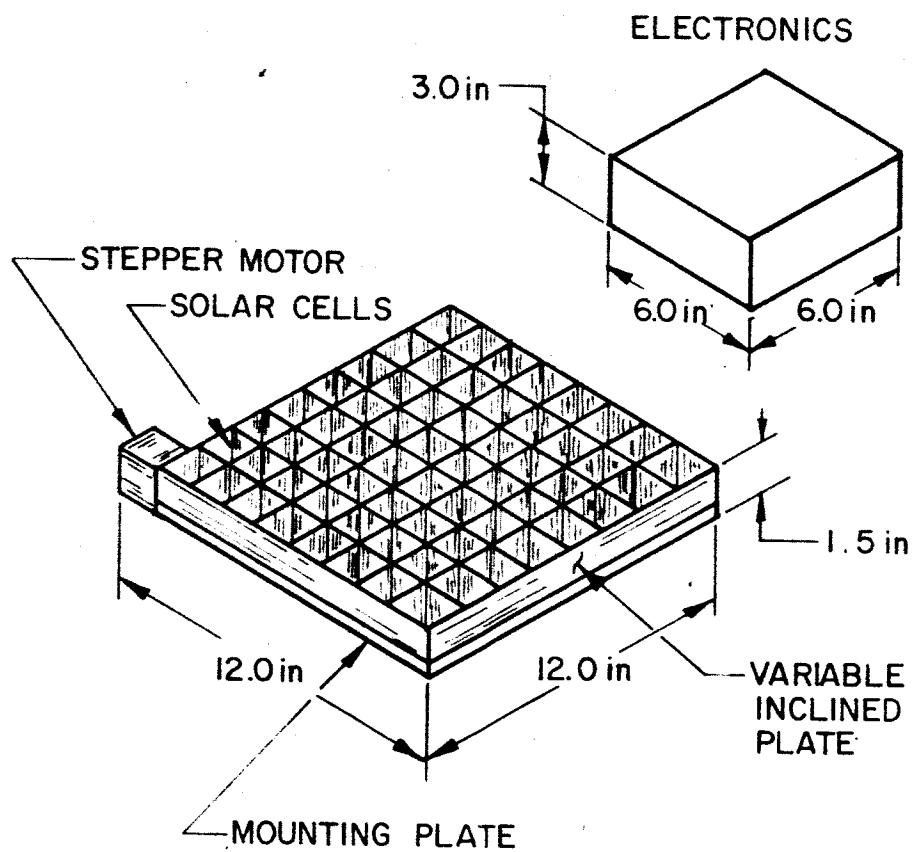


FIG. 2 SKETCH OF SOLAR CELL ANGLE OF INCIDENCE EXPERIMENT

EXPERIMENT I-B  
OPTICAL TRANSMITTANCE TEST

1. BACKGROUND

The space environment has many deleterious effects on materials used in a satellite. For satellite equipment and surfaces that are used in optical operations, the space environment is especially damaging. Effects such as erosion of optical surfaces, discoloring of adhesives, and discoloring of optical glasses occur in the space environment. The causes for this damage are primarily thought to be bombardment, ultraviolet radiation, and particulate particle radiation.

Reaction to the space environment for a wide range of materials has been the object of much effort in recent years. Plastic films may be useful in the space environment in various applications, depending on how rapidly the films are damaged by this environment. One possible use of these films is to encapsulate thin-film cadmium sulfide solar cells, which might be used as sources of power in space. For this type of solar cell, the plastic film provides several functions: protection from the prelaunch environment, physical support, and a method of temperature control in space.

When a plastic film is used as an encapsulant, the effects of the space environment on the optical transmission and the mechanical properties are important. The films must remain reasonably transparent (80 to 90 percent) to most of the solar spectrum of interest.

The operation of optical equipment in the space environment must be known and the time dependent changes of the optical properties must be predictable in order to adequately design equipment for space use. Some of the prime materials to be investigated are solar cell coverglasses, plastics, and camera or telescope lenses. In the case of solar cell coverglasses, the effect of transmission loss (i.e., surface erosion or darkening) can cause a loss in power output of the solar array. Damage to the optical surfaces of telescopes and cameras causes degradation



in performance of this equipment during their respective missions. It is desirable to know the effect of the space environment as a function of time on the various optical surfaces used in a satellite.

This experiment is designed to accomplish the following objectives:

1. To determine the effect of the integrated space environment on typical plastic films as a function of time.
2. To determine the effect of the space environment on typical solar cell coverslide material as a function of time.
3. To determine the effect of the space environment as a function of time on typical telescope and camera optical surfaces.

## 2. EXPERIMENT DEFINITION

The selection of appropriate combinations of surface preparations for the optical materials to be investigated will allow for the determination of the mode of damage occurring on the optical surface. It is possible to differentiate the effects of micrometeoroid erosion, ultraviolet radiation, and charged particle damage by properly protecting samples with sun shields (UV), quartz glass (micrometeoroids), or a combination of these.

Damage to materials can result from meteoroids by erosion, perforation, spallation, and pressure shocks. The extent of damage is related to the flux rate, particle size and density, and impact speed. As it is generally true of other elements of the space environment, these data are not yet too accurately defined with respect to spacial distributions and are variable with time. Meteoroids may be classified as meteorites, meteors, and micrometeoroids or dust. These differ as to mass, density, orbit, and origin.

The fraction of the sun's energy at wavelengths in the ultraviolet and x-ray region (less than  $3000\text{\AA}$ ) is 1.2 percent. During periods of solar flares, the levels can be increased by several orders of magnitude for periods of a few hours. The main reason for interest in the

UV and x-ray mission is because the full-time energies are sufficiently high to initiate chemical reactions and ionization of materials. Such reactions can begin at wavelengths below  $3000\text{\AA}$  in a near ultraviolet period. In view of the transient nature of sun spots and solar flares, the most practical presentation of data is in terms of yearly averages since a test vehicle will almost certainly be in orbit for a fair fraction of a year for a meaningful task of space environmental effects on materials.

The trapped radiation fields and solar flare protons encountered in near-earth-space can cause damage in optical surfaces due to high energy sputtering and internal discoloration of the optical materials. In the case of solar cell coverglass, discoloration is due to the formation of F centers in the coverglass which is brought about by displacement of impurity items in the material.

In all cases, the time dependent degradation of the optical surface would be measured by noting the decrease of transmission through the optical material or, in the case of meteoroid erosion, measuring the increase in transmission through a coated surface.

One of the most important aspects of this experiment is to differentiate the various effects that are occurring simultaneously in the space environment. This is possible through the choice of selected materials and protective devices which will be placed above the test specimens.

The experiment shall consist of 15 optical surfaces each prepared in a specific manner to measure one or all parts of the space environmental degradation. Each specimen will be rotated over a photomultiplier tube to measure incident solar illumination. Figure 3 shows the mechanical configuration of a test apparatus.

Sample 1 consists of a 125-mil quartz plate coated with a thin layer of silver. This sample will determine the time dependent effect of meteoroid erosion on a reflective surface. Samples 2 and 3 will measure the effect of ultraviolet radiation on adhesives used to bond

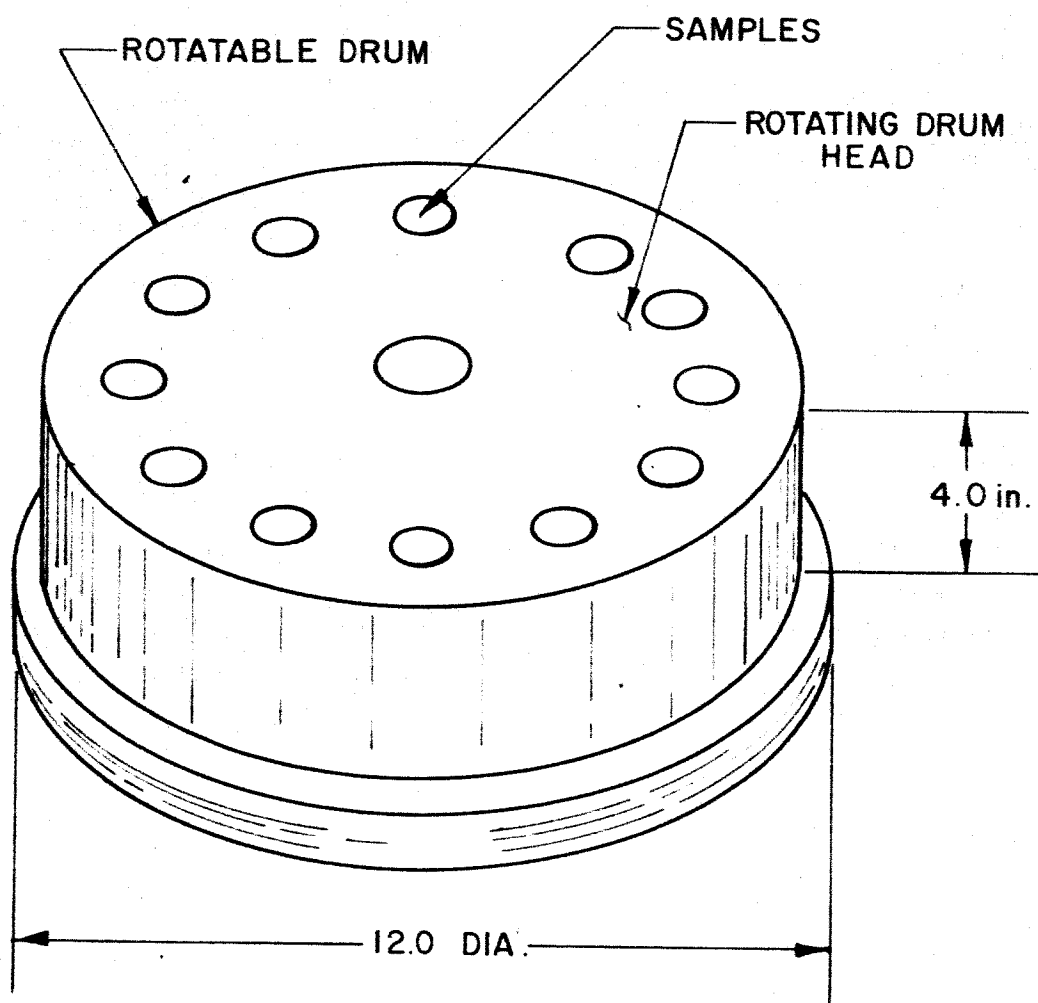


FIG. 3 SKETCH OF OPTICAL TRANSMITTANCE TEST

coverslides to solar cells. The basic structure of samples 2 and 3 is a sandwich design with a 6-mil quartz coverslide, adhesive, adhesive and a 125-mil quartz coverslide to protect the adhesive from charged particle radiation.

Samples 4 and 5 will determine the effect of charged particle radiation on coverslide adhesives. The structure is the same as for samples 2 and 3 except that the 125-mil quartz coverglass is replaced with a 3-mil quartz coverglass with a UV filter. Samples 6 through 10 will be various coverglasses and lens material which will see the entire space environment. Samples 11 through 15 are a 5-mil sample of H film mylar with separation of effects protective covers. Sample 14 and 15 are Aclar 22A and Tedlar 50 exposed to the total environment. The effect of the overall environment will be determined by measuring the change in the amount of light transmitted through the specimens with a photomultiplier tube as a function of time.

### 3. EXPERIMENT SPECIFICATION

The interface requirements for the optical transmittance experiment are summarized below (see Fig. 3):

Electrical power required:	8.0 watts for operation of motor, thermistors, photomultiplier tube, and electronics
Weight:	less than 15 lb
Size:	12 inches in diameter x 4 inches deep
Instrumentation:	1 analog voltage 0 to 5 volts (photomultiplier tube output), 15 temperatures (thermistors 0 to 5 volts)
Telemetry accuracy required:	1 percent of full scale reading
The experiment must be sun-oriented within approximately $\pm 5^\circ$ .	
Thermal:	$-30^\circ\text{C}$ to $+65^\circ\text{C}$

## EXPERIMENT I-C

### MEASUREMENT OF REFLECTIVE SURFACE DEGRADATION

#### 1. BACKGROUND

The performance of a solar concentrator depends on the geometrical accuracy and specular reflectivity of the concentrator surface. Success has been achieved in developing fabrication techniques that provide the required geometrical accuracies for solar thermionic systems, although verification that these accuracies can be maintained in space during thermal cycling is required. One area in which data are critically weak, however, is that of the durability of highly reflective surfaces in the space environment. This results from two factors: uncertainty of the space environment and the difficulty of simulating effectively those characteristics known to be present. The problems of simulation become particularly difficult when the necessity for long duration tests and combinations of physical effects are considered.

In recognition of the need for data on reflective surface durability, EOS recently performed a feasibility study to define a flight experiment for accurate determination of the performance of the reflective properties of solar concentrators in space. This study included evaluation of the space environment as it is presently known, selection of the solar concentrator surface samples to be tested, analysis and prediction of the performance of the samples in the space environment, and the generation of the experiment requirements. An experiment was designed which would test many substrate and surface material combinations for an extended period in space under conditions closely approximating those for an actual concentrator surface. The samples would be oriented toward the sun. Through the use of selective shielding, the influence of various environmental effects could be separated.

The following effects are most likely to damage the reflective surfaces:

1. Micrometeorites
2. Low-energy protons
3. Solar ultraviolet radiation

The results of this study are contained in EOS Report 4100-Final, Study of a Flight Experiment of Solar-Concentrator Reflective Surfaces, prepared for NASA/Langley Research Center. The satellite package, as defined in the study, is a cylinder approximately 2 feet in diameter and 8 inches thick. It carries 25 to 28 test samples and three calibration surfaces. Reflectance is measured by a moving arm reflectometer that sequentially tests the sample reflectance and compares each with a calibration surface.

Both NASA and the Air Force are considering flying an experimental package of this type. However, even if these flights take place in the near future, similar experiments should be flown on other vehicles for other vehicles for the following reasons:

1. The amount of statistical data available on reflective surface performance as a result of the first flights will be minimal. It is very important that additional tests of this type be made on other vehicles in order to increase the statistical reliability of the data.
2. Only a few different material combinations can be carried on each flight, because several identical samples of each material must be carried for redundancy and to allow separation of effects.
3. It is quite likely that the first reflective surface flight experiments will indicate possible coating improvements that must be verified in later flights.

There are at least three methods of measuring reflective surface degradation as a part of the experimental flight test:

1. Direct measurement of concentrator reflectance
2. Individual reflectance devices, each carrying a single surface sample
3. A multisample payload package such as that described above

The best approach depends strongly on the payload weight and volume allowances. For example, the complete 28-sample instrument is bulky and heavy. However, a similar, smaller device carrying fewer samples could be designed for nearly any vehicle. Individual sample instruments are in some ways less desirable because they are much heavier and more expensive per bit of data received. However, individual instruments can be located more conveniently in otherwise unused locations on the spacecraft.

Definition of the instrumentation also depends strongly on the number of different samples to be tested. Table 2 illustrates a typical selection of samples of interest for general concentrator applications. These include foam/Mylar, aluminum/epoxy, and epoxy substrates with aluminum or silver reflective layers and various undercoatings and overcoatings. For solar thermionic applications, the substrate selection could probably be limited to electroformed nickel and possibly electroformed copper since none of the other fabrication techniques has demonstrated adequate accuracy for thermionic purposes.

## 2. EXPERIMENT DESCRIPTION

The main design parameters of the simplified experiment are summarized in Table 3. Approximately 10 test samples plus three calibration surfaces would be carried. Both solar and artificial light sources would be used for redundancy and to provide better spectral data. The solar rays would be reflected from a convex spherical reflector. Reflectance measurements would be made for four wavelength regions as well as for the integrated solar spectrum. The spectral data are expected to aid in deducing the causes of degradation. By

TABLE 2

## EXPERIMENT SAMPLE SELECTION AND SEPARATION OF EFFECTS

No.	Substrate	Undercoat	Reflective Coating	Overcoat	Separation of Effects
1	Ni	SiO	Al		Surface mounted, no shield
2	Ni	SiO	Al		Partially recessed
3	Ni	SiO	Al		Fully recessed
4	Ni	SiO	Al	Si <sub>2</sub> O <sub>3</sub>	No shield
5	Ni	SiO	Al	Si <sub>2</sub> O <sub>3</sub>	Sun shield
6	Ni	SiO	Al	Si <sub>2</sub> O <sub>3</sub>	Particle shield
7	Ni		Ag		No shield
8	Ni		Ag		Sun shield
9	Ni		Ag		Particle shield
10	Ni		Ag		Total shield (control)
11	Foam/Mylar		Al		No shield
12	Foam/Mylar		Al		Sun shield
13	Foam/Mylar		Al		Particle shield
14	Foam/Mylar		Al	High e	No shield
15	Foam/Mylar		Al	High e	Sun shield
16	Foam/Mylar		Al	High e	Particle shield
17	Al/epoxy	SiO	Al	SiO	No shield
18	Al/epoxy	SiO	Al	SiO	Sun shield
19	Al/epoxy	SiO	Al	SiO	Particle shield
20	Epoxy	SiO	Al	Barrier layer	No shield
21	Epoxy	SiO	Al	Barrier layer	Sun shield
22	Epoxy	SiO	Al	Barrier layer	Particle shield
23	Epoxy		Al		No shield
24	Epoxy		Al		Sun shield
25	Epoxy		Al		Particle shield



TABLE 3  
SIMPLIFIED SURFACE COATING REFLECTANCE DEGRADATION  
INSTRUMENT SPECIFICATION

Weight	10 pounds
Diameter	9 inches
Thickness	6 inches
Number of samples	10
Sample diameter	1.5 inches
Calibration measurements:	
	1. 0 percent (black cavity)
	2. 100 percent (quartz prism)
	3. Aluminized standard mirror
Type of light source:	
	1. Solar (reflected from sphere)
	2. Incandescent tungsten
Type of detectors	Lead sulfide
Spectral regions detected:	
	1. 0.30 $\mu$ to 0.54 $\mu$
	2. 0.54 $\mu$ to 0.74 $\mu$
	3. 0.74 $\mu$ to 1.05 $\mu$
	4. 1.05 $\mu$ to 2.6 $\mu$
	5. 0.3 $\mu$ to 2.6 $\mu$
Type of sample temperature sensor	Solid state silicon temperature transducer
Total experiment power required	< 10 watts/reading
Data transmission rate	2900 bits/reading

measuring sample temperature at several points in the orbit, it will be possible to determine the  $\alpha/\epsilon$  ratio, which is required for calculation of minor equilibrium temperature and for estimation of thermal gradients. Supporting science sensors will be provided for monitoring the natural environment. This is necessary for proper interpretation of degradation rate. Instrumentation requirements for the experiment are summarized in Table 4.

The full 28-sample experiment is summarized below.

### 3. FULL-SIZE SURFACE COATING REFLECTANCE DEGRADATION INSTRUMENT SPECIFICATION

The interface requirements for the large solar concentrator reflective surfaces experiment are summarized below (see Fig. 4).

Electrical power required	10 watts for 10 minutes
Weight	25.0 pounds
Surface area required	452 in. <sup>2</sup> (a 24-in. diameter circle)
Volume	3616 in. <sup>3</sup> (cylinder 24-in. diameter by 8 in. long)
Instrumentation	5 voltages (0 to 20 mv) 30 temperatures (thermistors 0 to 5 v)
Telemetry accuracy required	1 percent of full scale reading

TABLE 4  
TYPICAL SUPPORTING SCIENCE INSTRUMENTATION  
FOR DEGRADATION OF REFLECTIVE SURFACES EXPERIMENT

Measurement	Typical Sensor	Range	Required Accuracy (percent)
Solar Ultraviolet	$\mu$ V-photomultiplier	2000-3000 Å	5
Solar Lyman-Alpha	Nitro oxide filled ion chamber	1100-1340 Å	5
Solar X-Rays	Shielded Geiger Tubes	2-20 Å	10
Solar Gamma Rays	Scintillation detector	1.0-200 MeV	10
Proton-Electron Radiation	Solid State (Cd S)	30-200 MeV (protons) 1.0-50 MeV (electrons)	5
Micrometeoroids	Crystal microphone detector	--	--

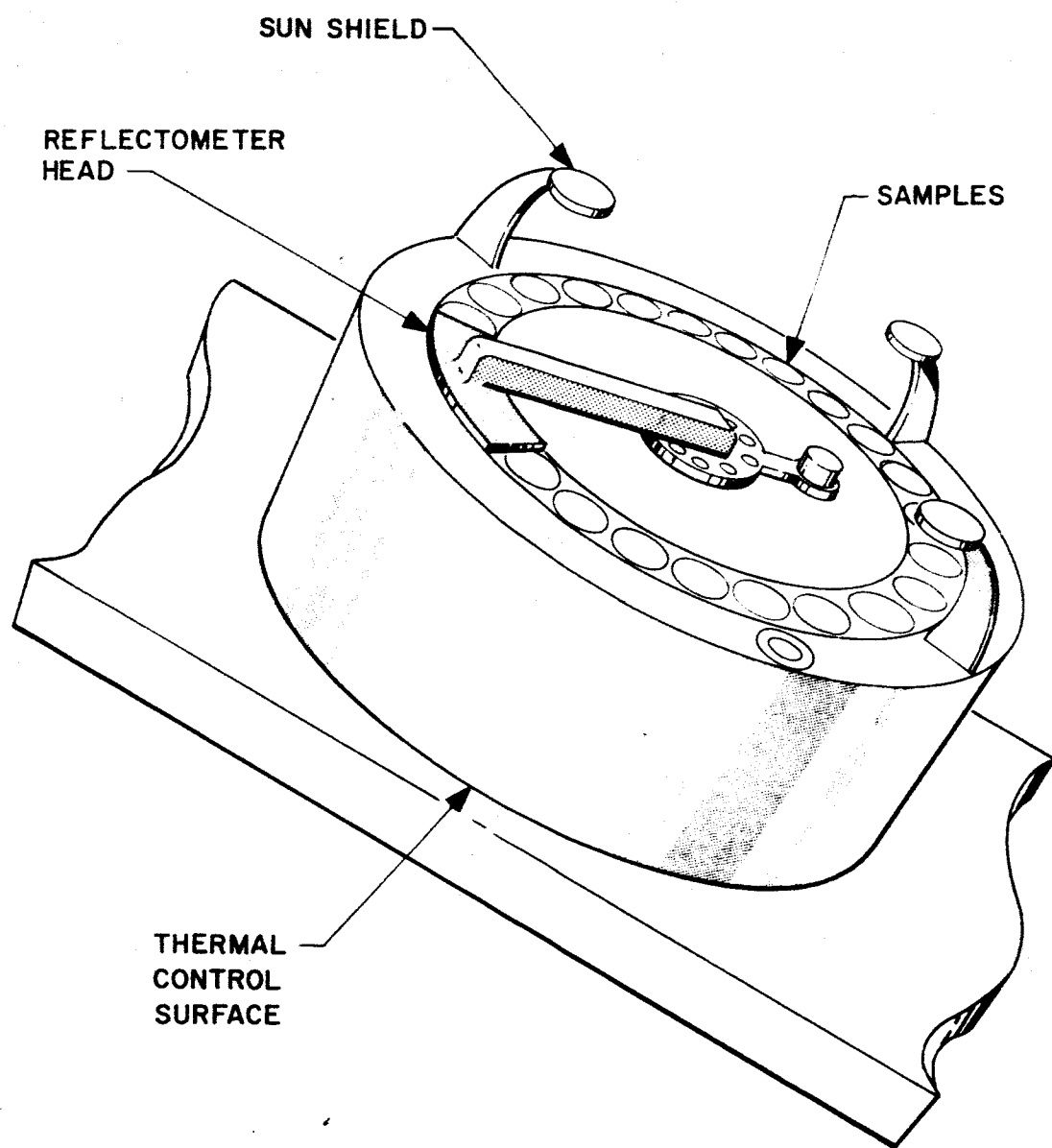


FIG. 4 REFLECTIVE SURFACES EXPERIMENT CONFIGURATION

EXPERIMENT I-D  
HEAT PIPE EXPERIMENT

1. BACKGROUND

The heat pipe is a device used in transporting thermal energy from one location to another with a minimal temperature drop. The device takes advantage of the high latent heat of vaporization of liquid metals. At the hot end, heat is transferred to the fluid which evaporates. The vapor is collected at the cold region whereby the latent heat of vaporization is liberated. The cooled fluid is returned to the hot end through capillary channels. Because the capillary force is small, the presence of gravity makes it difficult to evaluate the heat pipe performance in ground tests.

The importance of the heat pipe in advancing space power developments cannot be overemphasized. In the thermionic power application, there are at least two areas where heat pipes can be quite effective. For isotopic thermionic power supplies, the heat pipe can be used to collect thermal energy from low power density fuel and deliver it in a concentrated fashion to the diode or it can be used as a heat leveler by supplying a constant temperature to the thermionic diode. Similarly, it can be employed in the thermal energy storage (TES) application where ceramic oxide with low thermal conductivity is used. In both instances the heat pipe can reduce the temperature drop from 200°C with conventional means to something like 50°C. The same boiling and condensing principle may be applied to the design of a high temperature radiator. It was reported in Ref. 1 that a vapor fin radiator may result in a weight saving of as much as 30 to 40 percent.

Ideally, the experiment objectives should be:

1. To verify or improve the existing theory which predicts the device performance
2. To investigate the effect of the capillary channel geometry on the performance

3. To determine the upper and lower temperature limits and the maximum allowable heat flux for a given fluid.

Due to the limited amount of electrical power available and the minimum size dictated by fabrication limitation, the experiment objective will be curtailed to: Verification of performance prediction and investigation of the lower temperature limit of a cesium vapor heat pipe.

## 2. EXPERIMENT DEFINITION

The equipment required for this experiment consists essentially of:

1. Cesium vapor heat pipe with a sheathed heater welded to one end. The heater will be shielded to minimize heat loss. The heat pipe is a cylinder, 10 cm long and 2 cm in diameter. A construction detail is shown in Fig. 5.
2. Heater power control unit (HPCU) which is used to regulate the heater power. Figure 6 shows a typical circuit for the HPCU.
3. Associated instruments: There are 14 thermocouples required. Twelve thermocouples are mounted on the heat pipe exterior; 2 thermocouples are mounted on the outermost shield surface. Figure 7 shows the thermocouple mounting locations.

The input terminals of the HPCU are connected to the thermionic generator output. It is assumed that the generator power output of 140 watts is available, that the output is regulated, and that shunt loads are provided to take up the excess power when the heater is run at a lower power level, 30 watts, for instance.

The experiment will be conducted in the following manner: The heater power will be set for 30, 60, 90, and 120 watts. At each power level, the measurement will be made of:

1. Heat current and voltage to determine the actual power delivered to the heater

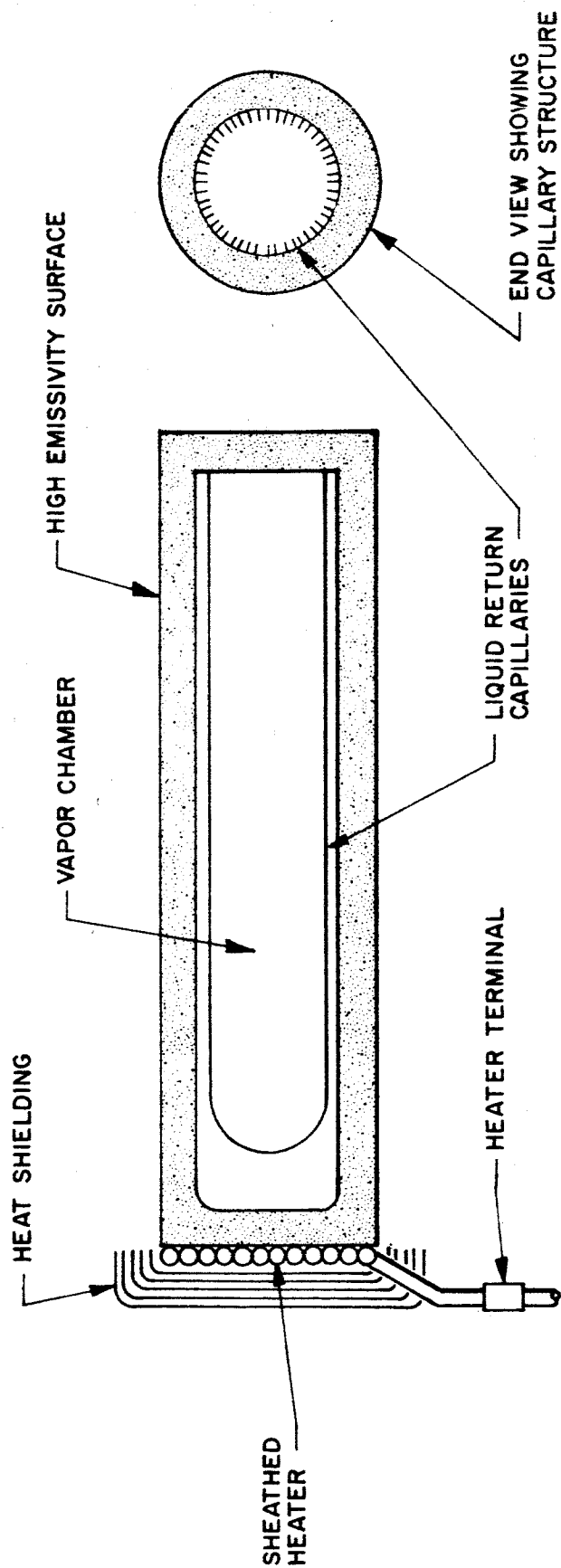
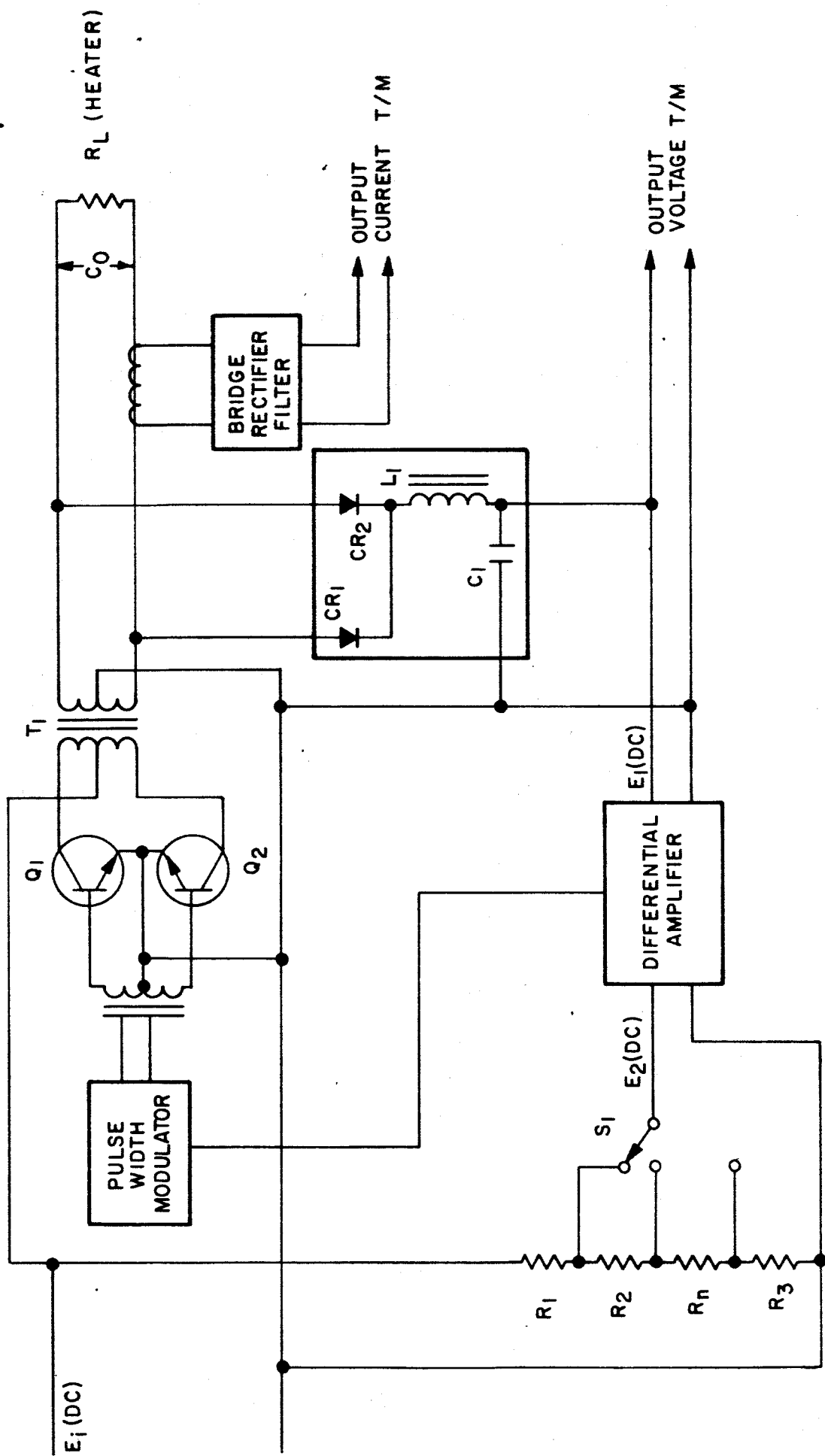


FIG. 5 CESIUM VAPOR HEAT PIPE



1.  $Q_1$  &  $Q_2$  CONVERTS THE INPUT DC VOLTAGE ( $E_1$ ) TO AC VOLTAGE THRU  $T$ , TO GIVE  $C_0$
2.  $C_1$  &  $C_2$  ARE PULSE WIDTH MODULATED TO PROVIDE CONTROL OF  $C_0$
3.  $C_0$  IS CONTROLLED BY MEASURING IT AND CONVERTING IT TO DC ( $E_1$ ) BY  $CR_1$ ,  $CR_2$ ,  $L_1$  &  $C_1$  AND REFERENCING  $E_1$  TO  $E_2$
4.  $E_2$  IS ADJUSTABLE (OR PROGRAMABLE) BY  $S_1$  USING  $R_1$ ,  $R_2$ ,  $R_n$  &  $R_3$
5. AC OUTPUT CURRENT IS MEASURED FOR TELEMETRY AS WELL AS AC OUTPUT VOLTAGE

FIG. 1. CIRCUIT FOR HEATER POWER CONTROL (TOP)



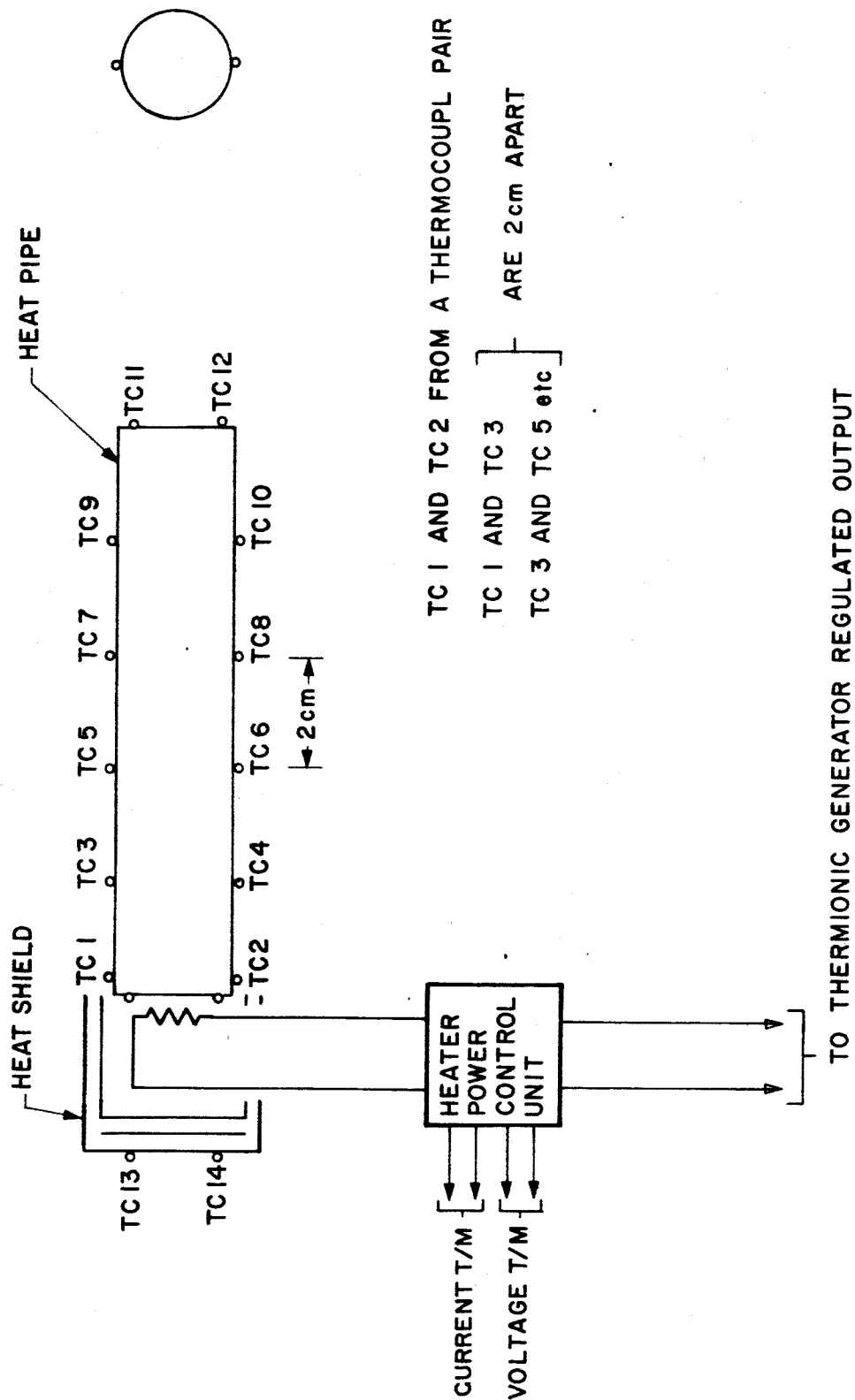


FIG. 7 HEAT PIPE EXPERIMENT INSTRUMENTATION

2. Thermocouples TC13 and TC14 which measure the shield surface temperature. Heat loss through the heat shield is calculated from known shield area and emissivity. The net power delivered to the heat pipe is the heater power minus the loss.
3. Readings of thermocouples TC1 through TC12 will be taken through a multichannel scanner. TC1 and TC2 form a coupling pair for the location closest to the heat source. TC3 and TC4 form another pair 2 cm away, and so forth. Past experience indicates that at least 2 couples for a given location are necessary. One acts as a backup and, in case both of them are in good condition, they will provide a good average.
4. From the temperature measurements, the heat pipe temperature profile can be obtained. It is expected that the pattern will be similar to that shown below in Fig. 8.

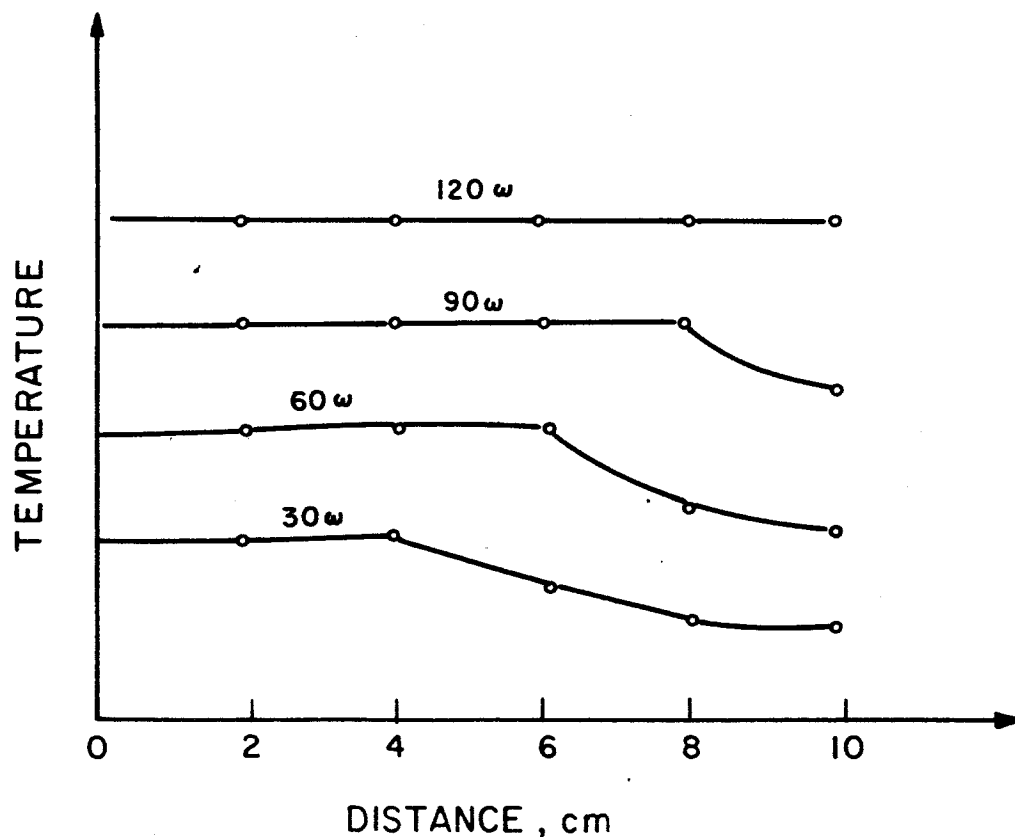


FIG. 8 HEAT PIPE PROFILE GRAPH

The measured temperature profiles will be compared to those predicted by the theory recently developed by Grover, et al (Ref. 2).

### 3. REFERENCES

1. Analysis and Evaluation of a Vapor-Chamber Fin-Tube Radiator for High-Power Rankins Cycles by Henry C. Haller, Seymour Lieblein, and Bruce G. Lindors, NASA Lewis Research Center, May 1965
2. The Use of a New Heat Removal System in Space Thermionic Power Supplies by G. M. Grover, J. Bohdansky, C. A. Busse, EURATOM Joint Nuclear Research Center, Ispra Establishment-Italy Direct Conversion Service, 1965

### 4. EXPERIMENT SPECIFICATIONS

Physical dimensions:	4 in x 1 in diameter
Weight:	3 lb (including electronics)
Electrical power requirement:	120 watts (maximum) of regulated power (assumed available from the thermionic experiment)
Duty cycle:	30 minutes to determine effects
Magnetic interference:	Some field due to dc current
Mechanical interface:	Must be shielded to prevent space-craft thermal control problems
Orbit:	Any orbit

## EXPERIMENT I-E

### CONCENTRATOR TEMPERATURE AND STRAIN MEASUREMENTS

#### 1. BACKGROUND

This experiment will provide an indication of the ability of the concentrator to maintain accuracy and reflectivity in space through measurement of skin, torus, and generator support temperature and strains.

If the thermionic system output does not deteriorate with time, it can be inferred that the mirror performance has not degraded. If, however, system power output falls off, diagnostic information on mirror performance is essential to pin down the cause of failure.

The torus-supported shell structure is conceptually simple. Its static and dynamic response to mechanical and thermal inputs, however, is difficult to analyze, particularly when the generator support arms are included. Measurement of the mirror's response to a varying thermal environment in space would be extremely useful for future design purposes. Two types of concentrator instrumentation are considered:

1. Temperature sensors to determine equilibrium temperatures and thermal gradients
2. Strain gages to detect bending of shell, torus, or support arms

A summary of the instrumentation requirements is given in Table 5.

#### 2. EXPERIMENT DEFINITION

The silicon semiconductor instrumentation is recommended since it can be attached to the concentrator with virtually no effects on performance, requires only very small lead wires, and is linear over a wide range.

Deformation of the shell and torus can be ascertained by mounting strain gages in critical locations. The greatest effect is expected to

TABLE 5

## CONCENTRATOR TEMPERATURE AND STRAIN INSTRUMENTATION

<u>Measurement</u>	<u>Sensor</u>	<u>Type</u>	<u>Number Used</u>	<u>Sampling Rate</u>	<u>Range (volts)</u>	<u>Accuracy (percent)</u>
Temperature of concentrator shell and torus	Temperature sensors	Silicon semiconductor	35	1/sec	0-5	1
Bending strain of concentrator shell and torus	Strain gages	Silicon semiconductor	40 pairs	1/sec	0-2	2

occur near the rim of the mirror shell. Strains can be correlated with thermal gradients by mounting temperature sensors at various points on the shell and torus and by noting the temperatures throughout the orbital cycles. Strain gages and temperature sensors would also be placed on the generator support arms to gain some indication of the absorber aperture misalignment and misfocus resulting from thermal deformation of the support arms. Figure 9 shows typical locations of the strain gages and temperature sensors on the shell, torus, and arms.

Each indicated strain gage is actually a set of two orthogonal pairs to allow measurement of both tensile and compressive strain in two directions. Temperature sensors would be placed immediately adjacent. The strain gages and temperature sensors are located to provide at least the following information:

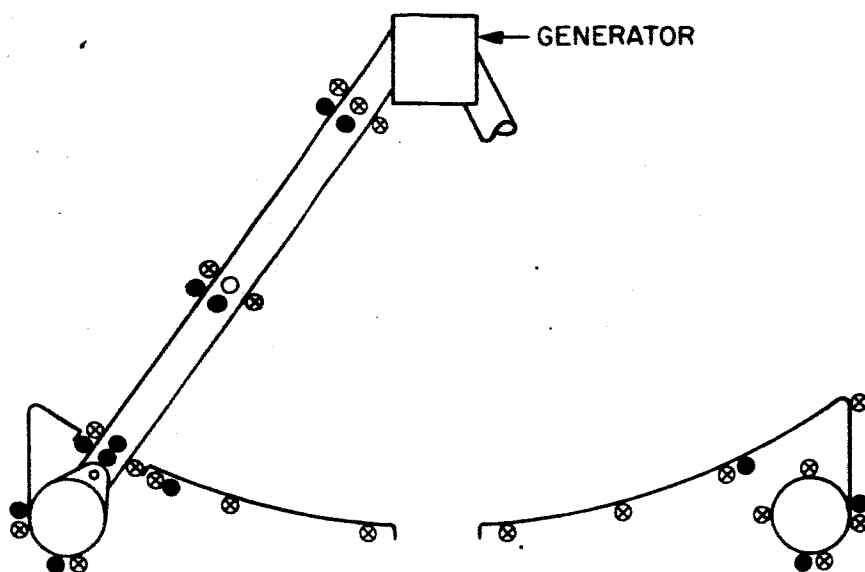
1. Thermal gradient from center to rim of mirror
2. Thermal gradient around torus and between torus and shell
3. Thermal gradient between shadowed (by arms) area and sunlit area on shell
4. Circumferential thermal gradients on shell and torus
5. Thermal gradients along support arms
6. Deformation of shell near rim
7. Deformation of torus at end near brackets
8. Deformation of torus between brackets
9. Deformation of support arms

Both the strain gages and the temperature sensors would probably be of the silicon semiconductor type for maximum sensitivity and minimum weight. Weight (or thermal mass) is particularly important on the shell because of the possibility of local distortion.

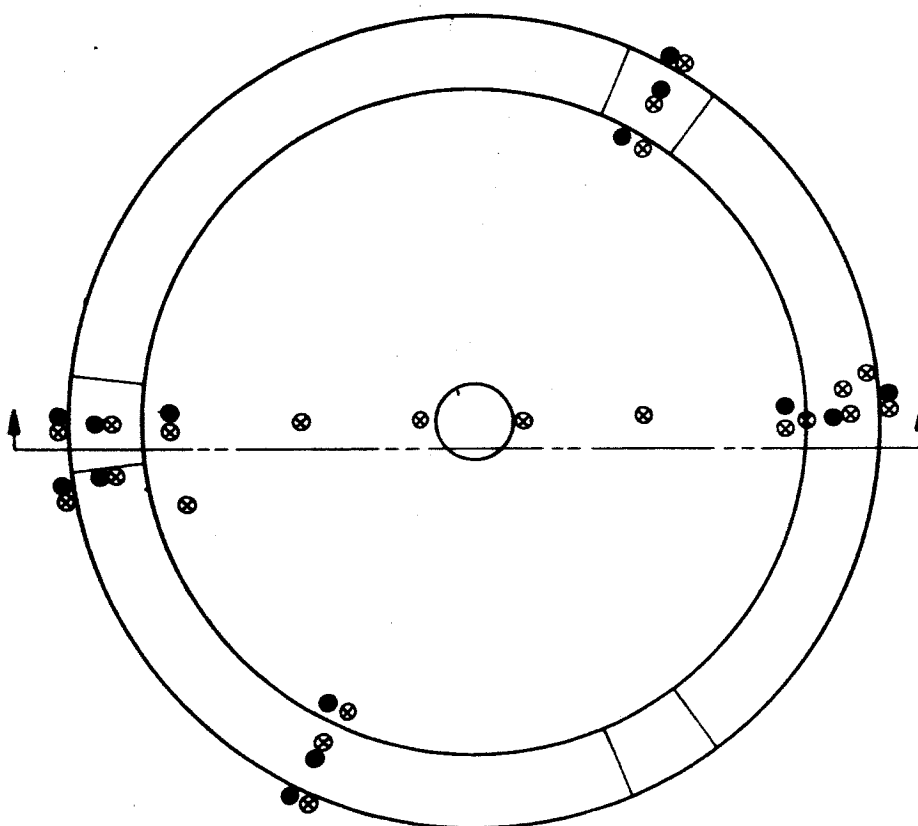
### 3. EXPERIMENT SPECIFICATION

Weight:	~2 lb (for 115 gages, including leads but not including bonding agents, etc.)
Volume:	Very small, distributed, each gage is size of pin

Physical interface: Need to be bonded with adhesive to surface  
Data interface: 1 bit/sec for each channel - 115 bits/sec  
sampled every 10 minutes



⊗ TEMPERATURE SENSORS  
 ● ↕ STRAIN GAGES



TORUS AND SHELL INSTRUMENTATION (NOT SHOWING SUPPORT ARMS)

FIG. 9 TYPICAL LOCATION OF STRAIN GAGES AND TEMPERATURE SENSORS



EXPERIMENT I-F  
CONCENTRATOR REFLECTANCE AND ANGULAR ERROR MEASUREMENTS

1. BACKGROUND

Direct verification of concentrator performance can be obtained from direct measurement of concentrator reflectance and angular deviation of the surface.

Reflectance measurements made directly on the concentrator would provide diagnostic information in case of a power loss from the solar-thermionic system. Without a means of measuring concentrator reflectance, it would be difficult to determine whether the power loss was due to concentrator or generator degradation.

The same is true for angular deformation. Both reflectance and angular deformation at selected locations on the mirror surface can be measured by the devices shown conceptually in Fig. 10. These involve small collimating light projectors that send beams of light to the mirror surface. The beams are reflected to sensors which detect either intensity or motion of the beams resulting from angular deformation of the surface. The reflectance detector could be a lead sulfide cell or silicon cell. The X-Y detector could be a lateral photocell (Radiation Tracking Transducer) or a photomultiplier tube. The instruments would be placed so as not to interfere with the main experiment.

The concentrator reflectance measurement would provide useful correlation of data obtained from the sample tests on the reflectometer experiment. For example, the sample experiments might involve testing several examples of the same material differing only, say, in the thickness of the reflective coating. If one of the samples were identical to the concentrator in terms of substrate and coating thickness, material, and application method, a direct correlation could be obtained between the small sample and a complete mirror. This would verify the results of the sample tests.

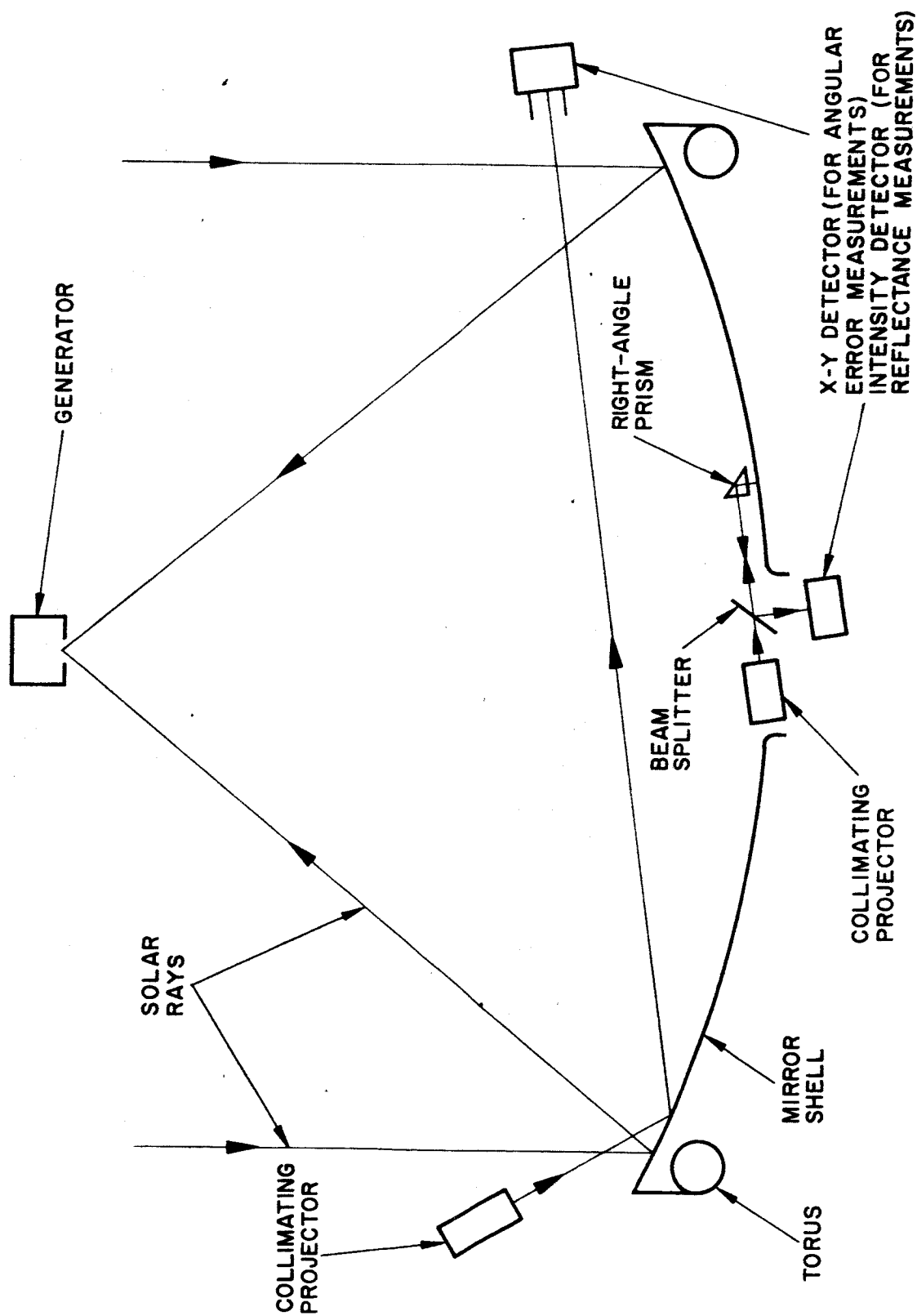


FIG. 10 TWO TYPICAL OPTICAL ARRANGEMENTS FOR MEASUREMENT OF MIRROR REFLECTANCE AND ANGULAR DISTORTION

The predominant mission effect would be that of thermal cycling. An orbit that involves both light and shadow would demonstrate the most important thermal effects which occur shortly after emergence into the sunlight.

The direct structural and thermal measurements on the concentrator and support arms involve only temperature sensors and strain gages which are available and well understood. If the direct reflectance and angular deformation measurements are made, some development will be needed on the instrument. However, since they involve no new optical instrumentation techniques, they do not present severe development problems.

## 2. EXPERIMENT DEFINITION

The method suggested for surface angular deviation measurement is to take the incoming solar radiation, condense, collimate, and filter it. Direct the collimated light beam to a preselected, polished spot on the surface of the reflector. The angle of reflection of this light beam is dependent upon the angle of incidence and on the angle of the normal to the surface. A triangular slit will define the vertical displacement of the light beam at the sensor, see Fig. 11.

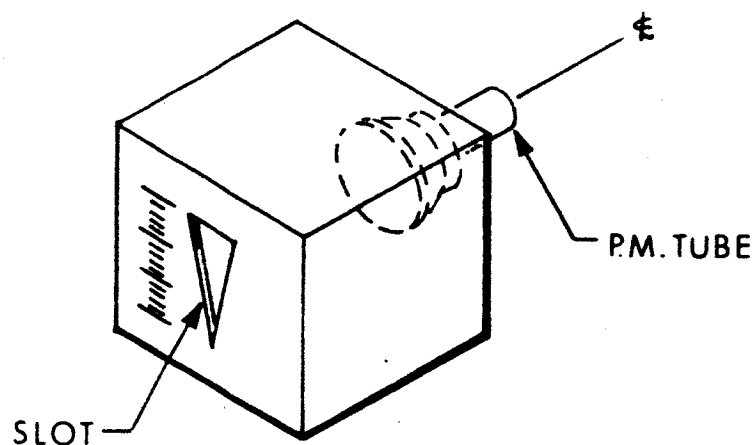


FIG. 11 DETECTOR FOR ANGULAR MEASUREMENTS

The sources can be artificial light if desired. It would take about 200 watts for 0.1 seconds for each data point for each source.

A typical set of instrumentation could consist of one source and 4 to 7 detectors located around the rim of the concentrator. Source and detectors would be mounted on the concentrator torus to avoid differential expansion problems between the vehicle and the concentrator.

The reflectance measurement could be mounted through the center of the concentrator on a rotating arm as shown in Fig. 12.

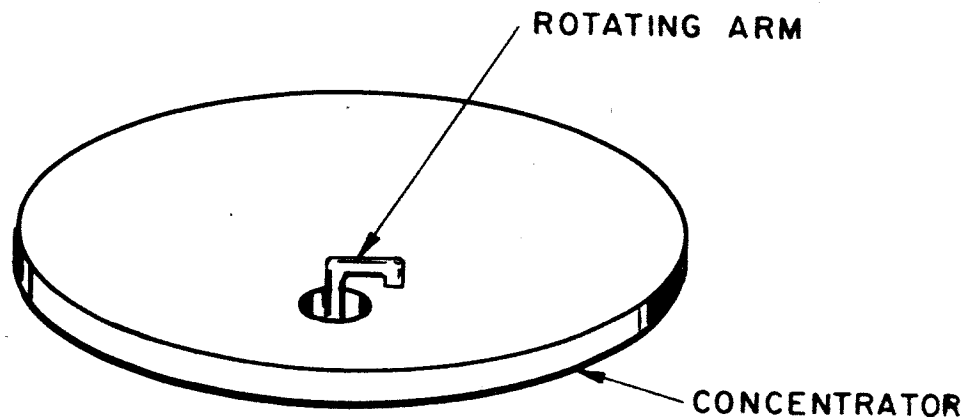


FIG. 12 CONCENTRATOR

### 3. EXPERIMENT SPECIFICATION

#### Reflectivity Experiment

Weight:	~ 5 lb (including electronics)
Volume:	6 in x 6 in x 6 in plus arm mechanism
Physical interface:	Must be mounted in center of concentrator, requires preflight calibration

Data handling:	Variable - typical 1 bit/sec
<u>Accuracy Measurement</u>	
Weight:	~ 5 lb (including leads)
Volume:	Small, distributed
Physical interface:	Must be mounted to torus, requires preflight calibration
Data handling:	Variable - typical 1 bit/sec for each detector channel

## EXPERIMENT I-G

### SOLAR CELL CALIBRATION TEST

#### 1. BACKGROUND

One of the major problems in the design of a photovoltaic power system is the accurate determination of the power output of solar cells under AMO illumination. Various methods are used, at present, to extrapolate a solar cell's performance at AM = 1 to that of AMO. The best method used to date is utilizing solar cell standards that have been flown on balloons or aircraft and calibrated to approximate AMO conditions. However, these cells are only approximations to AMO standards and are useful to determine the output of a solar array to within 7 percent. Another method which is less precise than that of high-altitude standards is the use of solar simulators which give predicted solar array performances at AMO to within  $\pm 10$  percent.

For spacecraft that are weight or area limited, it is necessary to precisely determine the output of the solar array in order to minimize either the weight and/or area of the array in order to optimize the spacecraft design. Knowledge of the output of the solar array under true AMO conditions would aid greatly in the optimization of a solar array design.

This experiment is designed to accomplish the following objectives:

1. Determine the AMO output of solar cells under the total spectrum and in various bandwidths of the spectrum.
2. Obtain a set of calibrated standard cells for use in earth (AM = 1) measurements of solar arrays.

#### 2. EXPERIMENT DEFINITION

The selection of appropriate bandpass filters for use with the test solar cells will allow the determination of the performance of the solar cells in various wavelength bands in the incident spectrum. The integration of the power output in these bandwidths would be

correlated with the output of a solar cell seeing the entire spectrum in order to determine the effect of filtering and spectral response on the solar cells. Specifically, the experiment would be composed of the following solar cell assemblies. Eight solar cells with appropriate bandwidth filters with a minimum cutoff of less than 350 mμ to a maximum cutoff greater than 1.2μ. One solar cell with a clear coverglass (at least 125-mils-thick quartz) which would allow the entire spectrum to be incident upon the solar cell. No adhesives would be used between the filter and the solar cell in order to eliminate the spectral effect of the adhesive. All filters would be deposited on 125-mils-thick fused silica, i.e., quartz, in order to eliminate the effect of particulate particle radiation damage. There would be two sets of these cells (9 cells per set), one of which would be used on the flight panel and the other would be a laboratory standard. The flight panel must be oriented to the sun at all times in order to obtain accurate data.

In order to obtain a reliable laboratory standard for use at earth test stations, it is necessary that the flight and laboratory test assembly be accurately matched for all parameters before the actual flight testing. The cells must be matched for temperature sensitivity, spectral response, and general overall performance. These matching tests can be performed either in the laboratory under solar simulation or at the Table Mountain test site, Table Mountain, California. The bandpass filters must also be matched for both the flight and laboratory standards.

The flight specimens will be mounted on an orientable array in order to obtain normal incidence of the solar illumination. The test solar cells shall be 2 x 2 n-on-p solar cells, 10 ohm cm with a series resistance of less than 0.4 ohms. The bandpass filters will be chosen to cover the range of 350 mμ to 1200 mμ, i.e., the overall response range of a solar cell. The E-1 Characteristic Curve of each test specimen will be recorded and then used to calibrate the earth standards for AMO performance (see Fig. 13 for schematic).

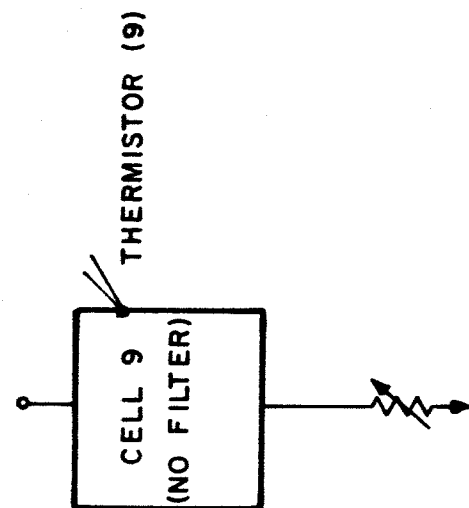
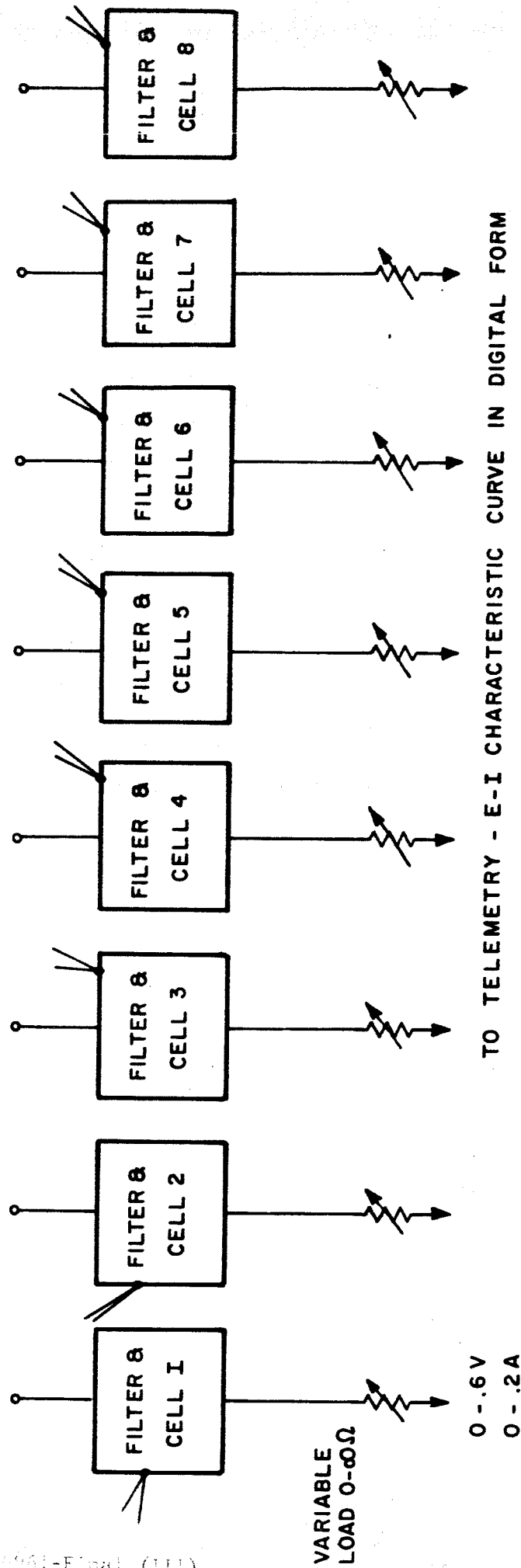


FIG. 13 SCHEMATIC FOR SOLAR CELL CALIBRATION TEST



### 3. EXPERIMENT SPECIFICATION

The interface requirements for the solar cell requirement (assuming a total number of 9 solar cells) are summarized below.

Electrical power required: 0.2 watts for operation of 9  
thermistors; 2 watts to vary load  
line

Weight: Less than 0.5 lb

Size: 15 sq in x approximately 1 in deep

Instrumentation: 9 voltages (0 to 1 volt);  
9 temperatures (thermistors 0 to 5  
volts); 110 bits/sample

Telemetry accuracy required: 1 percent of full scale reading

The experiment must be sun-oriented within approximately  $\pm 5^\circ$

Thermal:  $-30^\circ\text{C}$  to  $+70^\circ\text{C}$

EXPERIMENT I-H  
SOLAR CONSTANT OF THE SUN

1. BACKGROUND

The solar constant is the total radiant energy flux per unit area from the sun at the mean distance of the earth, and is fundamentally important to understanding the solar energy budget in the design of a solar power system. A numerical value of  $1.94 \text{ cal/min cm}^2$  or  $1350 \text{ watts/meter}^2$  was generally accepted until Johnson made some measurements which indicated that  $2 \text{ cal/min cm}^2$  is a better estimate, and now this is the generally accepted value.

These values were derived from measurements made from within the earth's atmosphere and since the atmosphere is completely opaque to large portions of the ultraviolet and infrared, considerable corrections are applied to the experimental results.

At present the solar constant is known to a  $\pm 2$  percent accuracy (see Fig. 14). The satellite heliometer developed by NASA/Goddard indicates an accuracy of  $\pm 0.2$  percent is achievable; and with this accuracy observations of the variations in solar output are possible.

2. EXPERIMENT OBJECTIVES

This experiment is designed to accomplish the following objectives:

1. Measure the solar constant with  $\pm 0.2$  accuracy
2. Monitor variations in the solar constant

3. EXPERIMENT DEFINITION

The method used to measure the solar constant is a blackbody exposed to the sun. The equilibrium temperature of the isolated body is recorded and telemetered back to earth. The energy balance of the black detector is governed by the Stefan-Boltzmann law:

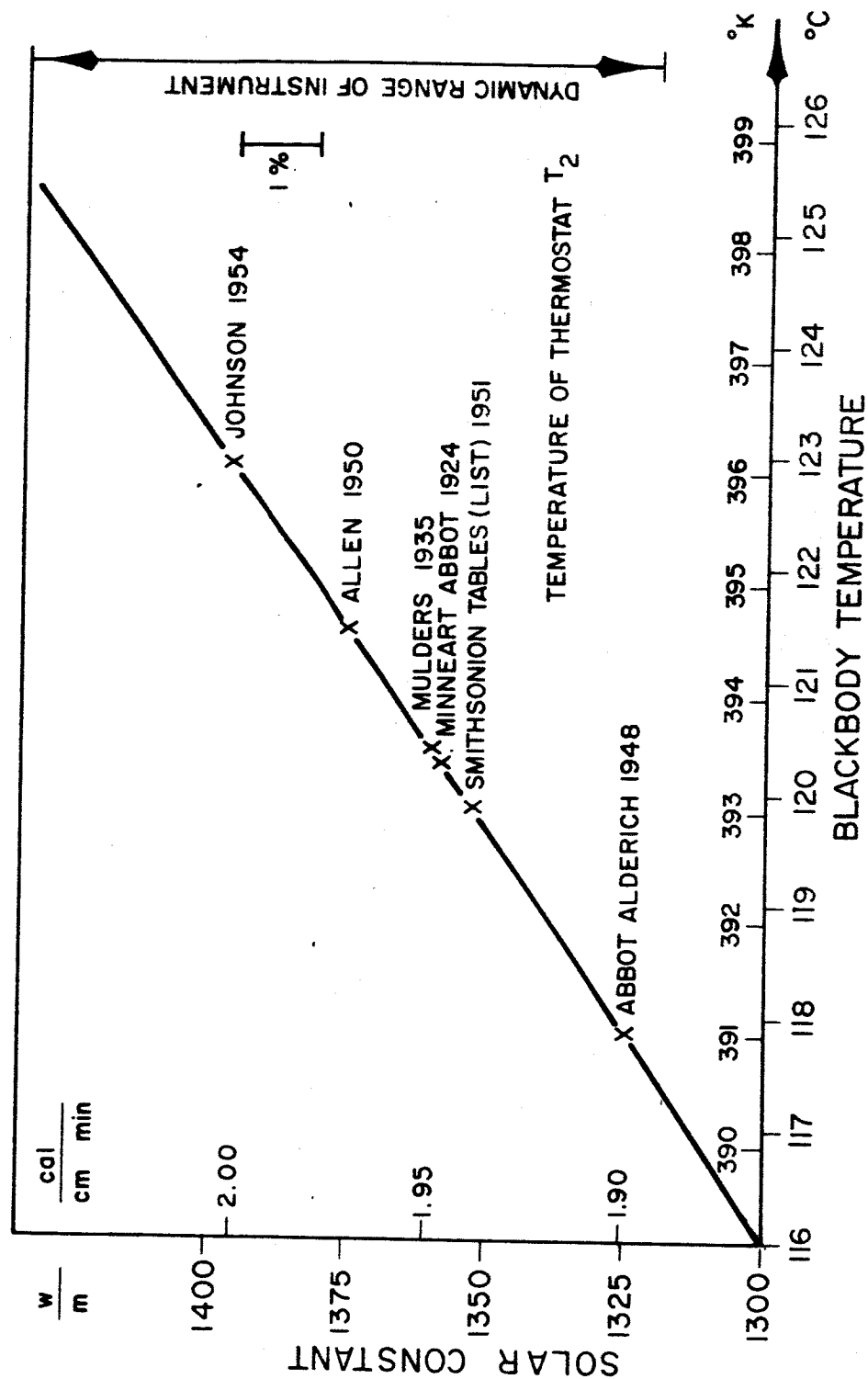


FIG. 14 TEMPERATURE OF AN IDEAL BLACKBODY EXPOSED TO THE SUN OUTSIDE OF OUR ATMOSPHERE AS A FUNCTION OF THE SOLAR CONSTANT

$$W = \sigma T^4$$

where  $W$  = total energy flux

$\sigma$  = Stefan-Boltzmann constant

$T$  = temperature

The value of  $\sigma$  is a well known constant; therefore, the variables are energy flux and temperature.

In the experiment to achieve the desired accuracy, the blackbody will depend mainly on the geometry of the cavity, not on surface coatings such as paints or coatings.

A conceptual drawing of the detector assembly is shown in Fig. 15.

The possible error in the measurement caused by misalignment of the blackbody with respect to the sun is shown in Fig. 16. The angle  $\alpha$  is the angle between the satellite-sun line and the normal to the aperture. In the equation,  $\cos \alpha$  can be taken equal to unity if the pointing accuracy is better than  $\pm 1$  degree. The experiment can be performed equally well with a lower accuracy of orientation, but then  $\alpha$  must be recorded and taken into account in the data reduction.

#### 4. EXPERIMENT DESIGN

The temperature sensor must truly average over the whole sphere; this requirement favors the metal film bolometer. Aluminum is deposited in spiral form on the outer surface of the blackbody and serves a dual function, as a bolometer and as a thermal radiation barrier. In the expected temperature range of  $120^\circ$  to  $130^\circ\text{C}$ , metals exhibit temperature coefficients in the order of  $0.004/^\circ\text{C}$ . They are very stable and well suited for the environmental conditions of outer space. The blackbody could be made also of plated material forming a junction of a thermocouple. The metal bolometer, however, is capable of absolute temperature measurements and allows the use of alternating bridge currents, which is more convenient in electrical circuitry. To measure the temperature  $T_1$  accurately to  $1/10$  degree, which is necessary

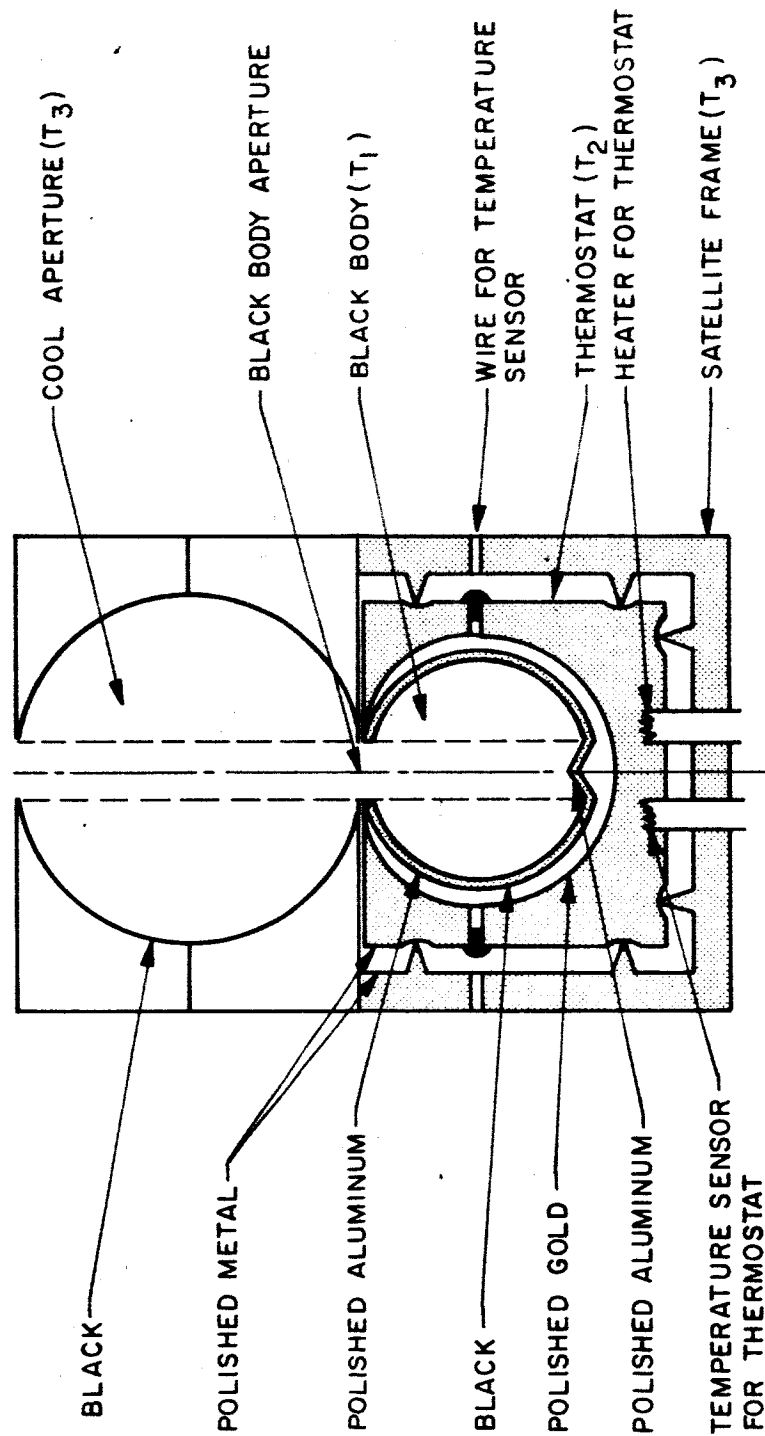


FIG. 15 DETECTOR ASSEMBLY. THE BLACKBODY IS IMBEDDED IN A THERMOSTAT SET TO THE MIDRANGE OF EXPECTED TEMPERATURES

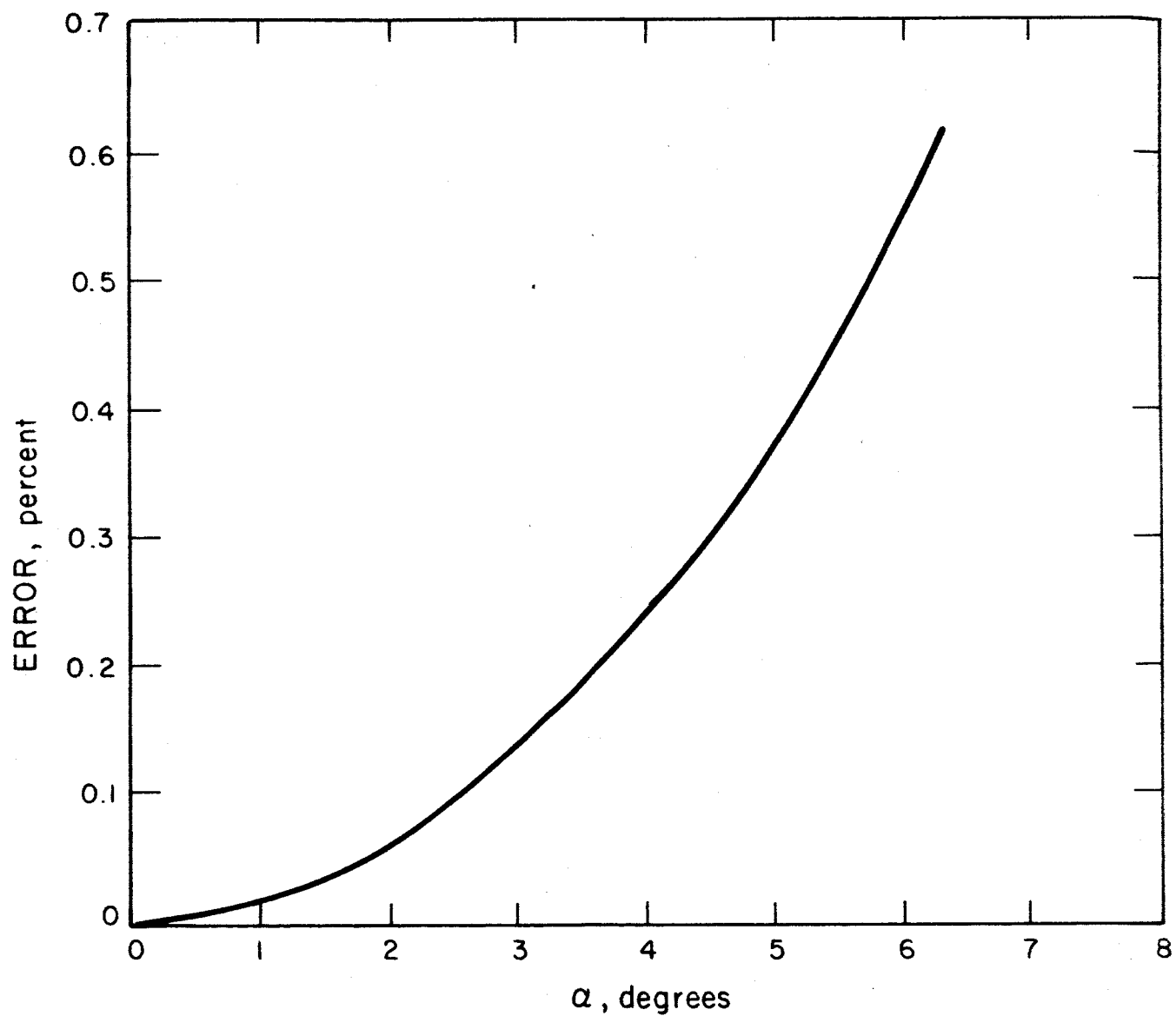


FIG. 16 . THE ERROR CAUSED BY MISALIGNMENT OF THE BLACKBODY WITH RESPECT TO THE SUN

to maintain an overall accuracy of 0.2 percent, requires a resistance measurement of  $4 \times 10^{-4}$ . The voltage change of a bridge with equal branches is 1/2 the resistance change and, therefore, the unbalance of the bridge voltage has to be sensed to  $2 \times 10^{-4}$  or to 200  $\mu\text{v}$  if one volt is fed to the bridge.

A block diagram of the circuit is shown in Fig. 17. The temperature of the thermostat,  $T_2$ , may be telemetered only once each orbit to indicate proper operation. A certain redundancy is provided if both signals,  $T_1$  and  $\Delta T$ , are telemetered. In practice it is convenient to have different ranges assigned to each channel as shown in the diagram. Requirements on the stability of amplifiers and other electronic components are moderate and well within normal instrumental standards.

#### 5. EXPERIMENT/SPACECRAFT INTERFACE REQUIREMENTS

The nominal interface requirements for the solar constant experiment are summarized below.

Electrical power required:	1.5 watts at 28 volts
Weight:	1.0 lb detector assembly 1.0 lb electronics
Size:	Detector 4" x 3" x 3" Electronics 6" x 2" x 6"
Instrumentation:	5 voltages (0 to 5 volts)
Telemetry accuracy required:	$\pm 0.5$ percent full scale reading
Sample time:	Once per orbit 100 bits/sample
Orientation required:	Experiment should be sun-oriented within $\pm 0.5$ degree

TEMPERATURE RANGE	118-126°	90-130°	120-124°C
MAXIMUM VARIATION	$\pm 4$	$\pm 20$	$\pm 2^\circ\text{C}$
ACCURACY	$\pm 0.1$	$\pm 0.5$	$\pm 0.05^\circ\text{C}$
MINIMUM S/N	32 db	32 db	32 db

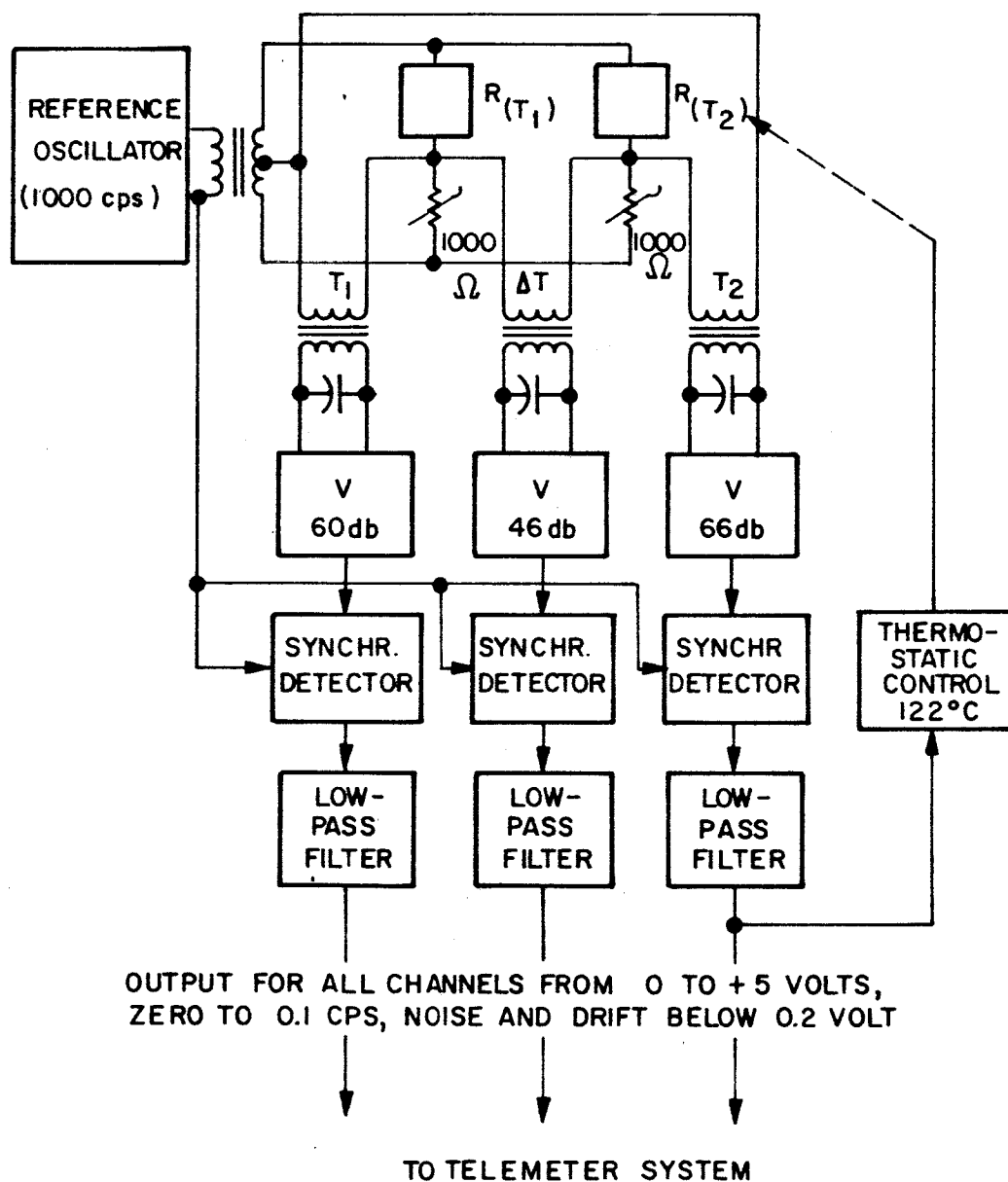


FIG. 17 THE BLOCK DIAGRAM OF THE ELECTRONIC INSTRUMENTATION TO MEASURE THE SOLAR CONSTANT



EXPERIMENT I-I  
MEASUREMENT OF SPECTRAL DISTRIBUTION OF SPACE SUNLIGHT

1. BACKGROUND

This experiment measures the spectral distribution of space sunlight by means of filtered photovoltaic solar cells. Spectral selection is accomplished through the use of interference filters with suitable blocking absorption filters. The region to be measured extends from 4000 to 11,000Å and is divided into 14 channels.

At the time of fabrication of these devices, 10 sets of identical sensors are prepared. The flight package and a possible back-up package provide the primary telemetered information. The other eight 14-channel sets can be utilized for calibration of simulators and to provide a supplement of the telemetered data issuing from the primary cells.

Silicon cells have been used to power satellites since the very earliest space experiments (Vanguard, 1958). They have proven to be extremely reliable devices with highly predictable characteristics. In the proposed experiment, these devices are to be used in a properly spectrally-modified manner in a multichannel spectrometer to determine the spectral distribution of sunlight in the visible and near-visible region. Previous measurements of the solar spectral distribution have been made in the determination of the solar constant by the Smithsonian Institute over a period of approximately 30 years (Ref. 1). These measurements were made from the earth surface, usually in locations of high altitude, and the solar constant was obtained by using an air mass extrapolation. Obviously, such an extrapolation was meaningful only if some energy was able to reach the sensing bolometer in the spectral region of interest. Subsequent measurements outside the atmosphere were made by F. S. Johnson (Ref. 2). The data of Johnson is based upon his own high-altitude rocket measurements, the data of Dunkelman and Skolnik (Ref. 3), and of Perry Moon (Ref. 4), see Fig. 18.

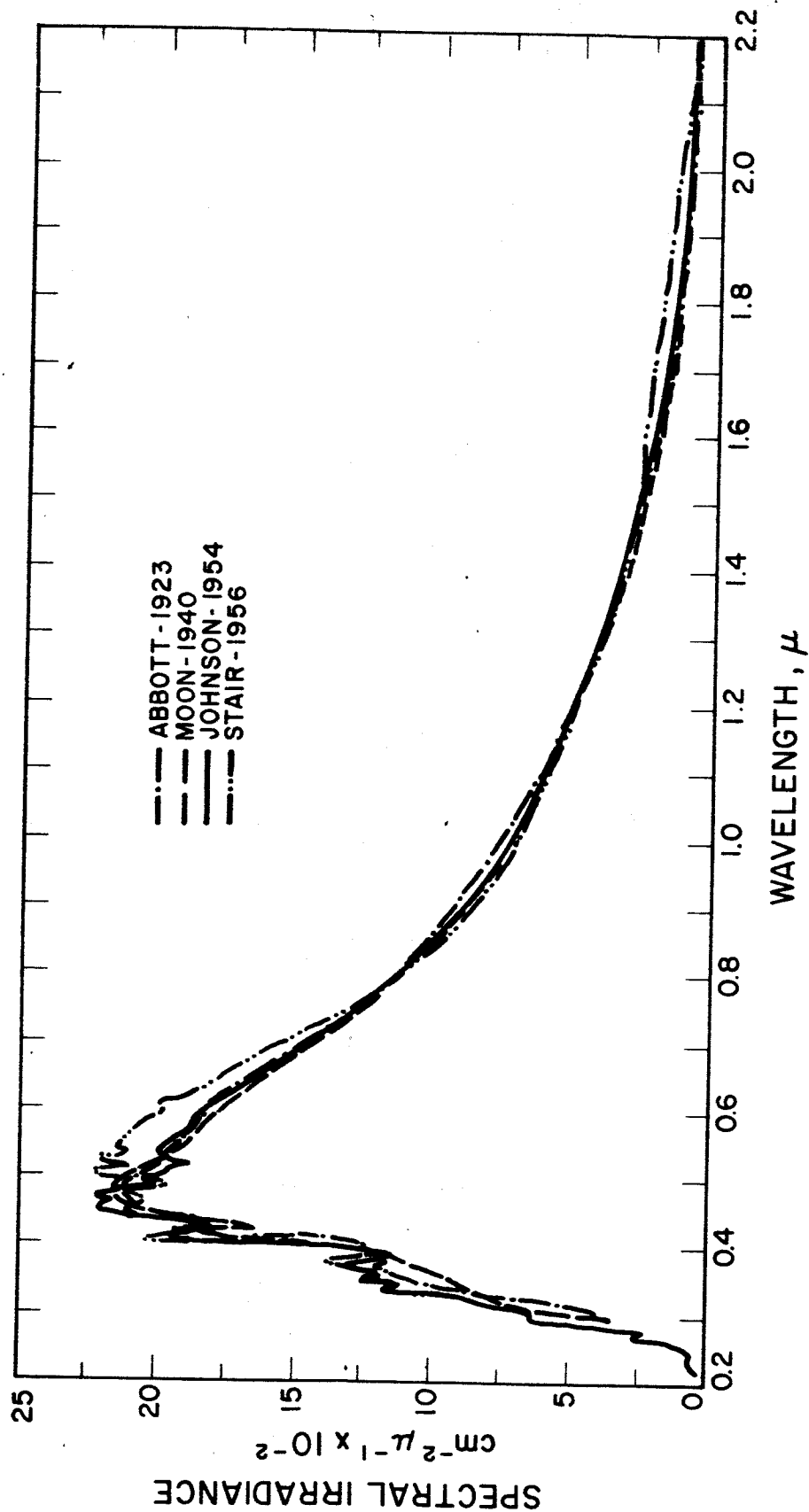


FIG. 18 SPECTRAL DISTRIBUTION OF THE SUN IN SPACE

The use of data from different investigations in the different spectral regions required the adjustment of absolute values in the overlap bands. It is, therefore, desirable to obtain a measurement which extends over at least two of the regions in the Johnson determination.

## 2. DESCRIPTION OF THE INSTRUMENTATION

Solar cells have a spectral response as shown in Fig. 19 in the near-visible region the onset of sensitivity occurs at approximately 3500Å rising to approximately 60 percent at 5000Å, peaking at approximately 8500Å, falling off rapidly beyond the peak and going to zero at approximately 12,000Å. While it would be most desirable to have rectangular, bandpass filters for use with the sensor devices, this is, unfortunately, not within the present state of the art. Optical interference filters with suppressing of harmonics by use of absorption blocking filters have become commercially available within the last 10 years. The use of silicon energy converters of 2 cm<sup>2</sup> area will permit a sufficient amount of electrical signal to modulate telemetry with little electronic complication. The current voltage characteristic for various energy inputs can be seen in Fig. 20. It may be noted that the short-circuit current is a linear function of the illumination level under consideration. Thus by operating each optical channel into a low-impedance load, such that the photo current output is close to short-circuit current, one may directly modulate each telemetry channel. To satisfy the linearity condition, the best choice would be a telemetry modulation between zero and 100 MV. Near the extremes of wavelength response, this could be achieved by having 2 cm<sup>2</sup> of photovoltaic active area per device operating into a 1 kilohm impedance. This assumes that filters allowing transmission of 50 percent of the desirable light wavelength are used.

Due to the considerable amount of information that has become available, both as a result of space experience and as a result of ground testing, the performance of solar cells and glasses in radiation

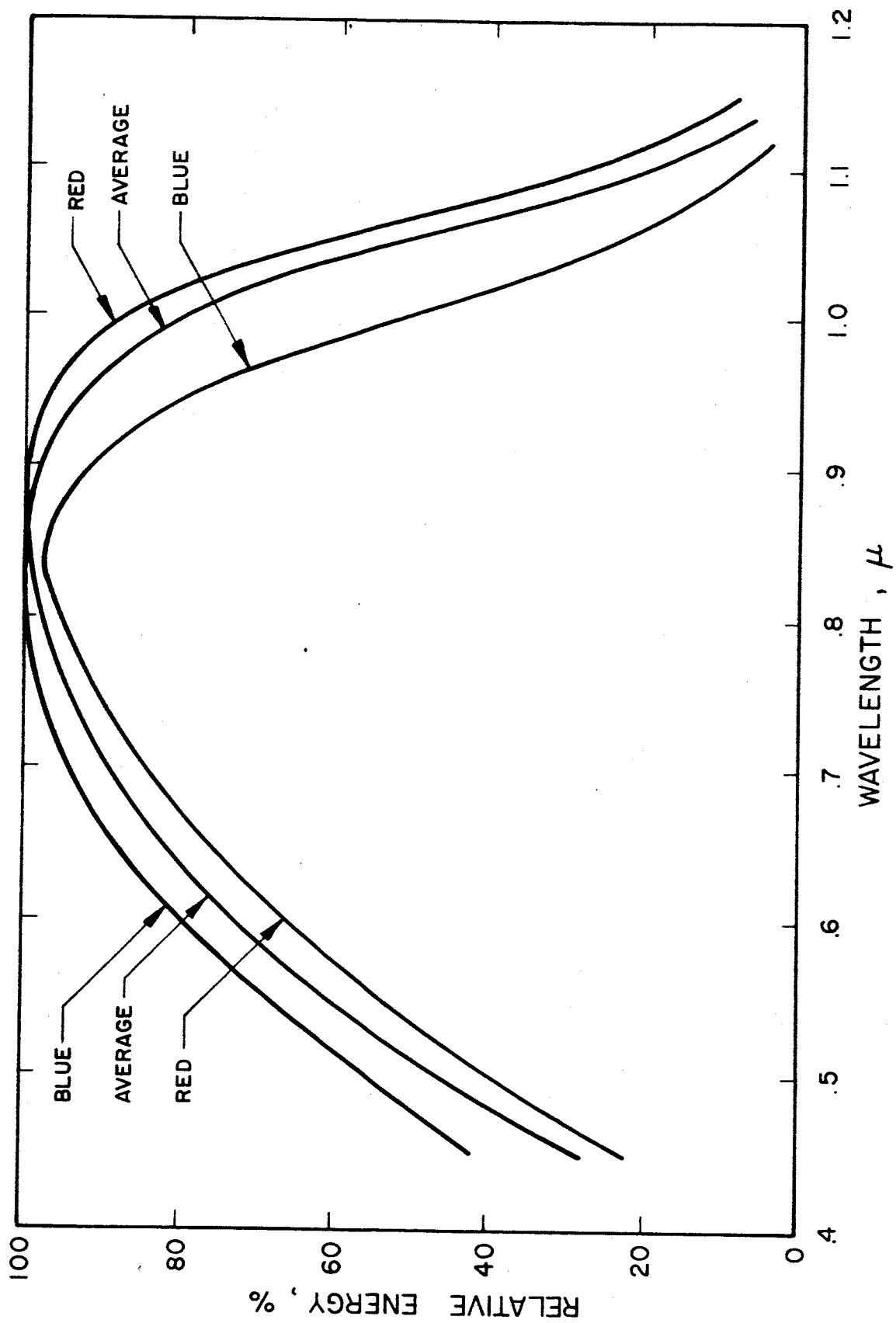


FIG. 10 RELATIVE SPECTRAL RESPONSE AND RED AND BLUE LIGHTS OF TYPICAL N/P SOLAR CELLS

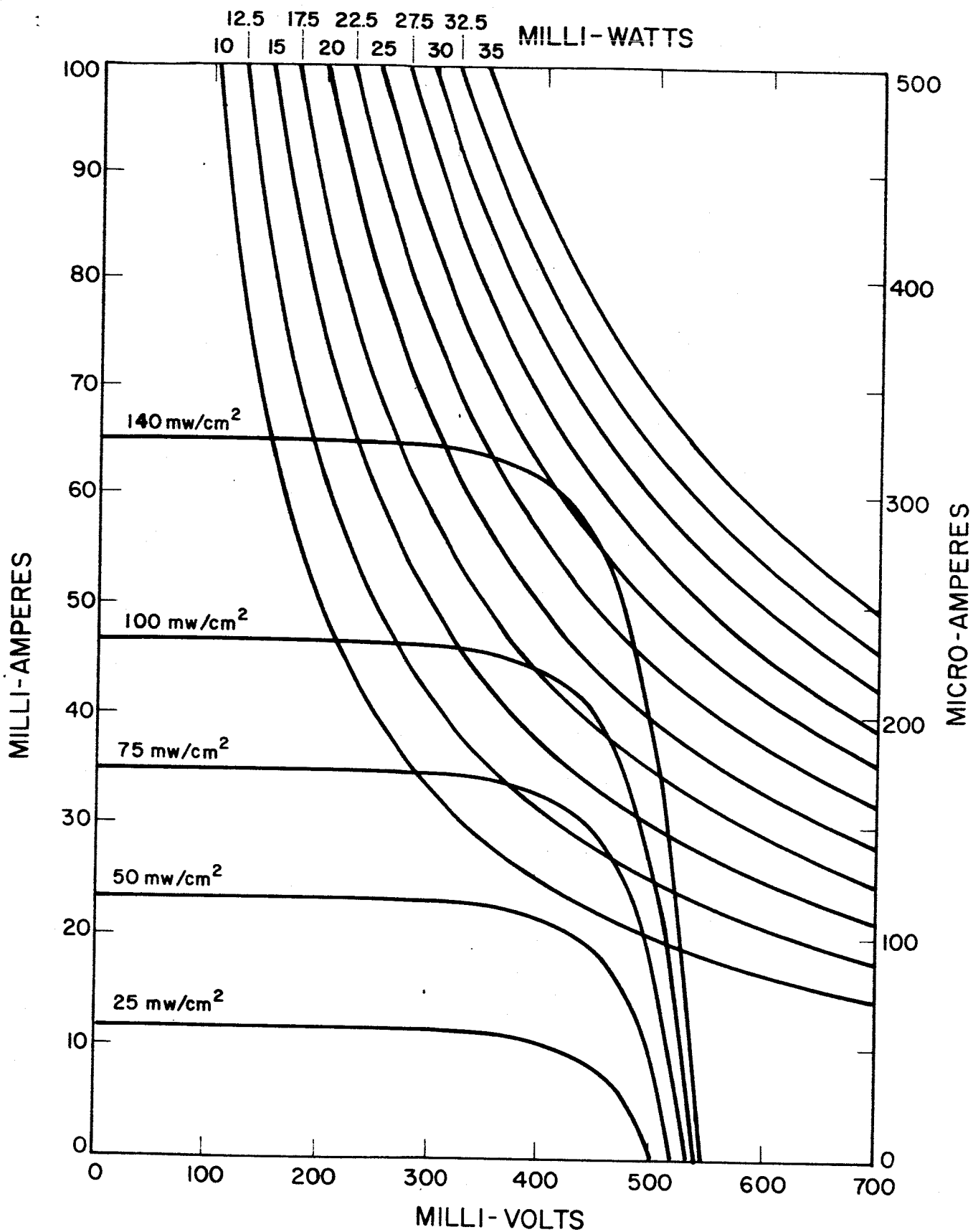


FIG. 20 VOLTAGE-CURRENT CHARACTERISTIC VS. INTENSITY  
(AIR MASS = 0 TEMPERATURE =  $28^{\circ}\text{C}$ )

environments is highly predictable. Figures 21 and 22 show short-circuit current degradation and spectral response degradation as a function of integrated flux. Degradation of these parameters becomes severe after considerable exposure, which implies long storage in a radiation environment. Since the instantaneity of information arrival is determined only by the telemetry rate, the desired information can be obtained in the very early stages of the experiment; therefore, energetic particle degradation need not be a factor adversely affecting the experiment.

If one wishes to examine the long-term stability of solar spectral intensities, radiation degradation would become a detrimental factor after some time. Degradation of the pertinent parameters must be evaluated in terms of storage in space, i.e., length of mission, and appropriate estimates of error may be made.

The multichannel optical spectrometer which is proposed here is an extremely simple instrument. Each sensor is self-powered and weighs, with filter and appropriate optical encapsulation, approximately 5 grams. For purposes of better control, it is recommended that a cell filtered only by equivalent thickness of glass be added to the 14 spectral channels. This will allow an integration of the total amount of light seen, in addition to providing for an assessment of the effects of temperature and radiation degradation. A separate temperature measurement for the common isothermal substrate is also recommended. Electric and magnetic fields are not expected to have any effect upon this experiment.

While the close matching in selection of solar cell filter combinations, in order to result in matched sets, may appear to be a formidable problem, this is actually not the case. The only regions of spectral response that must be matched within a particular wavelength band set encompass a single wavelength interval. Thus, a set of 10 cells must be selected, for example, to have relative spectral responses which are nearly identical over a wavelength interval from 4000 to 5500Å. Manufacturing experience has taught that this is not a difficult problem.

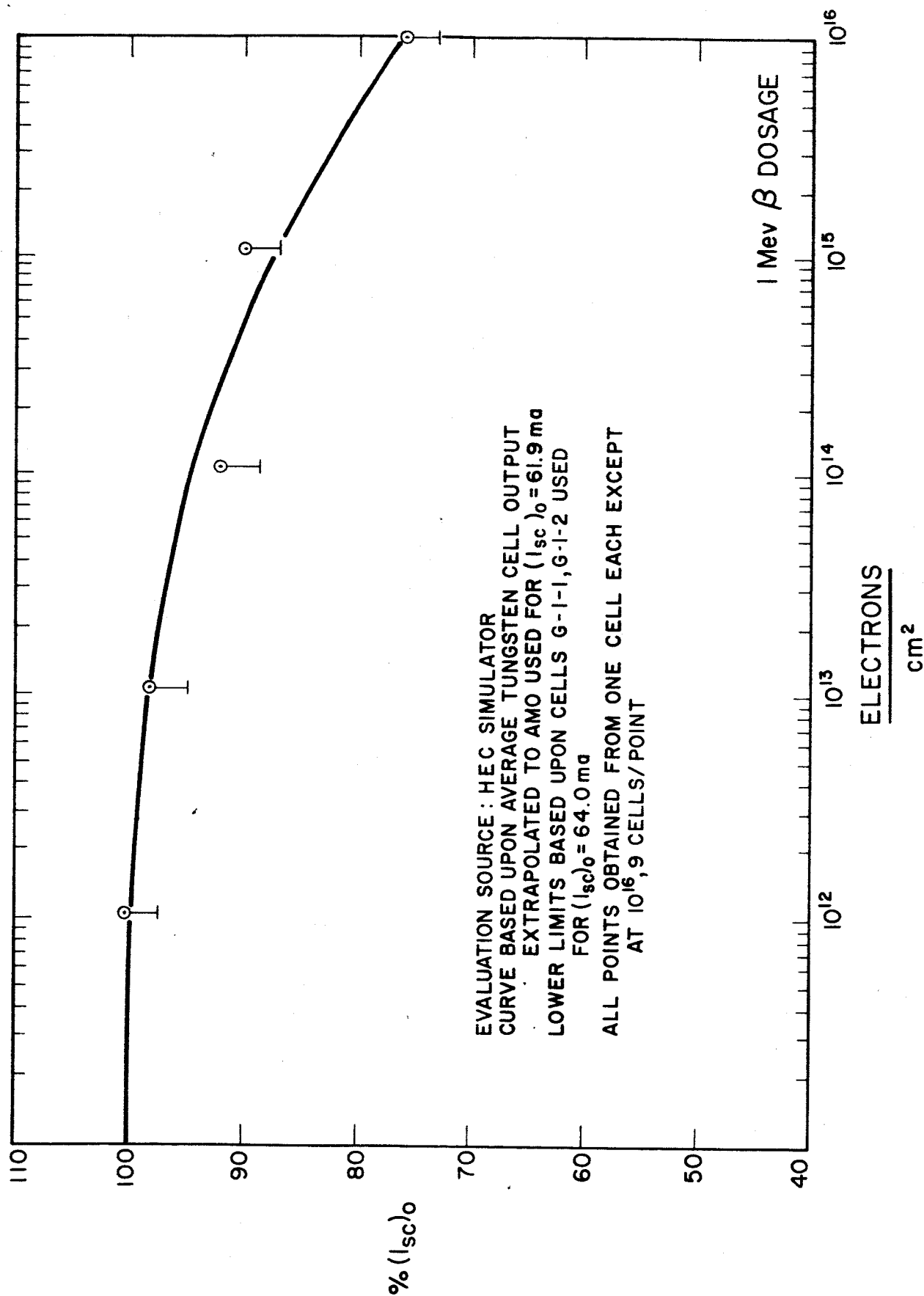


FIG. 21 SHORT CIRCUIT CURRENT DEGRADATION OF N/P HOFFMAN SOLAR CELLS UNDER 1 MeV ELECTRON BOMBARDMENT

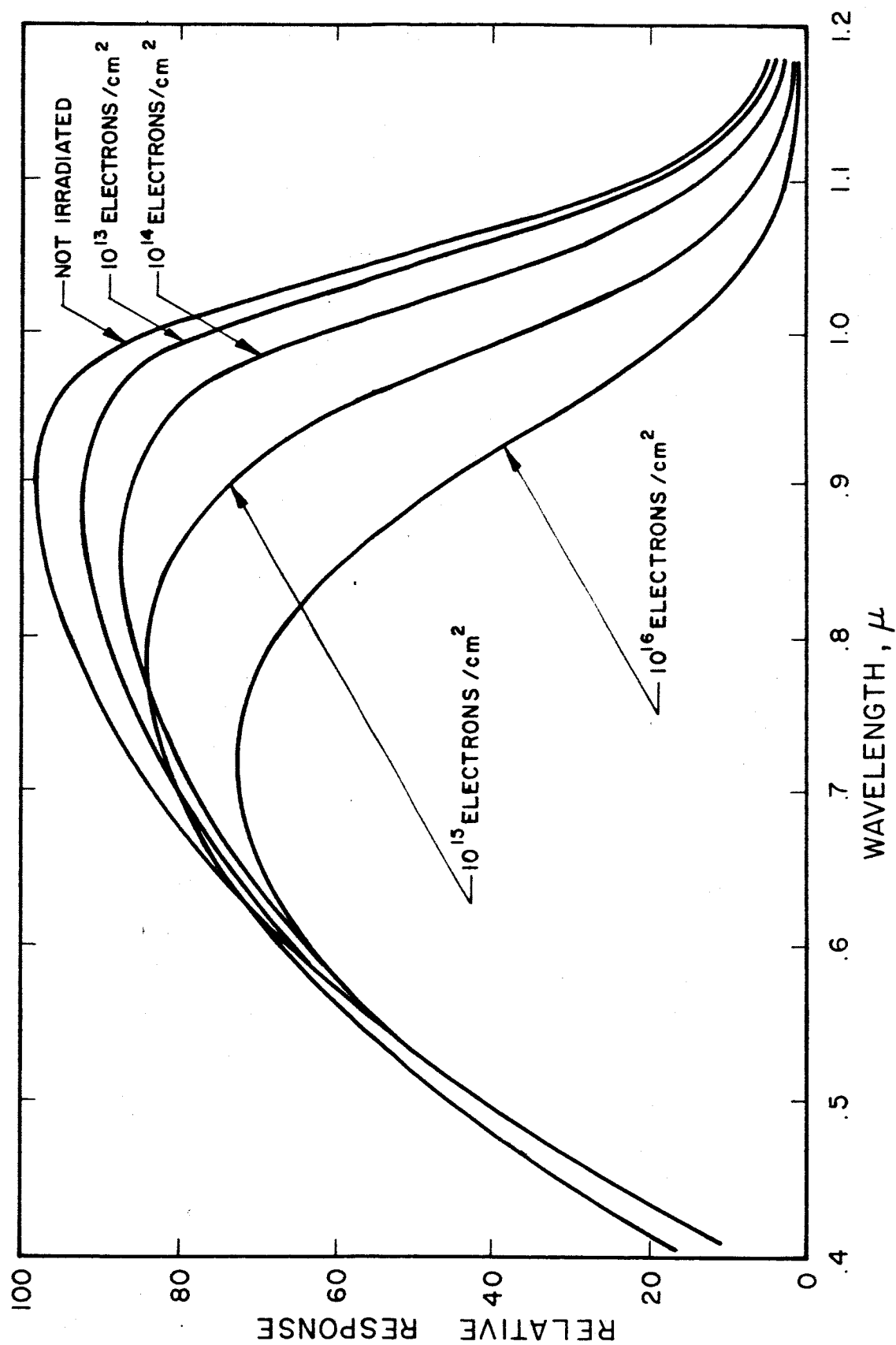


FIG. 2.2 SPECTRAL RESPONSE OF HOFFMAN N/P SOLAR CELLS AFTER BOMBARDMENT WITH 1 MeV ELECTRONS



The electronic circuitry consists only of a programming-control unit to scan the sensors periodically. The sizes of the cells have been chosen so that the outputs will not require amplification and can go directly to telemetry.

### 3. INSTRUMENT SPECIFICATIONS

Physical dimensions:	3 in x 7 in x 2 in
Weight:	1 lb
Electrical power requirements:	28 volts (nominal); 10 mA during scan, 0 mA standby
Duty cycle:	2 seconds scan time; 1 hour standby
Dynamic range:	0.4 to 1.1 $\mu$ in 14 0.05 $\mu$ -bands
Magnetic interface:	None
Thermal interface:	None (cells are mounted on a 0.125-inch-thick Al plate to ensure all are at the same temperature)
Mechanical interface:	Must be mounted facing the sun
Orbit:	Modified sun-synchronous is a slight preference; experiment can be flown in any orbit so long as sensors face the sun (to within a few degrees) for a few seconds at 1- to 2-hour intervals

### References

1. L. B. Aldridge and W. H. Hoover, "The Solar Constant," Science 116, 3 (1952)
2. F. S. Johnson, "The Solar Constant," J. Meteorol. 11, 431 (1954)
3. L. Dunkelman and R. Skolnik, "The Solar Spectral Irradiance and Vertical Atmospheric Attenuation in the Visible and Ultraviolet," J. Opt. Soc. Amer., 49, 356, (1959)
4. P. Moon, "Proposed Standard Solar Radiation Curves for Engineering Use," J. Franklin Institute, 230, 583, (1940)

## EXPERIMENT I-J

### EVALUATION OF CONVENTIONAL BATTERIES IN ZERO GRAVITY

#### 1. BACKGROUND

A major portion of a space power system is the energy storage unit--usually conventional batteries (AgO-Zn, AgO-Cd, or NiCd). All the effects of space environment on these batteries can be readily obtained in the laboratory except that of zero gravity. As long ago as 1958 (Ref. 1) it was pointed out that certain processes in a battery are gravity sensitive. Briefly, the portions of a battery mechanism that are gravity dependent are the mass transport of ions and electrolyte, the solution and dissolution of matter or species within the electrolyte, and the effect of gases that are generated during charge, overcharge, overdischarge, and corrosion of anodic electrodes that will not separate from the electrolyte.

Up to the present time, the instrumentation on batteries for space applications has been minimal (voltage, charge-discharge current, temperature) and any data applicable to solving or better defining the above effects is nonexistent. Therefore, to obtain some of these answers the following experiment is suggested.

#### 2. EXPERIMENT DEFINITION

The experiment will utilize the near-zero-gravity environment provided by the JPL spacecraft. Conventional batteries will be packaged, instrumented, and installed to determine the extent of zero gravity effects on the life cycle, individual electrode polarization, and overcharge gas recombinations. The experiment will be conducted with commercially available batteries by implanting a reference electrode to determine individual electrode polarization and a pressure transducer to determine pressure within the cell. The experiment will be cycled repeatedly in zero gravity and the individual electrode will be

monitored to determine its voltages and currents. Recombination studies will be conducted by progressively increasing the overcharge current and by monitoring the internal pressure within the cell. The cell will be cycled for a specified period of time on an established charge-discharge regime, and the polarization and recombination measurements of the individual cells repeated.

The experiment will be conducted in parallel with standard tests to show the effects of zero gravity on these areas.

### 3. EXPERIMENT SPECIFICATION

Dimensions:	8" x 7" x 6"
Weight:	10 pounds
Power:	5 watts, continuous
Thermal:	+10°C to +40°C
Data:	~ 150 bits/min (continuous or cycled every 5 minutes)
Preferred orbit:	Any

#### Reference

1. Morris Eisenburg, "The Effect of Weightlessness on the Performance of Batteries and Fuel Cells," Proceedings 12th Annual Battery Research and Development Conference, 21-22 May 1958

EXPERIMENT I-K  
EVALUATION OF REGENERATIVE HYDROGEN-OXYGEN  
FUEL CELL IN ZERO GRAVITY

1. BACKGROUND

The rechargeable fuel cell is basically a combination of  $H_2/O_2$  fuel cell and a water electrolysis cell in one compact package (Ref. 1). During the charge mode of operation, water contained within an asbestos matrix, separating the electrodes, is electrolyzed to produce hydrogen at the anode and oxygen at the cathode. The gases evolved are stored in appropriate integral tanks. During discharge, the stored gases are recombined to form water which returns to the asbestos matrix. In this concept, the electrolyte liquid is "immobilized" in the matrix and the reactant gases enter and leave the back side of the porous electrodes.

A multicell unit is constructed by stacking bipolar plates having appropriate gas manifolding. The cell stack is placed within a cylindrical storage vessel having a partition to divide the  $O_2$  and  $H_2$  gas storage sections. A volume-compensating bellows is provided to assure that the 2-1 volume ratio is maintained, since it is desirable to avoid differential pressures.

No actual long-term zero-gravity experiments have been conducted on the regenerative cell, but preliminary work by Allis Chalmers for the Air Force concluded that the units are not gravity-sensitive.

Therefore, the purpose of this experiment is to discharge the regenerative fuel cell in a long-term zero-gravity environment to demonstrate the capillary action and verify that there is no gas-liquid mixture. Also, on charge the unit would demonstrate the ability of hydrogen-oxygen electrolyzer systems to function in zero gravity without the problem of gas-liquid separation. The cycling of a unit of this type in long-term zero gravity would demonstrate the capabilities of the regenerative fuel cell and remove an important unknown in its development.

Ref. 1 "The EOS  $H_2/O_2$  Secondary Battery," Contract NAS3-2781

## 2. EXPERIMENT DEFINITION

The basic unit of this experiment is a 75-watt, 6-cell battery (see Fig. 23). In actual ground tests it develops 90 watts and has a capacity of about 10 amp hours.

Extensive ground tests have been conducted on this unit and the present performance capabilities are shown in Table 6. Typical charge-discharge cycle data are shown in Fig. 24 for this 6-cell unit. This nominal cycle is for a 300-nautical-mile orbit, i.e., 65 minutes of charge and 35 minutes of discharge. The linear pressure rise and decline with the flat charge-discharge characteristics are evident in Fig. 25.

TABLE 6  
PRESENT PERFORMANCE

Watt hours per pound	10 to 12
Amp hours per pound	16
Operation temperature (maximum)	350°F
Power level	110 watts
Thermal sterilization capability	Sterilizable
Cycle life	> 300 full depth
Operating current density	100 ma/cm <sup>2</sup>
Overload capability	2:1

## 3. EXPERIMENT SPECIFICATION

Dimensions:	8" diameter x 9" length
Weight:	15 pounds
Power:	~ 10 watts charge
Thermal:	50°C to +175°C
Instrumentation:	2 pressures, 6 voltages, 2 temperatures (0 to 5 volts)
Data:	120 bits/min continuous
Mounting:	Not critical
Preferred orbit:	Any

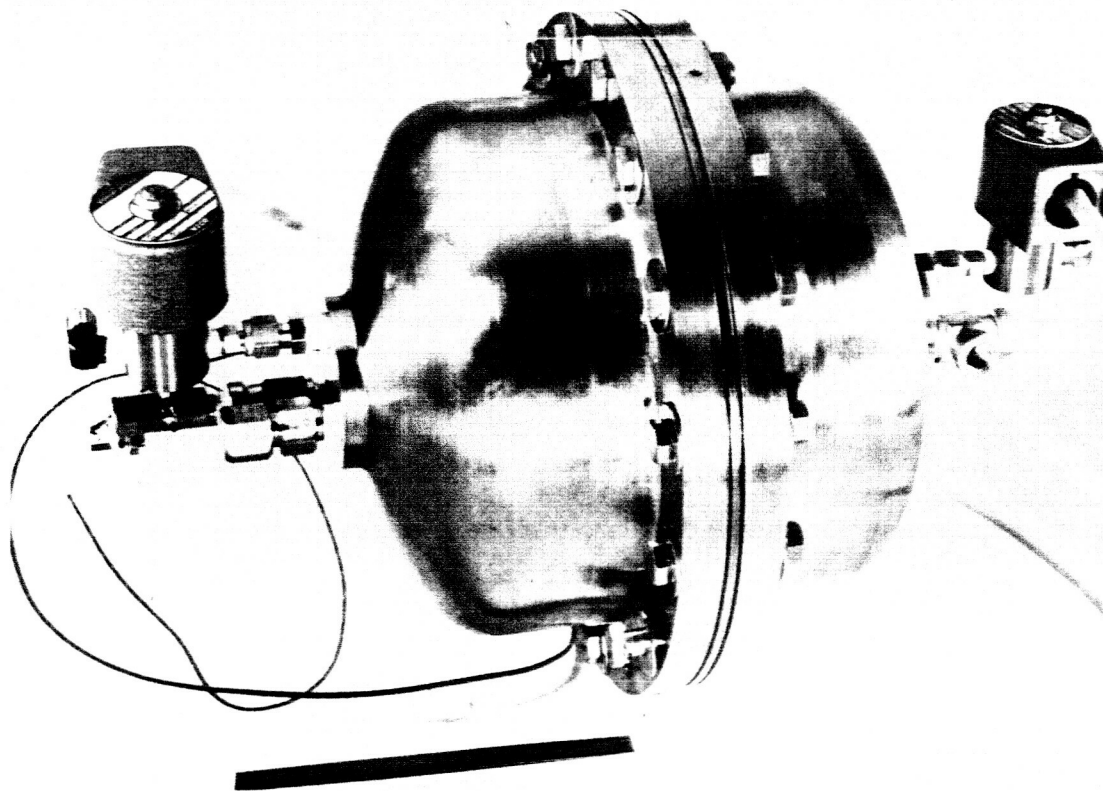


FIG. 23 75-WATT FUEL CELL ASSEMBLY

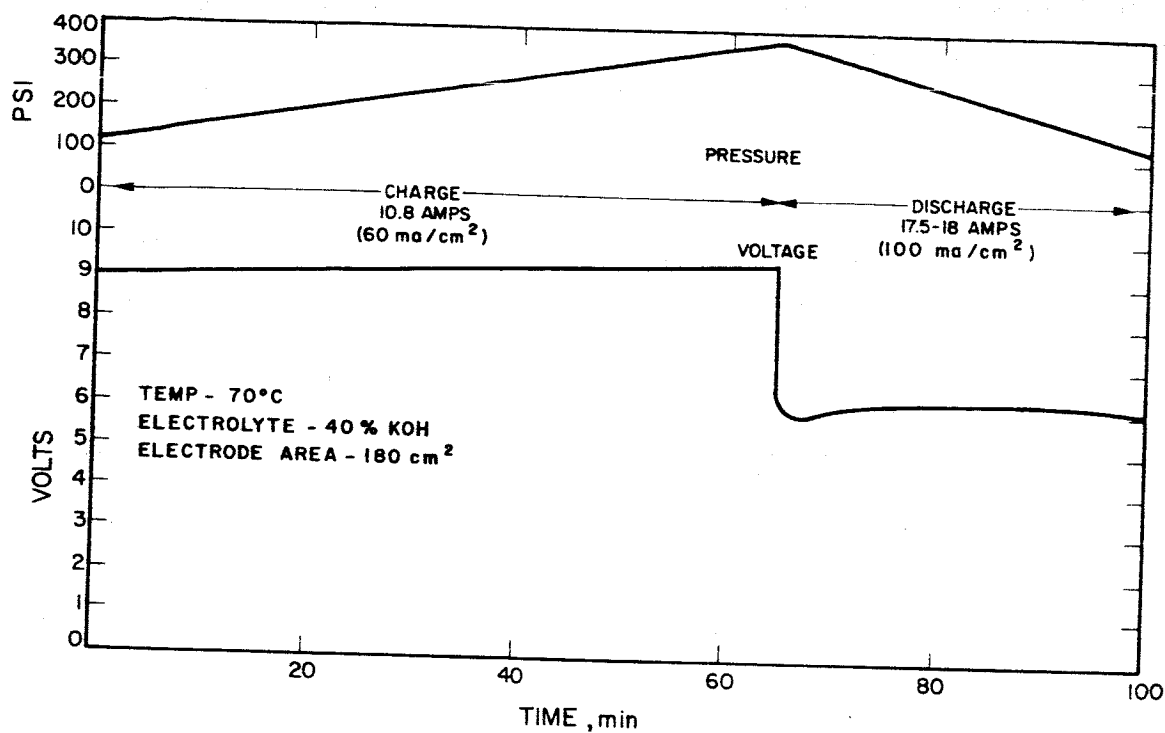


FIG. 24 H<sub>2</sub>/O<sub>2</sub> REGENERATIVE CELL PERFORMANCE

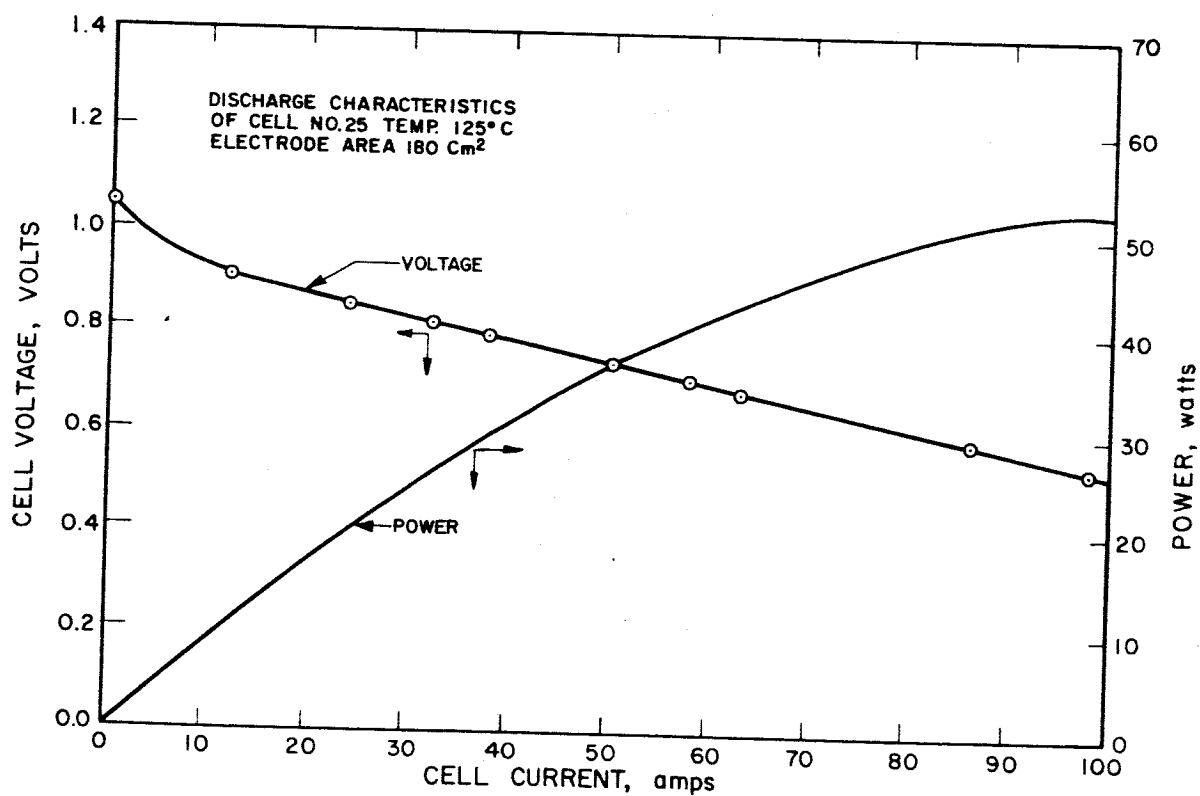


FIG. 25 CELL PERFORMANCE AT 125°C

## EXPERIMENT I-L

### RADIATION EFFECTS ON SOLAR CELLS

(This experiment was taken from the G. E. Report)

#### 1. BACKGROUND

Of all the components found on present state-of-the-art spacecraft, the solar cell array generally exhibits the highest vulnerability to space radiation damage. As a result, considerable attention must be given, when designing a space vehicle, to the shielding required to protect the solar array from the expected space radiation environment. The required shielding and oversizing of the solar array to account for the expected radiation damage can represent a very significant weight penalty. To minimize this weight penalty, it is important to: (a) know the radiation environment accurately, (b) thoroughly understand the effect of radiation on solar array performance, and (c) be able to accurately predict the protection afforded by shielding. However, present methods of predicting damage are approximate and, in addition, a large uncertainty in the expected environment exists. Space experiments are needed to better understand this problem and to provide the necessary design information.

The normal solar array configuration consists of solar cells covered with a fused silica coverglass. The coverglass shields the solar cells from the radiation environment. A filter is vapor-deposited on the coverglass, which is held to the solar cell by an organic bond. Each of these four components: solar cell, coverglass, filter, and organic bond to some degree exhibit a damage vulnerability.

In general, solar cell damage results from lattice defect production generated by collisions between higher energy particles and the lattice atoms. This produces a reduction in the minority carrier lifetime which lowers the short-circuit current.

Degradation in the organic bond results from a change in its chemical composition induced by ionizing interactions with the incident



radiation. Similar ionizing interactions with ultraviolet and particle radiation cause reduction in the transmittance of the filter and fused silica shield. These other effects, then, also degrade the short-circuit current since they reduce the amount of light reaching the cell surface.

This experiment is designed to accomplish the following objectives:

1. Separate and determine the relative importance of damage in the solar cell, organic bond, filter, and shield.
2. Determine the relative degree of protection afforded by shielding of different thickness and provide evidence on the "hardness" of the incident spectrum.
3. Monitor the spacecraft solar array degradation.
4. Verify, or provide information for correcting, laboratory damage estimates to improve the efficiency of solar array design.

## 2. EXPERIMENT DEFINITION

The selection of appropriate combinations of components for the solar cell assembly will allow damage in either the cell, shield, filter, or bond to prevail in producing degradation in the short-circuit current. Therefore, the experiment would contain various combinations of shield, bond, etc., to allow a determination of the relative significance of damage in each. Shields of varying thickness would be used to indicate the effectiveness of this parameter on radiation hardening and the hardness of the incident spectrum. To complete the complement, cell assemblies, identical to those in the spacecraft array, would be included for the purpose of monitoring the array degradation. Specifically, the experiment would be composed of these solar cell assemblies.

### Type A Assembly

This assembly would consist of solar cell and shield with no filter or bond. The shield would be mechanically clamped to the cell and any

degradation in the short-circuit current would be due mainly to cell damage induced by the residual spectrum. There would be two Type A assemblies present; the shield on one would be 6 mils thick while the other would be 60 mils. Comparison of data for these two shields would indicate relative shield effectiveness and the incident spectrum hardness.

#### Type B Assembly

This assembly would consist of a pre-irradiated solar cell, shield, and filter with bond. Pre-irradiation of the solar cell would render it relatively immune to additional damage, therefore, any degradation in the output would be due mainly to damage in the shield, filter, and bond.

#### Type C Assembly

This assembly would consist of a pre-irradiated solar cell, bond, and shield with no filter. Therefore, degradation in the output should be due solely to damage in the bond and shield. A comparison of data from this assembly with data from Type B would indicate the amount of damage incurred by the filter.

#### Type D Assembly

This assembly would consist of a pre-irradiated cell, with shield, filter, and no bond. Therefore, degradation in the output should result mainly from damage in the shield and filter. A comparison of data from this assembly with Type B would indicate the degree of damage incurred by the bond.

#### Type E Assembly

This assembly would consist of a pre-irradiated cell and shield with no filter or bond. Any degradation occurring greater than approximately 5 percent would indicate damage in the shield

#### Type F Assembly

This assembly would be representative of the vehicle array. It would contain identical bonding, shield thickness, filter, and cells. Therefore, this data would be used to monitor the vehicle array

degradation. Also, comparison with data from Type B would indicate the degradation that would be suffered by the cell alone.

In an experiment of this nature, duplication to gain statistical confidence in the data is a necessity since no two samples will exhibit the same damage sensitivity. Therefore, in order to gain sufficient duplication using one vehicle, a scheme has been adopted which utilizes ten 1/2 by 1/2 cm solar cell segments connected as shown in Fig. 26. Each segment for an assembly would be cut from a different 1 by 2 cm cell. The remaining segments cut from the cell would be used in other assemblies. Every assembly would then consist of segments from 10 different cells, however, the total output for each of the assemblies would represent the average of the 10 cells. This is equivalent to using identical cells on each assembly and duplicating the entire experiment 10 times. The segments in an assembly would be mounted in thermal contact with, but electrically insulated from, a common base plate. All would be covered by a single shield and filter piece. If  $V_T$  is the voltage across the total string and  $V_i$  is the voltage on each cell, then

$$V_T = \sum_{i=1}^{10} V_i$$

To measure the short-circuit current, a 1-ohm resistor would be connected across each segment. Therefore, the average short-circuit current would be

$$\bar{I}_{sc} = \frac{V_T}{10}$$

Then only one quantity,  $V_T$ , must be measured to obtain the average short-circuit current for the 10 segments and the same statistical validity is obtained as if 10 separate cell assemblies were exposed and measured separately. This scheme enables each assembly to be effectively duplicated 10 times with no increase in the number of

INPUT TO TELEMETRY 0-50 MV

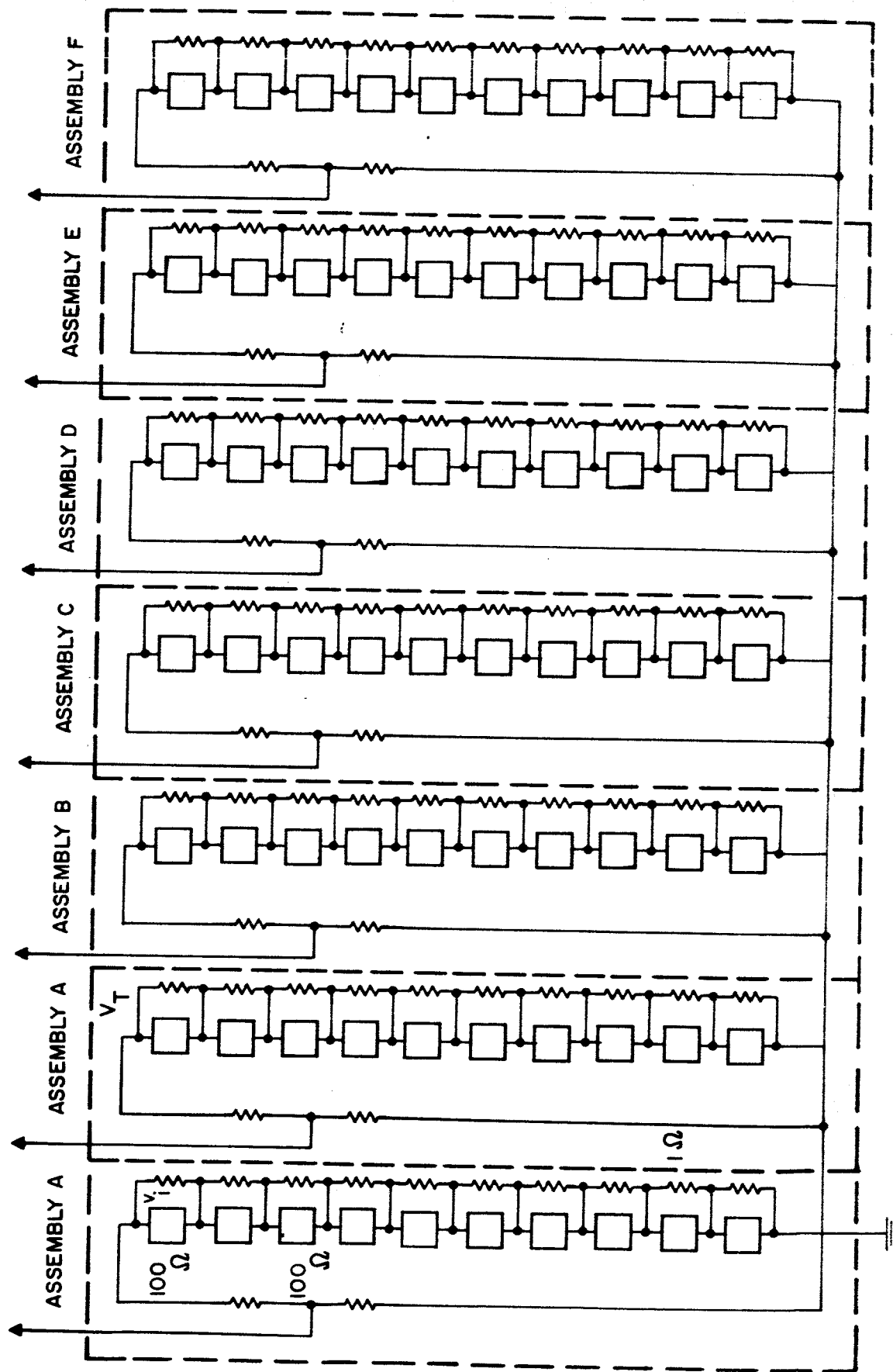


FIGURE 8. EFFECT OF SOLAR CELL RADIATION EFFECT IS EXPERIMENT

readings required and an increase in required surface area of only about 1 cm<sup>2</sup>. Although the size of a segment is 1/8 that of a normal cell, no insurmountable mounting or soldering problems are foreseen since the technology in this area is well advanced.

The short-circuit current is a temperature sensitive quantity and, since variations in temperature are expected, the requirement for temperature information exists. If all the assemblies were mounted on a good common thermal sink, all the cell temperatures should be approximately equal and only the sink temperature would have to be measured.

Solar cell output is also sensitive to sun orientation. The experiment would be sun-oriented making use of the orientation system employed by the primary solar thermionic experiment. Since measurement of the orientation accuracy will be required for evaluation of the solar thermionic experiment, this information would be available for the secondary experiments as well.

### 3. EXPERIMENT SPECIFICATIONS

The interface requirements of the solar cell experiment (assuming a total number of 7 solar cell assemblies) are summarized below.

Electrical power required:	0.04 watts for operation of 2 thermistors
Weight:	Less than 0.5 lb
Size:	4.5 in <sup>2</sup> by 1 in deep
Instrumentation:	7 voltages (0-50 mV); 2 temperatures (thermistors 0-5V)

Telemetry accuracy required: 1 percent of full scale reading

The experiment must be sun-oriented within approximately  $\pm 5^\circ$

EXPERIMENT I-M  
VEE-RIDGE (G.E. EXPERIMENT)

1. BACKGROUND

Solar photovoltaic arrays are currently the major means of supplying electrical power in space and are expected to be the best source of power for many missions in the future. The state of the art has evolved to the solar-oriented flat paddle of the Ranger, Mariner, Nimbus, and OGO systems. The present paddle designs will continue to be improved with the use of more efficient and more radiation resistant solar cells and other innovations. However, an advance in the state of the art of photovoltaic arrays to the use of V-ridge concentrators offers two potentially significant advantages: (1) a weight saving of 15 to 30 percent, and (2) a decrease in cost of up to 45 percent. The V-ridge reflective surfaces result in more solar energy being concentrated on the solar cells. This allows more power to be obtained from the same number of cells. This means a given power output can be achieved with a smaller number of solar cells, which accounts for the reduction in cost. Since the concentrating surfaces are lighter in weight than the solar cells they replace, this also yields an overall decrease in weight.

In the past three years, several companies, including General Electric and Boeing, have successfully developed and ground tested experimental V-ridge concentrating modules. The major uncertainty remaining is what effect, if any, will the space environment have on the performance of the concentrator surfaces. A space experiment is required to find the answer. This experiment is designed to verify the space performance of a typical photovoltaic array employing V-ridge concentrators. Of particular interest are the effects of ultraviolet radiation, ionizing radiation, micrometeorites, and thermal cycling on the performance of the reflecting surfaces.

2. EXPERIMENT DEFINITION

The selection of appropriate combinations of solar cells and concentrator surfaces will enable separate determination of solar cell performance

for both concentrated and nonconcentrated cases; and separate determination of any solar cell or concentrator performance degradation. The experiment would be composed of three assemblies (see Fig. 27).

Type A Assembly - This assembly would consist of a typical V-ridge concentrator panel from which temperature and power output measurements would be made.

Type B Assembly - This assembly would be a nonconcentrating section. Power output and solar cell temperature would be measured. A comparison of the performance between Assemblies A and B would provide a measure of the concentration ratio. Also, the data from these two assemblies would allow the solar cell performance to be factored out and the concentrator performance isolated.

Type C Assembly - This assembly would be identical to the Type A section but smaller. Solar cell temperature and short-circuit current would be measured. Since short-circuit current is primarily dependent on energy impinging on the solar cells and not cell temperature, it is another measure of concentrator degradation.

### 3. EXPERIMENT/SPACECRAFT REQUIREMENTS

The interface requirements for the V-ridge concentrator experiment are summarized below:

Electrical Power Required	0.16 watts (8 thermistors at 20 mw per thermistor)
Weight	2 pounds
Surface Area Required	130 in <sup>2</sup>
Volume	260 in <sup>3</sup>
Instrumentation	6 voltages (0-6.4 volts) 8 temperatures (thermistors 0-5v)
Telemetry Accuracy Required	1 percent of full scale reading

The experiment must be sun-oriented with an accuracy on the order of  $\pm 3$  degrees. It is also desirable to have a measure of the orientation accuracy. This could be obtained from the primary experiment.

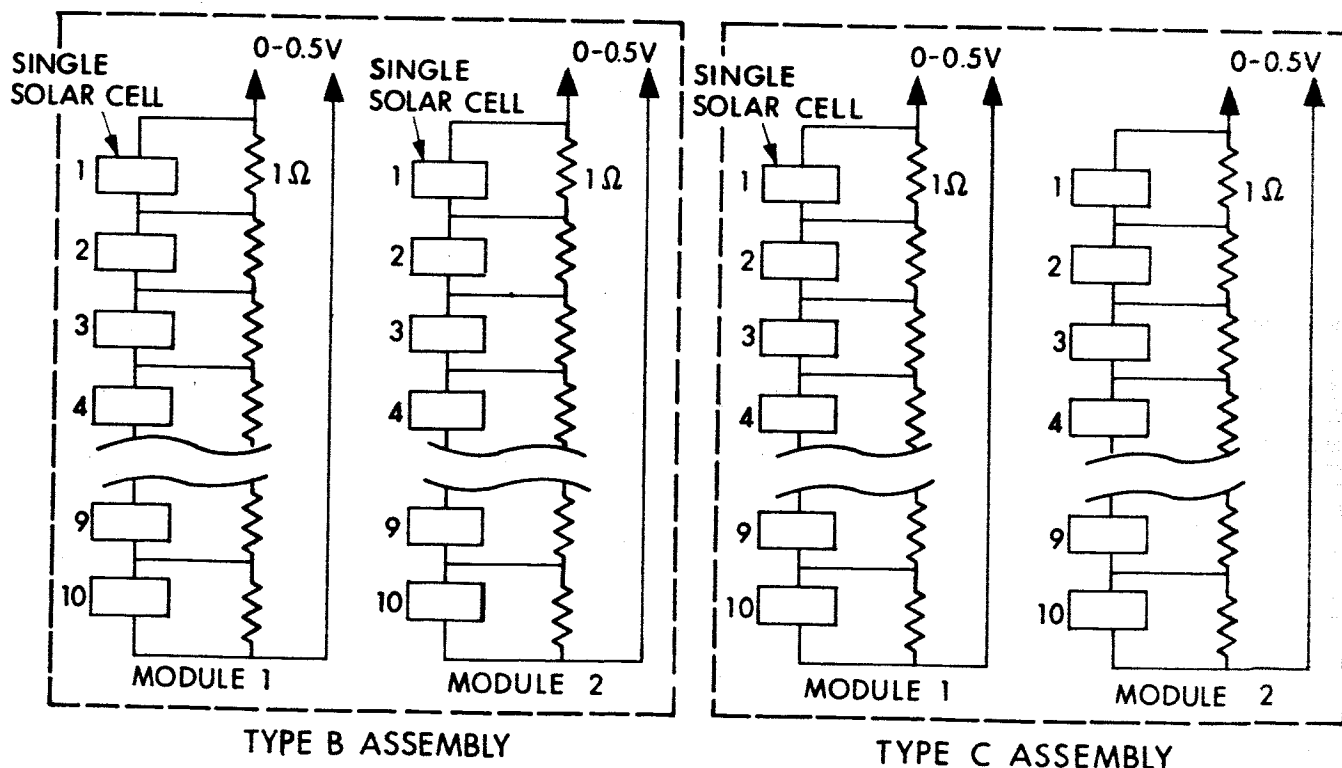
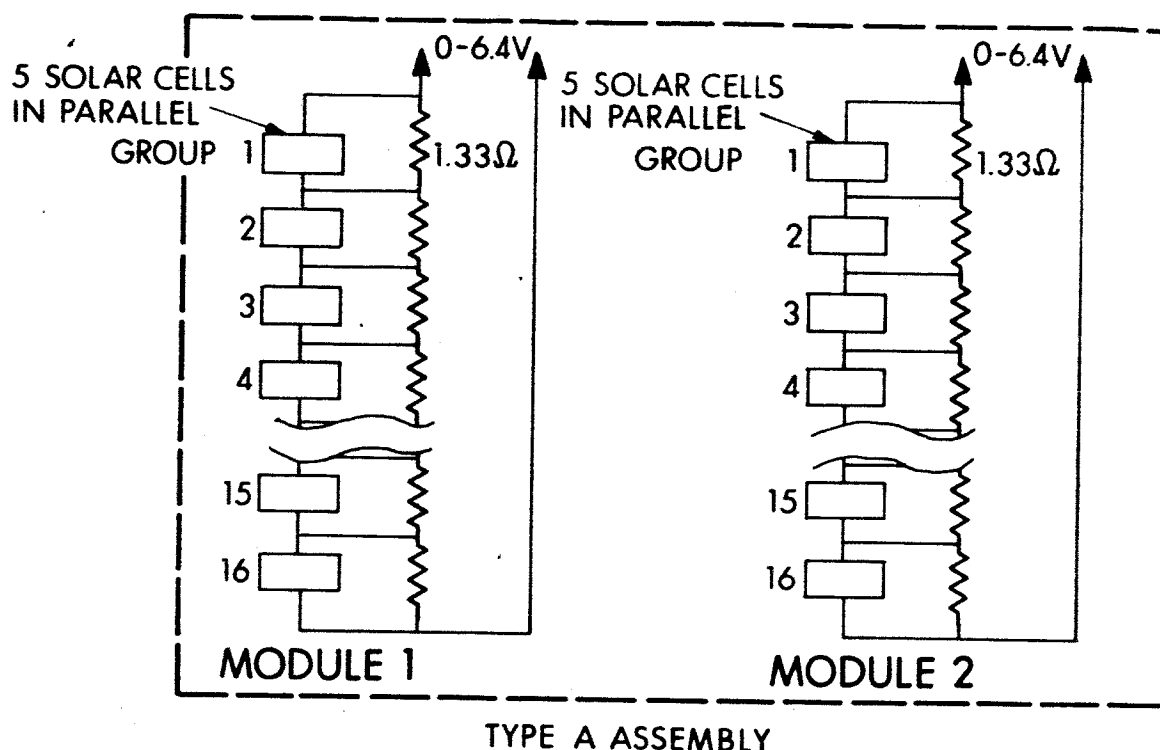


FIG. 27 V-RIDGE CONCENTRATOR EXPERIMENT SCHEMATIC



EXPERIMENT I-N  
THIN-FILM SOLAR CELLS (G.E. EXPERIMENT)

1. BACKGROUND

The development of high efficiency, thin-film solar cells could result in extremely lightweight space power systems. Consequently, research and development of thin-film cells is presently receiving considerable attention. However, this work is still in a very early state of development. This is true both from the standpoint of the theoretical understanding of thin-film cell operation and also from the standpoint of materials and fabrication techniques for making usable cells for space experimentation and application. A brief synopsis of the present state of the art of thin-film solar cells is given below, and will serve as a background upon which a space experiment will be defined. The materials being most aggressively investigated at present are cadmium sulfide (CdS), cadmium telluride (CdTe), and to a lesser degree, gallium arsenide (GaAs) and silicon (Si). Several techniques are being pursued in fabricating the CdS cells.

The development of fabrication techniques for thin-film GaAs and silicon cells are such that they cannot be considered for a space experiment at this time.

The laboratory work that has been done on the radiation effects on CdS and CdTe cells indicates that these cells are very radiation-resistant. Some tests results on CdS cells, fabricated by the techniques described previously, are given below.

Tests with electrons ranging in energy from 0.6 to 2.5 Mev show degradations of only five to ten percent for doses of  $10^{17}$  electrons per square centimeter. Similar results are seen for protons ranging in energy from 2 to 10 Mev for doses of  $10^{15}$  protons per square centimeter. These are extremely high radiation doses for space application. However, an interesting aspect of the electron irradiations, was that for doses above approximately  $10^{16}$  electrons per square centimeter, the effects of the

radiation appears to be very dose rate dependent. Degradations of 50 to 90 percent have been seen immediately after an irradiation of  $10^{17}$  electrons per square centimeter at a high dose rate. Complete recovery of the cells occurred, however, within a few days after the irradiation with the cells exposed to room ambient light and under no load. This recovery shows a strong dependence on cell loading during the annealing.

A space experiment with CsS and CdTe cells could shed light on a number of questionable areas. For example, will the moisture degradation for at least one type of CdS cell be a problem, or will the cells quickly recover once they are in space, regardless of the previous moisture degradation history? Will the CdS be stable in the combined space environment of deep vacuum, ultraviolet radiation, particle radiation, and temperature; or will a protective coating have to be applied to stabilize the surface? Are the cells stable against the low dose-rate space particle radiation while under full solar illumination and power loading conditions? Do the cells have to have some minimum shielding against the intense, very low-energy particle radiation? Will micrometeorites create an erosion problem on unshielded film surfaces?

A space experiment can be designed that would attempt to answer some of these questions for the CdS and CdTe cells. Specifically, the objectives of the experiment would be to investigate:

1. The recovery of moisture degraded cells in space
2. The effect of intense low-energy particle radiation and micrometeorites on thin film surfaces
3. The need for surface stabilization against evaporation in the space environment
4. The effect of low dose-rate energetic particle radiation on cell output
5. An accurate determination of thin-film cell efficiencies in space.

## 2. EXPERIMENT DEFINITION

The experiment would be composed of various combinations of cell assemblies, surface coatings, and shielding in order to investigate

the above listed objectives. Specifically, these cell assemblies would be:

Type A Assembly - This assembly would utilize the Type A CdS cell described previously. The cells would be encapsulated in Dupont H-film and would not have suffered moisture degradation prior to launch. No additional shielding would be used. This assembly would indicate the stability of this cell type and construction in the space environment. It would also measure the space conversion efficiency of this cell type.

Type B Assembly - This assembly would utilize the Type A CdS cell, however, it would not be encapsulated and would have had considerable moisture degradation prior to launch. The assembly would be shielded, however, to prevent low energy particle radiation and micrometeorites from impinging on the film. The shield would be mechanically clamped over the cell assembly. The degree of recovery of this assembly in space would give a measure of the need for ground protection against degradation.

Type C Assembly - This assembly would also utilize Type A CdS cells. The cells would be encapsulated with an evaporative material to prevent moisture degradation prior to launch. The films would also have a surface coating such as  $\text{SiO}_2$  to stabilize the surface against evaporation in space. A mechanical shield similar to that in Type B assembly would also be used. This assembly would test the stability of the films in space.

Type D Assembly - This assembly would also utilize Type A CdS cells. The cells would be encapsulated in an evaporative material to prevent moisture degradation prior to launch. No shield would be used. This assembly would expose the film surface to the space environment of low energy particle radiation and micrometeorites and would give a measure of the effects of this environment on cell output.

Type E Assembly - This assembly would utilize the Type B CdS cells. No shielding or surface coatings would be used. This assembly would

give an indication of the effect of the space environment on this cell type and would also measure its space conversion efficiency. Type F Assembly - This assembly would utilize the Type B CdS cells with a shield similar to that used in the Type B assembly to prevent low energy particle radiation and micrometeorites from impinging on the film surface. This assembly would indicate the degree of evaporation of the film in space.

Type G Assembly - This assembly would be the same as Type F except a surface coating would be used to stabilize the films from evaporation. This assembly would serve as a reference for assemblies Type E and Type F so that the radiation, micrometeorite and evaporation degradation could be related.

Type H Assembly - This assembly would utilize Type C CdS cells. No shielding would be used. This assembly would indicate how well this cell type could withstand the space environment and would also give a measure of its space conversion efficiency.

Type I Assembly - This assembly would utilize the Type C CdS cells, with a shield similar to that used in the Type B assembly. This assembly along with the Type H assembly would give a measure of the effects of the radiation and micrometeorite environment on cell output.

Type J Assembly - This assembly would utilize the CdTe cell. No shielding would be used. This assembly would indicate how well this cell type can withstand the space environment and would also give a measure of its space conversion efficiency.

Type K Assembly - This assembly would utilize the CdTe cell with a shield similar to that used in the Type B assembly. This assembly along with the Type J assembly would give a measure of the effects of the radiation and micrometeorite environment on cell output.

### 3. EXPERIMENT/SPACECRAFT INTERFACE REQUIREMENTS

The interface requirements for the thin-film solar cell experiment (assuming a total of eleven assemblies) are estimated as follows:

Electrical Power Required	0.04 watts (2 thermistors at 20 mw per thermistor)
Weight	Less than 0.5 pounds
Surface Area Required	30 in <sup>2</sup> (10 in. x 3 in.)
Instrumentation	11 voltages (0-50 mv) 2 temperatures (thermistors 0-5 v)
Telemetry Accuracy Required	1 percent of full scale reading

The experiment would have to be solar-oriented and the solar orientation error measured.

## EXPERIMENT I-0

### SOLAR THERMOELECTRICS (G. E. EXPERIMENT)

#### 1. BACKGROUND

One of the potentially attractive means of supplying electrical power in space is by means of solar thermoelectrics. In the flat panel, solar thermoelectric generator design, heat from the sun is used to provide the temperature difference between the hot and cold junctions. A sandwich type construction is used wherein the thermoelectric elements are bonded between two thin aluminum sheets. One sheet, called the collector, is coated to produce a surface having a high solar absorptivity and a low infrared emissivity. This side of the panel is oriented toward the sun, absorbs energy from it, and produces the hot junction temperature. The heat absorbed is partially converted into electrical energy, and the remainder is transferred through the thermoelectric elements to the cold junctions and radiated from the other side of the panel.

The objectives of this experiment are:

1. Demonstrate the feasibility of solar thermoelectrics as a means of supplying space power.
2. Conduct a long term evaluation of a solar thermoelectric power supply in the space environment.

#### 2. EXPERIMENT DEFINITION

A spacecraft designed to conduct a solar thermionic flight experiment offers a very attractive platform for evaluating solar thermoelectrics. Unlike the space experiments conducted to date, the panels would always be oriented to the sun when the spacecraft was not in the earth's shadow. In addition, measurements of the solar intensity, radiation environment, orientation error and micrometeoroid density

would be available from the primary solar thermionic experiment. Therefore, the solar thermoelectric experiment would only require the addition of temperature and voltage instrumentation to provide a more complete evaluation than was possible from previous space experiments.

The experiment would consist of three, solar thermoelectric panels. Each of these samples would be approximately 4 inches by 4 inches by 0.115 inches. In each panel, a row of six n-type elements alternates with a row of six p-type elements. The elements in adjacent pairs of rows are connected in an electrical parallel circuit, and the three pairs of rows are connected in series. A wiring diagram is shown in Fig. 28.

Three panels would be used to allow evaluation of relative performance between samples and also to improve the chances of obtaining performance data over a long period (months) of time.

The power output for each sample is determined by measuring the voltage drop across a precision resistor located in the electrical circuit. In addition to the required voltage measurement, four temperatures would be measured on each panel (two on each surface). The orientation of the panels to the sun would be accomplished by the same orientation system employed by the solar thermionic system. Also, the orientation accuracy would be obtained from measurements made in connection with the primary solar thermionic experiment.

### 3. EXPERIMENT/SPACECRAFT INTERFACE REQUIREMENTS

The interface requirements for the solar thermionic experiment (assuming three test panels mounted together in one magnesium support frame) are summarized in the following:

Electrical Power Required:	0.12 watts for 6 thermistors
Weight:	1 pound
Surface Area Required:	14 in x 5 in
Volume:	8 in <sup>3</sup>
Instrumentation:	3 volts (0-1.2V) 6 temperature (thermistors (0-5V))

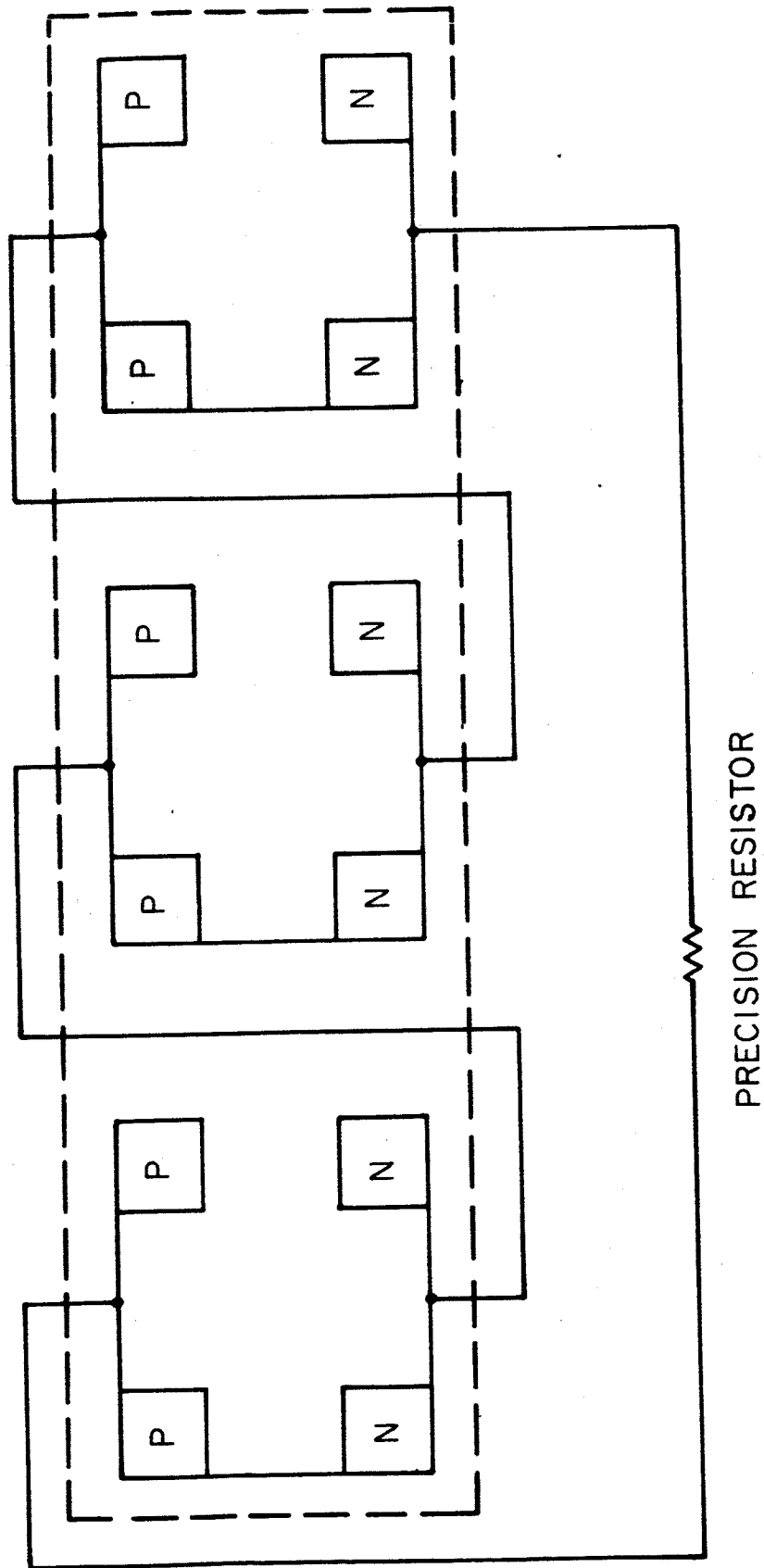


FIG. 28 SCHEMATIC DIAGRAM, 5 LAR THERMEELE TRIC TEST PANEL



This experiment requires sun orientation and, if possible, a measure of the orientation error. This could be obtained for the primary experiment. Although not absolutely necessary, it would be desirable to also have a measure of the radiation environment and micrometeoroid density. These two items would be obtained from the supporting science experiments included on the spacecraft.

EXPERIMENT I-P  
PYROMETER EXPERIMENT

1. BACKGROUND

Since all substances at temperatures above absolute zero radiate electromagnetic energy as a result of the atomic and molecular agitation, we have radiation pyrometry. The power emitted per unit area is  $W = \epsilon \sigma T^4$  watts/cm<sup>2</sup> where  $\sigma$ , the Stefan-Boltzmann constant is in watts/cm<sup>2</sup>/°K<sup>4</sup>, and  $T$  is in degrees K. The dimensionless factor  $\epsilon$ , called the total emissivity or emittance, is defined as the ratio of the radiation of the surface in question to what would be emitted by an otherwise comparable blackbody, i.e., another idealization, one that absorbs all incident radiation.

In this experiment, the pyrometer will view the radiated radiation from the interior of the thermionic cavity and furnish information on the "effective" temperature. The need for a pyrometer to measure temperature of the cavity in parallel with the thermocouples already supplied is threefold

1. The thermocouples degrade approximately 40°C per 100 hours.
2. The original calibration of the couples is off by 30° to 40°C.
3. Diffusion of emitter material into the couple and visa-versa causes contamination problems.

One type of pyrometer is the disappearing filament optical pyrometer, in which the unknown source is imaged onto a reference source and both observed through a microscope. The reference, the filament of a small vacuum lamp, can be made to "disappear" into the unknown source by varying the lamp current. Filters are used to reduce the apparent source if it is higher than the maximum obtainable lamp temperature (about 1500°C). If the instrument has been calibrated, and if the source is a blackbody, matching the brightness by varying the lamp current will give a temperature determination.

A fairly well-defined "effective wavelength" is achieved in the optical pyrometer by a filter, usually red, nominally centered at 6500Å. Red is used because it works at lower temperatures, stable sharp-cutoff filters are available in this range. The brightness sensor sets the fundamental limitation in the precision attainable in this optical pyrometry. Within its range (4000 to 7000Å), the sensor can match brightness well enough to reduce the uncertainty to as little as 0.2°C at 1400°C, 1.6°C at 1800°C, and 1 to 1.5°C at 2900°C.

Another practical method utilizes color, or polychromatic pyrometry. The color temperature of a nonblackbody may be defined as the temperature to which it is necessary to heat a blackbody so that its radiation will match the visual color of the nonblackbody. In particular, if we choose two wavelengths (colors),  $\lambda_2 > \lambda_1$ , in the 4000 to 7000Å range, we can measure a  $T_c$  by taking the ratio of powers radiated from an incandescent body at the wavelengths  $\lambda_1$  and  $\lambda_2$ .

## 2. EXPERIMENT DEFINITION

The pyrometer experiment consists of two types of pyrometer contained in a single instrument (see Fig. 29). The disappearing-filament optical pyrometer is represented in the top path, where the incoming radiation from the cavity is matched by a brightness sensor against the light from the calibrated adjustable lamp filament until the brightness of images match. The two color pyrometer, indicated by the lower light path is separated into two bands, which are alternately admitted by the rotary chopper to the detector. The two levels are telemetered back and compared.

The pyrometer instrument is mounted in the shadow formed by the thermionic generator to prevent direct sun light from entering its optical system.

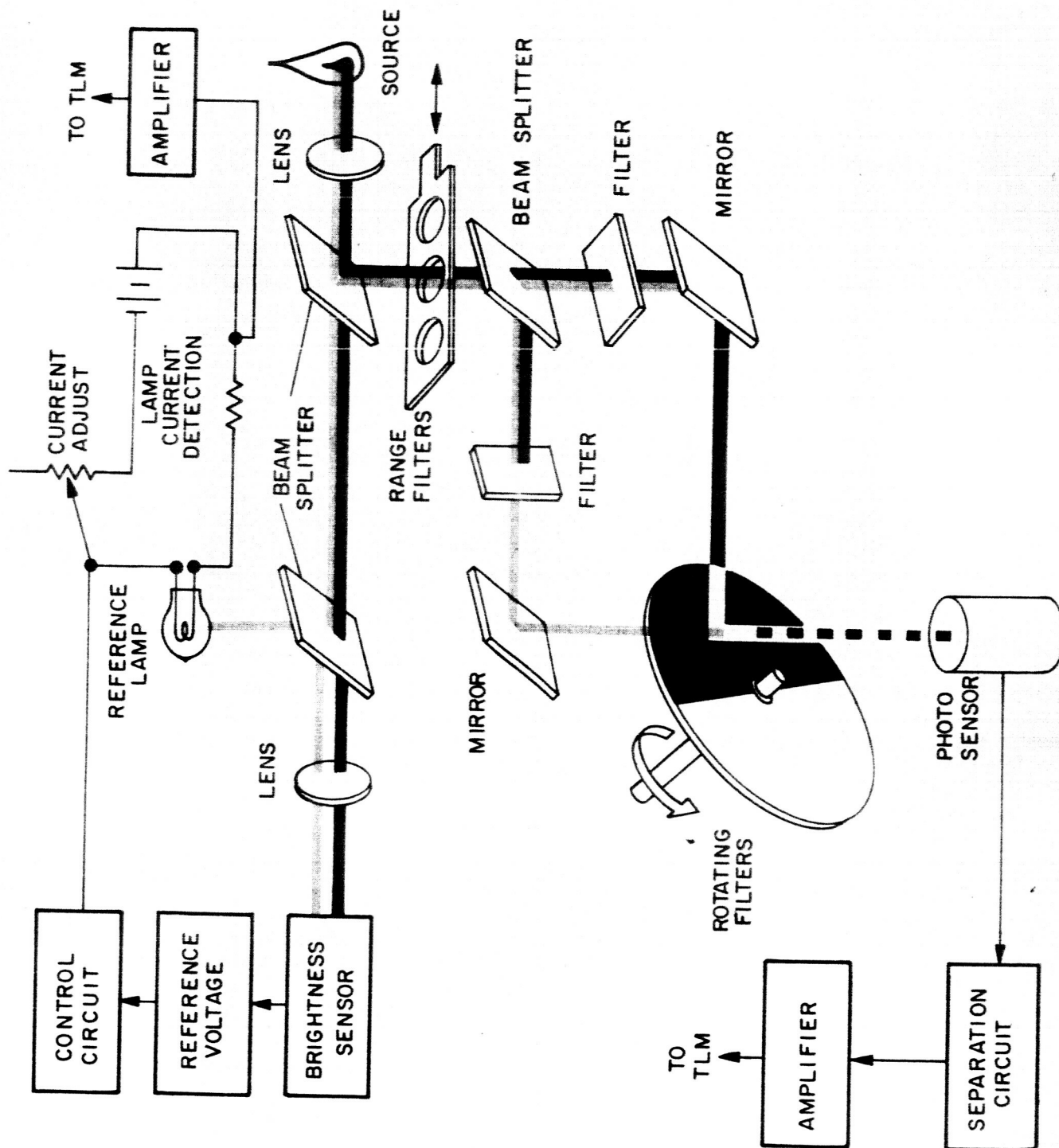


FIG. 29 SCHEMATIC REPRESENTATION OF PYROMETER EXPERIMENT

The effects of stray and/or reflected sunlight will be accounted for by ground calibration tests.

3. INSTRUMENT SPECIFICATIONS

Dimensions:	4" diameter x 7" long
Weight:	5 pounds
Power:	6 watts at 28 volts
Thermal:	-20°C to +80°C
Data:	~ 96 bits/readout
Mounting:	At center of parabolic reflector in shadow of thermionic generator
Preferred Orbit:	any

EXPERIMENT II-A  
FLIGHT QUALIFICATION OF A  
BRUSHLESS DC TORQUER-REACTION WHEEL

1. BACKGROUND

Attitude control is one of the vital functions of almost all spacecraft. A widely accepted method of maintaining attitude control is by reaction wheels. They provide fast continuous control and use only replenishable electrical energy, in contrast to the limited fuel of a gas jet system.

A conventional dc motor reaction wheel is shown in Fig. 30. The use of a dc motor for reaction wheels is attractive because dc motors are about twice as efficient as ac motors of similar size and weight, thus the power demand for a dc motor is less, but the hazards of sliding contact brushes have made dc motor usage undesirable.

This experiment utilizes electronic commutation and other features of the brushless dc torquer which are very significant in simplifying the attitude control system.

Figure 31 illustrates the simplification to the system by utilizing the capabilities of the electronic commutation and the dc torquer. The gear train is eliminated by the use of the torquer which can provide the torque directly; the brushes are not needed, eliminating a source of friction and improving performance and reliability. Reversibility is obtained by logic at a milliwatt power level and without requiring the additional power and voltage drops of a bridge reversing circuit. No power amplifier is necessary since only a signal level input can control the output with good linearity.

The rotating assembly is completely inert. Problems with windings or lamination movements affecting the balance of the rotating assembly do not exist. The thermal situation is improved by reducing the power required and the fact that no power is dissipated on the rotating assembly.

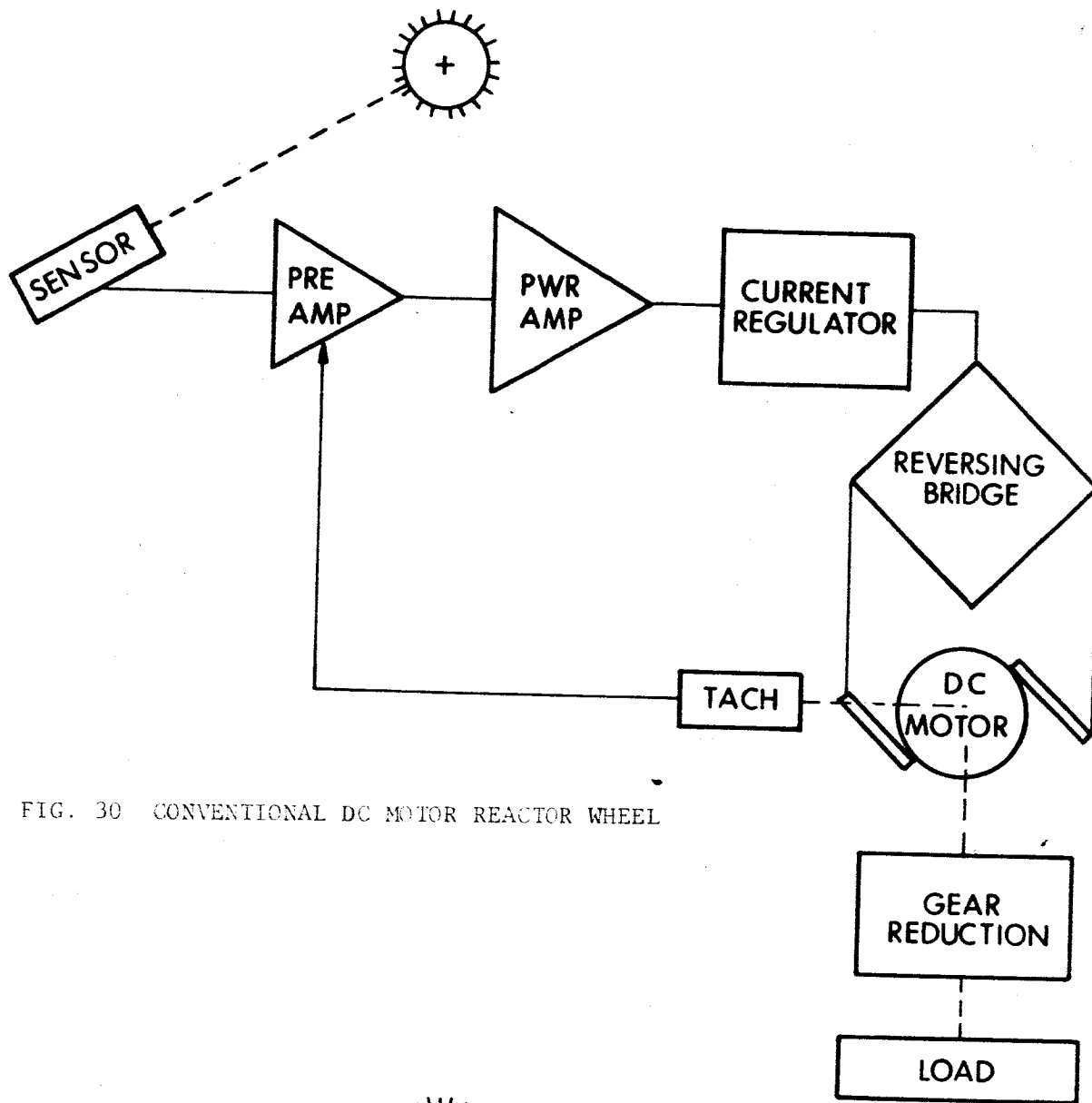


FIG. 30 CONVENTIONAL DC MOTOR REACTOR WHEEL

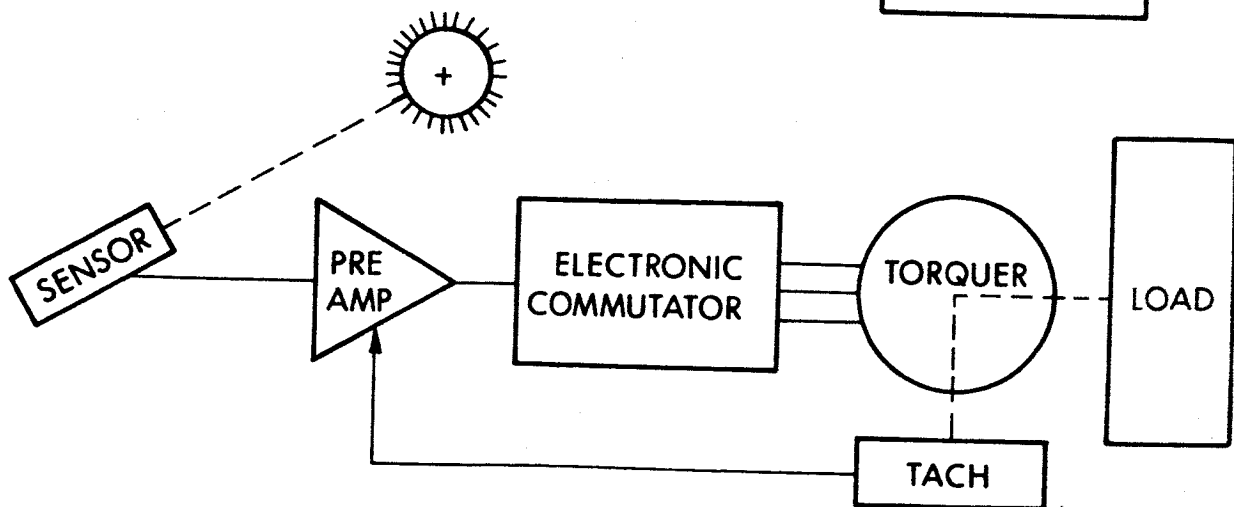


FIG. 31 SYSTEM WITH BRUSHLESS TORQUER

Low-speed operation of the torquer also provides better bearing operation and life.

## 2. EXPERIMENT DEFINITION .

The dc torquer-reaction wheel experiment is based on the work performed by the Sperry Farragut Company (Ref. 1) for NASA Goddard Space Flight Center (Ref. 2).

The experiment will be flown as a "passenger" with the conventional reaction wheels already provided for the attitude control system. The switchover to the brushless dc torquer will be made and its performance monitored. The dc torquer will be left in the system as long as its performance meets the mission requirements. If at any time its operation is questionable, the original reaction wheel will be switched back into the loop (manually or automatically). In this fashion, the brushless dc torquer can be "flight proven" and not be a primary component in the attitude control system.

Design details are available in Refs. 1 and 2.

## 3. EXPERIMENT SPECIFICATION

Size: dc torquer: 12-inch diameter, 3-inch height

Electronics: 6" x 6" x 1"

Weight: dc torquer: 12.5 pounds

Electronics: 1.5 pounds

Power: 25 watts maximum

Thermal: -30°C to +60°C

Data: 50 bits/minute

Mounting: On control axis

Preferred Orbit: Any



#### REFERENCES

1. Control of Brushless dc Torquer-Reaction Wheel, W. M. Casaday, Sperry Farragut
2. NASA Publications TND 2108 and TND 2819

EXPERIMENT II-B  
ATTITUDE CONTROL BY ELECTRIC THRUSTORS

1. BACKGROUND

Of the various types of electric thrusters under development, only the ion engine and resistojet can be considered sufficiently advanced for application on this spacecraft. Arc jets and plasma jets have not been developed with the low thrust levels required, and it is doubtful that sufficient power efficiency can be achieved in the thrust range required (10  $\mu$ lb to 10 mlb). The hydrogen-oxygen electrolysis thruster may eventually offer advantages for satellites with 1- to 2-year lifetimes, but their characteristics are not yet well defined and the hardware is not sufficiently advanced. The experiment considered for this spacecraft uses the ion engine.

Surface Contact Ion Engine. A surface contact ion engine is an electrostatic ion accelerator in which the source of ions is a hot metal surface upon which the propellant is ionized. The exhaust velocity or specific impulse is controlled by the applied voltages. The propellant used is cesium, an alkali metal, carried as liquid in a reservoir where a portion of the volume is heated to create a vapor pressure sufficient for the desired flow rate.

EOS has developed such engines over the past 6 years, ranging from submillipound sizes through 2, 10, 30, and 100 millipounds of thrust. Devices of this type have been operated for a thousand hours and have been tested successfully in suborbital and orbital flights.

A thruster system consists of a power-conditioning and control (PC&C) unit, propellant feed system, ionizer and accelerator assembly, and neutralizer. Table 7 gives a preliminary weight breakdown for three thrust levels.

TABLE 7  
WEIGHT BREAKDOWN FOR TYPICAL CONTACT ION THRUSTORS

(Thrust)	(10 $\mu$ lb)	(300 $\mu$ lb)	(10 mlb)
Engine Weight	0.4 lb	1 lb	2.3 lb
Neutralizer Weight	0.1 lb	0.1 lb	0.2 lb
Feed System Weight (for 1 year total running)	0.2 lb	2.8 lb	75 lb
Power Conditioning and Control System Weight	1.0 lb	2.5 lb	15 lb
Total Weight	1.7 lb	6.4 lb	92.5 lb

Figure 32 shows a 10  $\mu$ lb thruster developed at EOS specifically for satellite attitude control and this engine is the one selected for the experiment. This device has a projected lifetime in excess of 10,000 hours. Figure 33 shows a typical 300- $\mu$ lb thruster.

Two solutions exist for the problem of neutralizing ion propulsion engines. Both provide an electron current equal to the ion beam current as required to maintain the spacecraft potential at or near that of the environment. Any large difference in potential would create decelerating fields outside of the spacecraft, which would result in a loss of thrust.

The conventional approach to neutralization is to place a thermionic emitter close to the ion beam. In the simplest case, this may be accomplished with a resistively heated, refractory-metal wire. The second method utilizes a cesium discharge as the electron source. The discharge forms a highly conducting path to the beam, resulting in high efficiencies. However, this neutralizer requires a cesium reservoir and has generally more power conditioning requirements.

The conventional thermionic neutralizer is, at present, more desirable for engines producing thrust levels up to about 1/2 mlb.

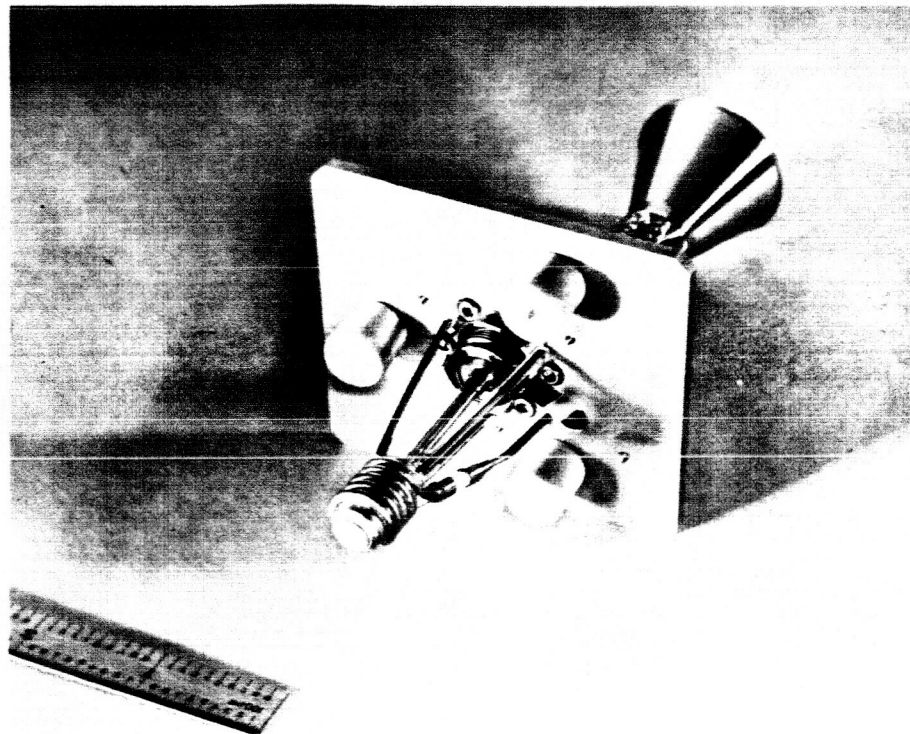


FIG. 32 TEN-MICROPOUND ION THRUSTOR

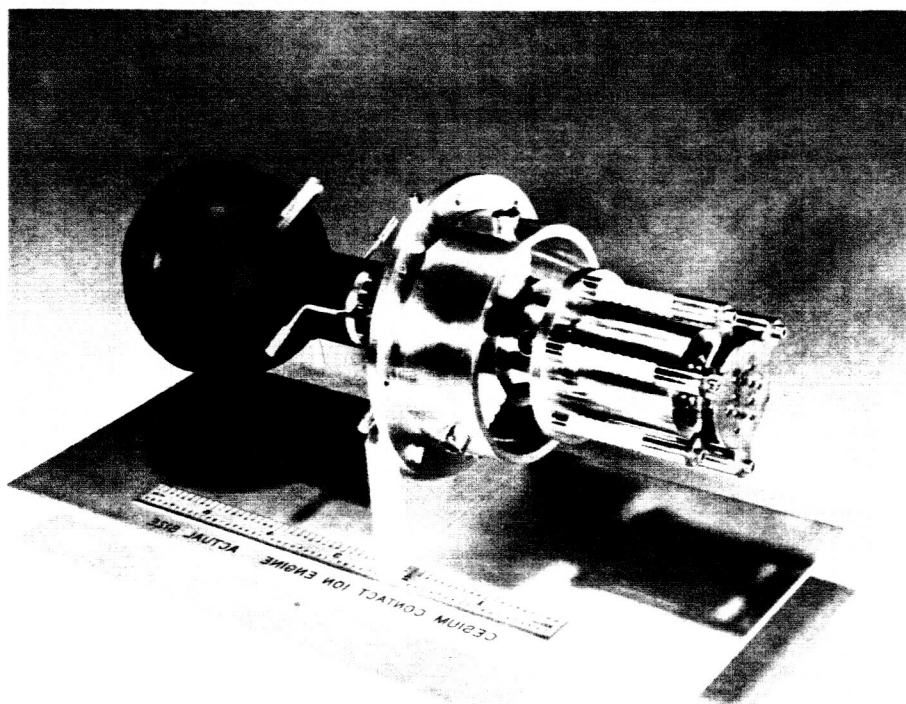


FIG. 33 300-MICROPOUND ION THRUSTOR

Cesium Electron Bombardment Ion Engines. The cesium bombardment engine under development at EOS for the NASA Lewis Research Center has demonstrated a 2600-hour lifetime with negligible loss of performance or structural integrity. Projected lifetimes are in excess of 20,000 hours.

The bombardment engine produces ions by electron bombardment of cesium vapor in a discharge chamber. Ions are extracted through apertures in a screen electrode and accelerated through matching apertures in an accelerating electrode. The feed, neutralizer and power conditioning, and control systems are similar to those of the contact ion engine.

Propellant systems for use with cesium ion engines have been under development for several years at EOS. The type that has evolved through this effort has been found to be simple and reliable. This has been achieved by designing a no-moving-parts system where the surface tension forces the propellant are utilized almost exclusively to pump the propellant and to maintain stable liquid-vapor interfaces within the system during zero-g operation.

Figure 34 shows the components of a typical system. The main cesium reservoir contains a series of fins which converge along the central axis. Because of the surface tension forces, the cesium propellant is directed to the central axis. Here the propellant is picked up by the porous rod and carried by capillary action to the vicinity of the vaporizer where the cesium is vaporized and delivered to the ion engine.

The system shown in Fig. 34 has a capacity of 5 lb of propellant. Smaller systems can utilize the same basic geometry or can use a new geometry which has recently been developed. This configuration is shown in Fig. 35 which shows an exploded view of a system having a capacity of about 30 grams. In place of the fin structure, a series of truncated cones are used as the surface tension elements. The porous rod is retained in this system to carry the propellant to the vaporizer.

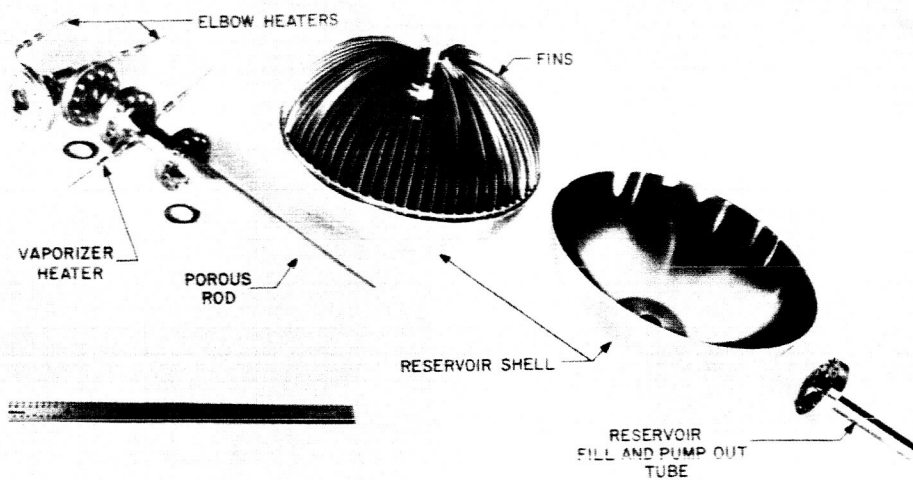


FIG. 34 COMPONENTS OF 5-POUND CAPACITY FEED SYSTEM

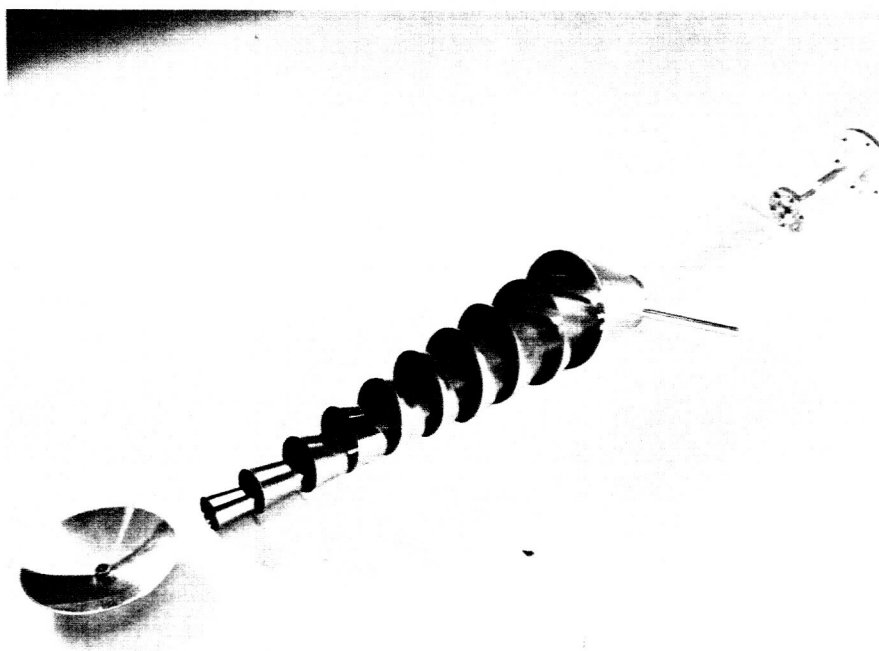


FIG. 35 ZERO-g FEED SYSTEM WITH CONICAL VANES

Thruster Power Conditioning and Control. Power from the primary source must be conditioned to provide the necessary voltages and power levels required by each thruster. Tables 8, 9, and 10 compare the input and output power for power conditioning of the ion engine and the bombardment thruster. The development by EOS of supporting electronics for the suborbital and orbital flights of ion engines led to extensive study and development over the wide range of 10 mlb to 100 mlb and 10 watts to 30 kw.

## 2. EXPERIMENT DEFINITION

The state of development of the low thrust electrical engine has reached the point where a space experiment is in order. The primary reason for such an experiment is to prove this type of propulsion in the space environment. Also, space offers an ideal environment for measuring the electric engines extreme low thrust ( $10^{-6}$  to  $10^{-5}$  pounds), which because of the need for a zero-g environment, isolation from vibration and a deep vacuum is difficult to do on earth.

This experiment proposes to use electric engines for control of the spacecraft roll rate. The experiment would be designed so that upon ground command, control of the spacecraft roll rate would be switched from the cold gas system to the low thrust electric engine experiment. The capability would also be provided to switch back to the primary cold gas system by means of ground command.

Based on the anticipated disturbance torques, a total impulse of approximately  $10^{-3}$  lb-sec per cycle would be required once every 1.2 days. This would be accomplished by two sets of engines firing in the roll plane. Each set of engines would have thrust capability in two opposite directions. Thus, if thrust were desired to counter a clockwise roll of the spacecraft, the counterclockwise engine in each engine set would be fired.

The engines will be mounted on the tips of the solar arrays and the power conditioning will be shared between opposite sets of engines.

TABLE 8  
POWER CONDITIONING INPUT POWER

<u>Contact Ion Thrustor</u> <u>Level</u>	<u>10 Micropound</u>
Assumed Power	16.5 w
Voltage	28 v
Current	0.579 amp
<u>Bombardment Ion Thrustor</u> <u>Level</u>	<u>10 Micropound</u>
Assumed Power	22.9 w
Voltage	28 v
Current	0.818 amp

TABLE 9  
POWER CONDITIONING OUTPUT POWER, CONTRACT ION THRUSTOR

<u>Function</u>	<u>Voltage</u>	<u>Current</u>	<u>Power (w)</u>
<u>10 <math>\mu</math>lb Contact Ion Thrustor</u>			
V+	+3.0 kv	0.5 ma	1.5
V-	-1.0 kv	50 $\mu$ amp	0.05
Ionizer Heater	2.5 v	3.0 amp	7.5
Neutralizer Heater	1.4 v	0.71 amp	1.0
Feed Heater	2.0 v	2.0 amp	<u>4.0</u>
			14.05

TABLE 10  
POWER CONDITIONING OUTPUT POWER, BOMBARDMENT ION THRUSTOR

<u>Function</u>	<u>Voltage</u>	<u>Current</u>	<u>Power (w)</u>
<u>10 <math>\mu</math>lb Bombardment Ion Thrustor</u>			
V+	+1.0 kv	1.0 ma	1.0
V-	-500 v	0.1 ma	0.05
Magnet	1.0 v	0.2 amp	0.2
Arc	9.0 v	0.6 amp	5.4
Cathode	2.0 v	1.0 amp	2.0
Neutralizer	1.3 v	0.6 amp	7.8
Feed Heater	1.5 v	2.0 amp	<u>3.0</u>
			19.45



3. EXPERIMENT SPECIFICATIONS

Dimensions: Electronics: 6" x 6" x 4" total

Engine: 2" diameter x 4" long (each)

Weight: Electronics: 2 pounds (total)

Engines: 3 pounds (4 engines)

Power: 28 watts (total)

Thermal:  $-30^{\circ}\text{C}$  to  $+75^{\circ}\text{C}$

Data: 10 voltages (0 to 5 v)

~ 1000 bits/readout

Mounting: On tips of solar arrays

Preferred Orbit: 325 nautical mile circular

EXPERIMENT III-A  
THERMAL CONTROL WITH PHASE CHANGE MATERIALS (PCM)

1. BACKGROUND

Experience has shown that the reliability of a satellite or spacecraft is greatly enhanced if its dependence upon power and upon moving parts is eliminated or at least reduced to a minimum. The exploration of various possible means of passive thermal control systems is, therefore, attractive for long-life satellites and spacecraft. A passive thermal control system is here defined as one that does not incorporate moving parts or moving fluids, and does not require any power for its operation.

When the incident orbital heat fluxes on a satellite vary over a wide range, or the on-board equipment heat dissipation is widely fluctuating, passive thermal control by the application of phase-change materials (PCM) presents an attractive approach. Basically, the PCM thermal control system consists of a core filled with a substance capable of undergoing a phase change (solid to liquid and vice versa) at a predetermined temperature. The core is sandwiched between the equipment to be controlled and a space radiator. The scheme is shown schematically in Fig. 36.

As the outer satellite surface (space radiator) is exposed to external radiation or to internal equipment heat dissipation, the phase-change material will absorb the excess heat and melt at a constant temperature (the material melting temperature). When the satellite outer surface faces space, away from the sun, and heat is being lost, or if the heat generating equipment is shut off, the PCM will solidify and give off the heat it absorbed during melting. The equipment will thus be in a stabilized temperature environment regardless of the fluctuations in the incident external or internal heat fluxes.

A comparison with other (semiactive) thermal control systems, on an analytical basis, shows that the PCM thermal control scheme has, in addition to being completely passive (absence of moving parts and

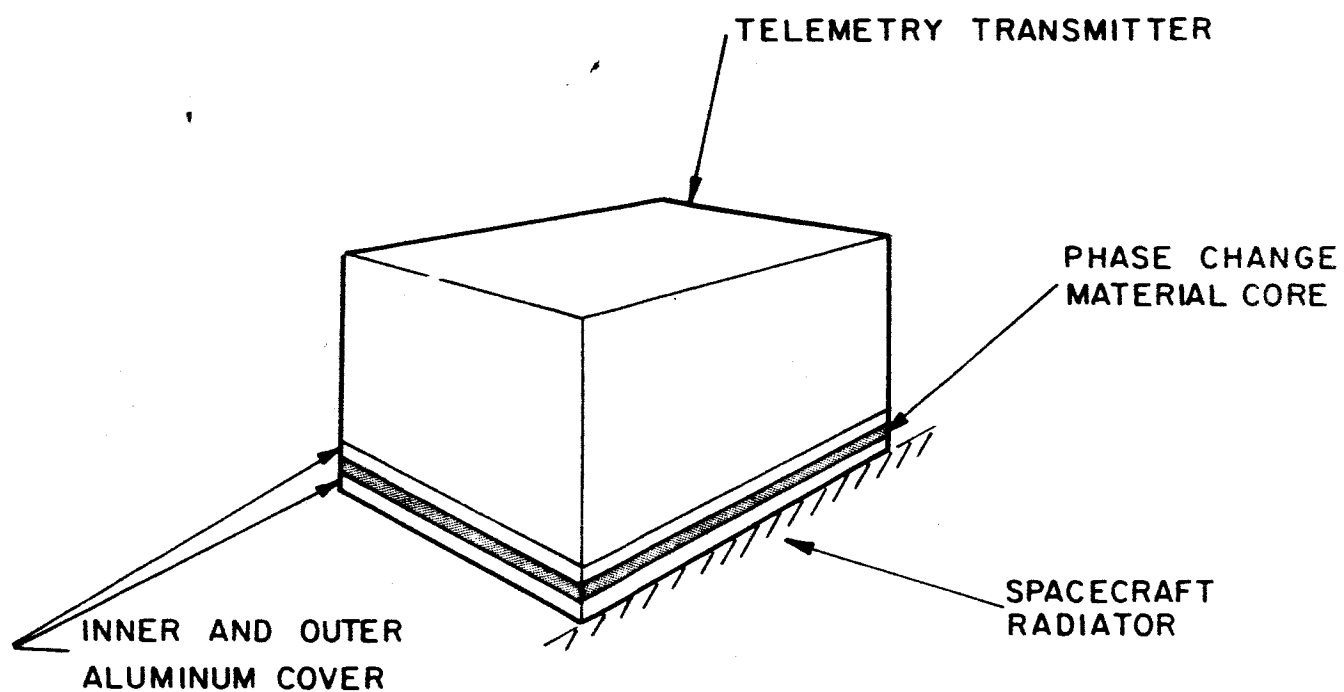


FIG. 36 SCHEMATIC REPRESENTATION OF PCM THERMAL CONTROL EXPERIMENT

nondependence on external power), a definite weight advantage over louvered or forced circulation systems. With presently available phase-change materials (heat of fusion = 130 Btu/lb), it is possible to attain a weight index (weight of phase-change material needed per unit of absorbed heat) of 0.00385 Btu/lb.

Two different phase-change materials, technical eicosane ( $C_{20}H_{42}$ ) and polyethylene glycol (carbowax 600), and two different PCM core designs (finned and finless configurations) were tested in the Republic thermal-vacuum chamber.

Ground test results show that satellite temperature control by phase-change materials is feasible; that it is possible with a PCM thermal control system to maintain satellite equipment and structural components within narrow temperature limits under widely fluctuating satellite external heat loads. Most of the test data indicated that the PCM thermal protection system reduced on-board equipment temperature fluctuations by at least 75 percent (compared to an unprotected satellite). Much better results could be expected with phase-change. The objectives of this experiment are:

1. Design and test a PCM thermal control in space and verify ground tests.
2. Improve the analytical and design techniques with space data.
3. Develop substances especially suitable for PCM thermal control systems.

## 2. EXPERIMENT DEFINITION AND DESIGN

The basic test approach for the PCM thermal experiment is to construct a test panel. The test panel will have a layer of phase-change material interposed between the redundant telemetry transmitter and its radiator or heat sink. The other transmitter will be mounted to the heat sink with conventional techniques. Both transmitters are subjected to nearly identical external and internal heat loads and the resulting temperatures recorded and compared. This approach provides a fairly direct comparison.

The phase-changer materials to be evaluated during the experiment will only be used after extensive ground testing. The materials should have the following properties:

1. High heat of fusion
2. Reversible solid-to-liquid transition
3. Melting temperature in the range of 50°F to 100°F (can be altered to suit specific requirements)
4. Low coefficient of volumetric expansion in both the liquid and solid phases
5. High density
6. Low change in density during change of phase
7. Nontoxic and noncorrosive
8. High thermal conductivity in both phases
9. Low vapor pressure in the vicinity of the melting point
10. High specific heat in both phases

The two transmitters and test panel will be instrumented with thermocouples adequate to define the thermal levels and differentials.

### 3. EXPERIMENT/SPACECRAFT INTERFACE REQUIREMENTS

Dimensions	4 inches x 2 inches x 1/2 inches
Weight	< 0.5 pound
Power	0.6 watt for 10 minutes
Thermal	-10°C to +60°C
Data	36 bits/sample; sample twice/orbit
Preferred orbit	any

EXPERIMENT III-B  
THERMAL COATINGS (G. E. EXPERIMENT)

1. BACKGROUND

The optical characteristics of the surfaces of a spacecraft are fundamental parameters in controlling the spacecraft temperature. Thus, a major effort has been made in recent years to determine the optical properties of various surfaces and even to develop surfaces which have special desired optical characteristics and environmental stability.

The need for adequate temperature control of spacecraft was never more apparent than during the anxious hours in December of 1962 as Mariner II approached the Planet Venus, and the temperature inside the vehicle rose well above that considered safe for the electronic components and batteries. The difficulty apparently stemmed from incomplete knowledge of the required pattern of temperature-control coatings on the spacecraft. In addition, the coatings undoubtedly deteriorated somewhat during the three-month voyage. This event in the Mariner flight points up the importance of the role of thermal control in space vehicle.

The objectives of this experiment are:

1. To measure, in the space environment, the solar absorptance and total hemispherical emittance of selected thermal coatings.
2. To determine the changes with time of the optical and adhesive characteristics of the selected thermal coatings in the space environment.

The Ames Research Center has developed a sensor and mounted six of them on a common structure. In this sensor, each test coating is applied to a metal-disk substrate one-inch in diameter which is placed in a mounting cup. The disks are mounted on three small plastic supports to minimize the conduction path. Radiant heat exchanges with the mounting cup are minimized by the use of four

radiation shields. Surface temperature is measured by means of a thermistor soldered to the underside of the test disk. The radiation sensors are arranged in a circular cluster with a reference surface in the center. The reference surface is composed of razor blades stacked together to form a large number of notches, which cause multiple reflections and eventual absorption of most of the incident radiation. As a result, the reference surface is essentially a black-body. Because of the large number of reflections, any change in the emittance or reflectance of the individual surfaces in the notches would have only a very small effect on the overall emittance or absorptance of the reference surface. To permit correction of heat exchanges between the test surfaces and the sensor mounting cups, the temperature of the base plate is measured with a thermistor. Since the cups are in intimate thermal contact with the base plate, it is assumed the cups are at all times at base-plate temperature.

## 2. EXPERIMENT DEFINITION

The two most important optical properties in thermal design are the absorptance of the surface with respect to solar radiation,  $\alpha_s$ , and the total hemispherical emittance of the surface in the far infrared,  $\epsilon_T$ , ( $T$  denotes surface temperature). Of somewhat lesser importance, generally, are the absorptance of the surface to earth radiation,  $\alpha_E$ , the spectral absorptance and emittance,  $\alpha_\lambda$  and  $\epsilon_\lambda$ , the directional absorptance and emittance,  $\alpha_\theta$  and  $\epsilon_\theta$ , and polarization effects. This experiment will be designed to measure the absorptance and total hemispherical emittance of selected thermal coatings.

## 3. EXPERIMENT SPECIFICATIONS:

Dimensions:	8 inch diameter by 3 inches deep
Weight:	2 pounds
Power:	0.2 watt for 20 minutes

Data: 100 bits/readout  
Thermal: -30°C to +70°C  
Mounting: Sun oriented; unobstructed view  
Perferred Orbit: any



EXPERIMENT IV-A  
COLD WELDING IN INTEGRATED SPACE ENVIRONMENT

1. BACKGROUND

Recent advances in vacuum technology allow for attaining and measuring pressures below  $10^{-10}$  torr. This range increase from  $10^{-6}$  to  $10^{-10}$  torr as limited as it is has opened new areas of scientific investigations. Actual applications in these vacuum facilities are limited by pump capacity vs outgassing, lock problems and associated thermal control problems. At best the results of tests are based upon assumptions of outer space conditions. The real test facility is outer space.

The research experiment being considered here is designed to study the interaction of atomically clean surfaces with each other. Many chamber experiments between two surfaces of the same material have appeared in recent literature. It has been shown that both with metallic and nonmetallic materials the adhesive force in some instances approaches the tensile strength of the material. Consider an ideal curve where two surfaces are produced by breaking a material and then matching the surfaces together again. If one assumes that surface contamination and relaxation of the crystal structure did not take place the original bonds should reform on contact. The real situation, however, is not so restrictive. The strength of materials, even that of whickers, is far less than the theoretically calculated value because of imperfections of the crystalline structure. The measured strength is essentially that of the weakest grain boundaries. These are not hard to reproduce and thus in an ultra high vacuum environment on breaking and making of metal often 90 percent of the original tensile strength is regained. The essential requirement is to preserve the cleanliness of the surface and protect it from contamination from the gas phase. At  $10^{-10}$  torr, for example assuming a striking factor of 1 the surface would be covered with a monomolecular layer in 3 hours.

An experiment is reported by Borden who studied the friction of diamond on diamond at  $10^{-10}$  torr. Evidence is presented to show that "cold welding" took place and small pieces of diamond were torn out of one surface and attached to the other. Thus the frictional forces must have been equal to the shear strength of diamond itself.

## 2. EXPERIMENT OBJECTIVES

1. Study the adhesion between metal versus oxide.
2. Study the adhesion between metal versus silicate surfaces.
3. Study adhesion of metallic films to nonmetallic substrates.

## 3. EXPERIMENT DEFINITION

Several sets or pairs of metals/oxide and metal/silicates will be selected and classified as to thickness, method of plating or rating and types of metal (ferrous and nonferrous).

Each sample pair would consist of one oxide coated tub secured to a strain sensitive rod and a mating tub secured to a slug which when activated would apply one surface to the other for a predetermined length of time and then pull to separate the surface samples. The resultant strain to separation would be read as a detected peak and stored until sampled by telemetry. Knowing the resultant forces necessary to separate oxides from parent metal or metal from silicate surfaces it will be possible to determine whether the samples adhered and tore out the base metal or whether there was slight adherence (superficial).

## 4. EXPERIMENT DESIGN

Attached to a fixed base bar will be one half of each pair of mating surfaces to be tested. A movable bar will curtain the mating halves of each sample pair. At a predetermined time the pairs of samples will be brought into contact and held there under a known

preload. At some later time a linear solenoid will be activated to put a tensile (or shear) load in the movable bar. The stress on each secondary arm (gage length) will be recorded via high-output semiconductor transducers (5 Volt range) and stored for telemetry.

5. EXPERIMENT/SPACECRAFT INTERFACE REQUIREMENTS

Temperature:	50 <sup>0</sup> F to 100 <sup>0</sup> F
Elec. Power Required:	-2.25 watts (-3 minutes)
Size:	4" x 4" x 1.5"
Instrumentation:	5 voltages (0-5V) (2 minutes) 1 temperature (therm. 0-5V)
Weight:	2.0 pounds

EXPERIMENT IV-B  
SUBLIMATION OF MATERIALS IN SPACE

1. BACKGROUND

The purpose of the experiment is to measure the sublimation rate of samples of various materials under actual space vacuum. Literally hundreds of such measurements have been made in the laboratory<sup>1</sup>, but at pressures much higher than those found in space.

Measurements made on a satellite would not only give the sublimation rates under actual vacuum conditions, but could also yield the result of combined effects, such as X rays, charged particles, and UV radiation insofar as they affect the chemical stability and hence the mass loss.

2. DESCRIPTION OF INSTRUMENT

The basic problem is to find a method of weighing the samples at intervals in order to determine their weight, or more accurately the mass losses. Since the entire satellite system is in free fall, no ordinary weighing procedure is possible. The mass determination would be made by using the sample as a load on a vibrating spring and, in effect, measuring the resonant frequency of the system at specified intervals.

The principle is illustrated in Fig. 37. A conventional tuning-fork driving circuit maintains the oscillation of the reed spring and specimen. The reed is made of Elinvar, which has a zero temperature coefficient of elasticity. This will prevent the masking of small mass changes by changes in instrument temperature. A shield protects the reed and drive system from hard EM radiation and, to a large extent, from charged particles.

The resonant frequency of the system will obey a relation to the form

---

<sup>1</sup>L. D. Jaffee and J. B. Rittenhouse, "Behavior of Materials in Space Environments," JPL Tech. Report 32-150

$$\omega^2 = \frac{1}{m} \times \text{const}$$

where

= force constant, and

m = mass which, if the reed is very light, will be essentially the mass of the specimen.

Differentiating the frequency expression, we obtain

$$2 \frac{d\omega}{\omega} = - \frac{dm}{m}$$

As can be seen by studying the tables in Ref. 1, the loss rate, even of plastics, is quite slow at ordinary temperatures; thus there is a problem in measuring the small changes in frequency that would occur in short intervals, such as a week. If  $dm/m$  were, for example,  $10^{-4}$  the frequency change  $d\omega/\omega$  would be only  $1/2 \times 10^{-4}$ , which could be measured directly only by transmitting the frequency to the earth. However, by using the accumulated error over a sufficiently long period, an error even less than the one chosen for the example would become obvious. This would be done by allowing the amplifier to drive a clock for, say, 24 hours and then comparing the indicated time with a standard. Thus, if  $d\omega/\omega$  is  $5 \times 10^{-5}$ , the 24-hour error would be  $8.6 \times 10^4 \times 5 \times 10^{-5} = 4.3$  sec, about four times the daily rate of a good watch. One clock would suffice for a large number of samples since the rate of data accumulation is very slow. The clock would measure the rate of one oscillator for an appropriate interval and then would be switched to the next oscillator, etc. Only the oscillator actually under measurement would be driven, so the power demand could be very small. After the rates of the entire series of oscillators had been determined, the system could shut down for a week or a month, when a new series of determinations would be made.

### 3. INSTRUMENT SPECIFICATIONS

Dimensions: 1 x 1 x 2 inches (each oscillator, including electronics)  
1 x 2 x 6 inches (power, programmer and clock)

Weight: 2 ounces (each oscillator)  
0.5 lb (power, programmer and clock)

Power: 2 watts, except during shut-down periods

Magnetic Interference: Not susceptible. Shielded to protect other circuits.

Readout: Parallel or serial readout from clock once a day during sampling. 200 bits/sample

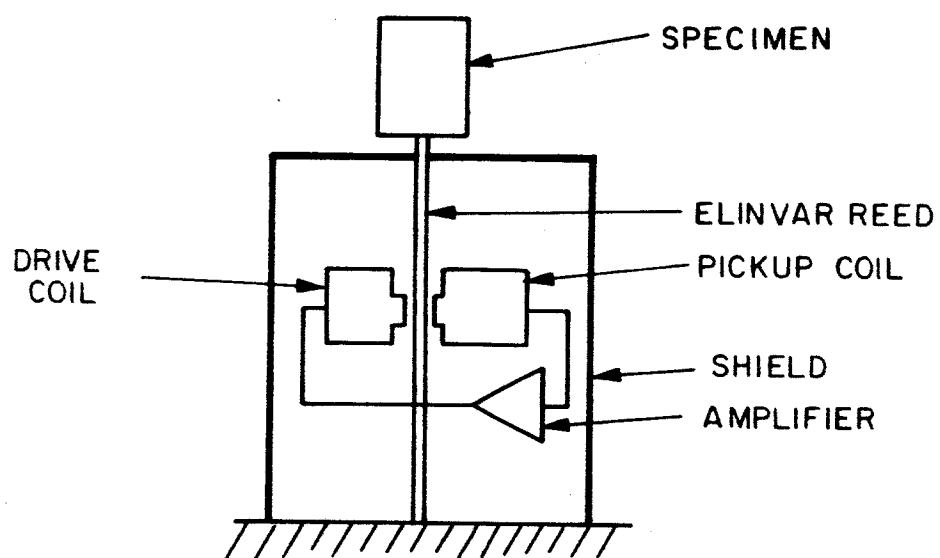


FIG. 37 RESONANT SYSTEM FOR MEASURING MASS LOSS

## EXPERIMENT IV-C

### METEOROID ARMOR TEST

#### 1. BACKGROUND

The future of prolonged manned spaceflight depends on the development of a lightweight meteoroid shield to protect the pressure hull. The pressure hull in which the astronauts live would be extremely heavy if it were called on to resist meteoroid penetration as well as retain the pressurized environmental system. Several designs have been presented that protect the pressure hull against all but the largest meteoroids, but there is no present capability of assessing the relative effectiveness. Much effort has been expended in attempts to simulate meteoroid impacts on earth-bound laboratories.

Most ground base test equipment cannot achieve the required velocities and/or mass of the postulated space meteoroids. The actual composition of the meteoroids is unknown; hence their hardness, cohesion, elasticity, plasticity, etc. so-that their behavior on impact with a shield is unknown. Some data are available on the probability frequency of encounters and on the likely mass of each encounter but this data is sparse.

#### 2. THE OBJECTIVES OF THIS EXPERIMENT

1. To test several meteoroid protection designs in the actual space environment
2. To determine the frequency of impact, size and penetration capability of the larger particles impacting some angle
3. To determine the average abrasion effect of small mass particles and of larger mass particles impacting a greater than their initial angle. Since the abrasion is an average, this part should be confined to the 2 circular orbit, unless a tenuous correlation is sought for the high elliptical orbit.



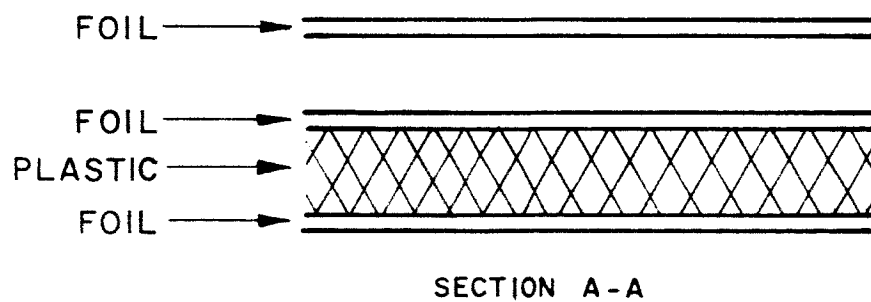
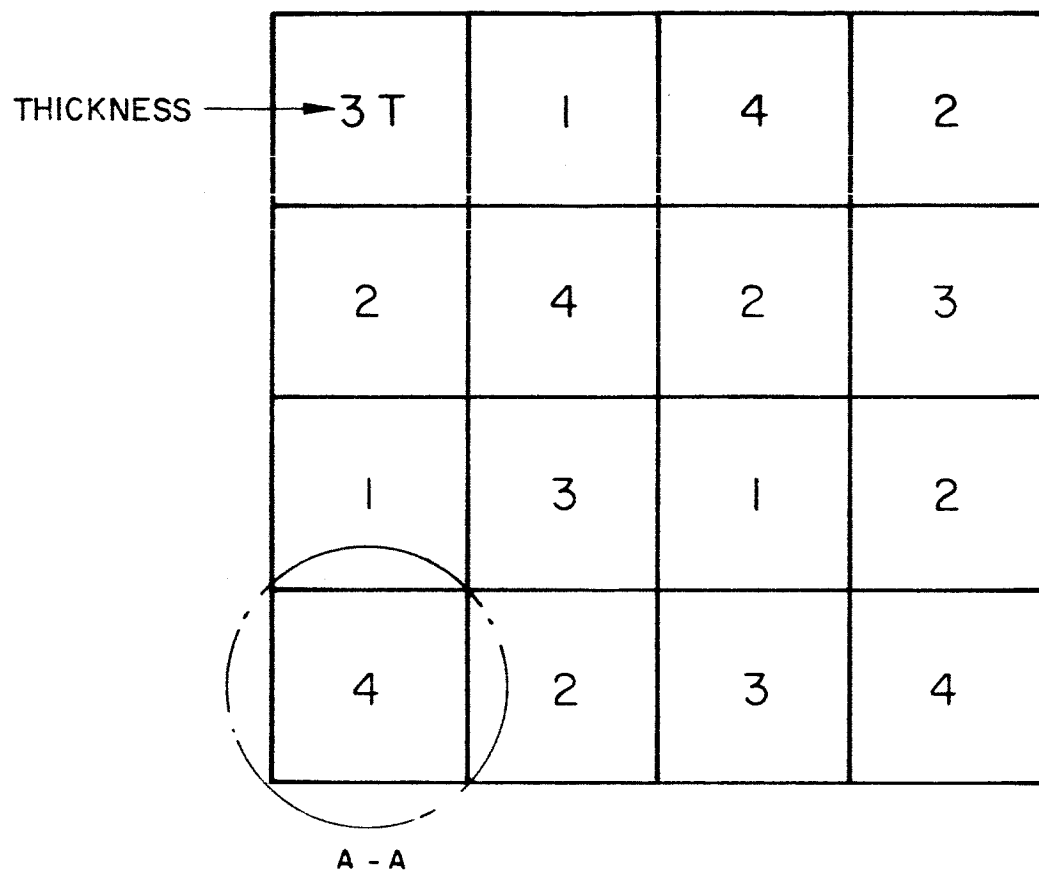


FIG. 38 METEOROID ARMOR TEST

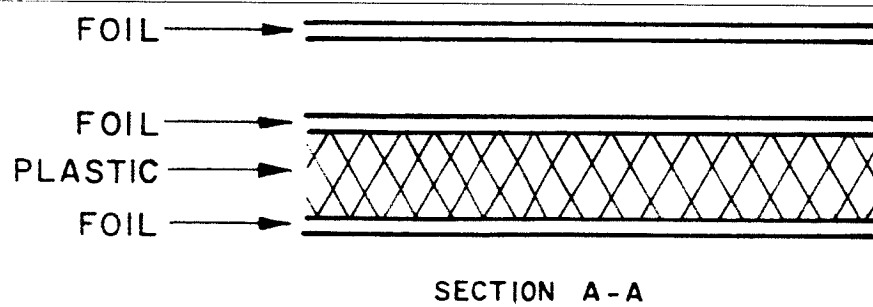
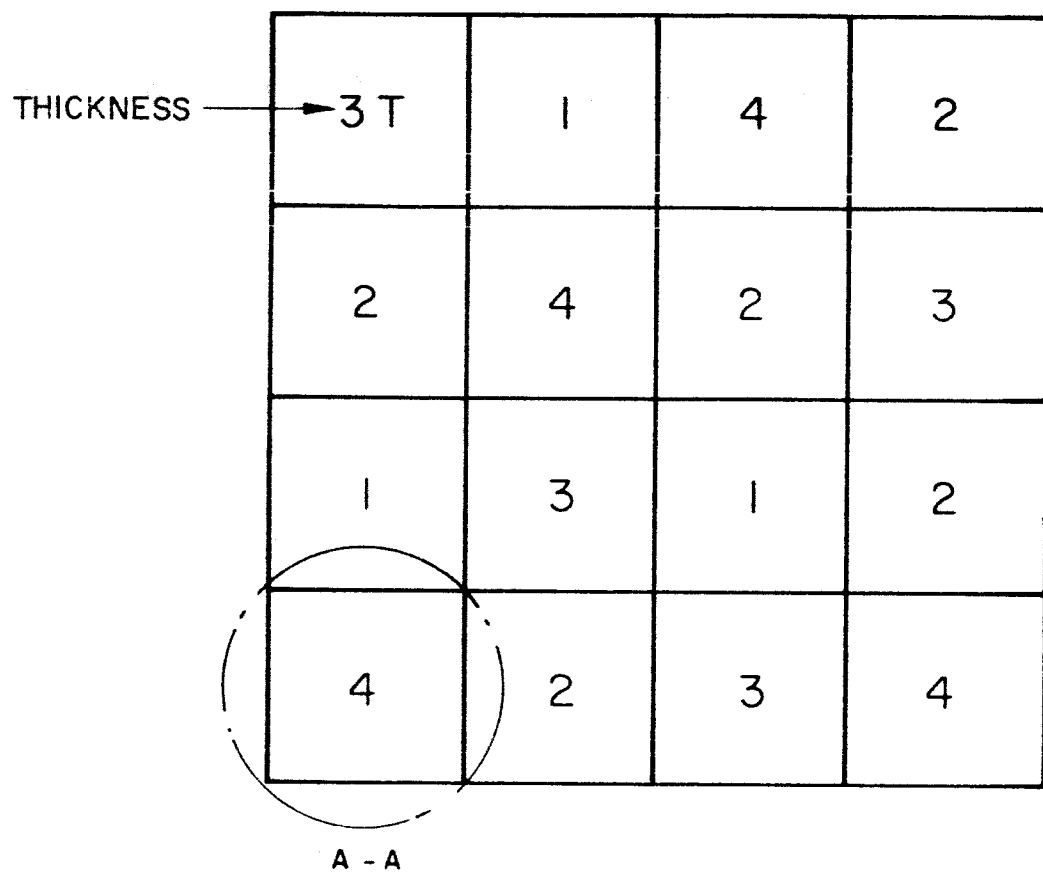


FIG. 38 METEOROID ARMOR TEST

meteoroids, or larger ones impacting at less than their critical angle, the temperature of the inner surface of the panel tends to rise. If there is a bright aluminum foil layer between the test panel and the interior of the satellite, the temperature between the foil and the panel will rise as the thermal coating is eroded away

Instrumentation would consist of thermistors for temperature measurement and pulse counters for registering impact.

#### 4. EXPERIMENT SUMMARY

Weight	6 pound (including electronics)
Size	4 inches x 12 inches x 12 inches panel plus 6 inches x 6 inches x 6 inches electronics
Physical interface	Mounted on side of vehicle
Data	Low bit rate
Power	~ 0.5 watts (average)

## EXPERIMENT V-A

### LASER EXPERIMENT

#### 1. BACKGROUND

The use of lasers for space applications has been under study and development for a number of years. The JPL spacecraft, as specified for this study, does not have the power or appropriate attitude control to carry a laser onboard. However, information necessary to solving many of the operational problems can be evaluated and valuable experiments can be performed by leaving the laser and the receiver on the ground and only providing a corner reflector on the satellite.

The type of information obtainable from an experiment of this type would be:

1. Feasibility of gravitational astronomy by use of ground-based laser tracking
2. Optical properties of atmosphere and space background
3. Feasibility of laser spacecraft communications with ground-based laser system

#### 2. EXPERIMENT DEFINITION

The spacecraft will carry corner reflectors which are illuminated by a ground-based laser. The laser return signal would be detected by a ground-based receiver. The corner reflectors are constructed of three reflecting planes orthogonally located with respect to each other. By moving one of the planes with respect to the other two, the return signal can be amplitude modulated and the amplitude modulation would be detected by the ground receiver.

A typical experiment sequence would be as follows: The gravitational astronomy and optical properties experiments would be performed. The optical properties experiment would provide a base line calibration for the communication experiment which would be performed by modulating one of the planes.

For minimum interference with the sun and maximum probability of performing the experiment, a corner reflector would be mounted on each of the 8 sides of the spacecraft.

The detail design and analysis of this experiment is beyond the scope of this study, but the techniques and hardware are within the present state of the art and the experiment provides valuable engineering and scientific information.

### 3. INSTRUMENT SPECIFICATIONS

Dimensions:	Corner Reflector: 6 in x 6 in x 6 in (each) Electronics: 6 in x 6 in x 1 in (total)
Weight:	Weight: 20 lb (total)
Power:	3 watts at 28 volts
Thermal:	-30°C to +60°C
Data:	~ 300 bits/acquisition
Mounting:	8 sides of spacecraft
Preferred Orbit:	1000 nautical miles; modified sun-synchronous

VI-A  
OPTICAL TRANSMITTANCE TEST

BACKGROUND

(See Experiment I-B Volume III)

EXPERIMENT DEFINITION

(See Experiment I-B Volume III)

A typical set of optical samples would consist of the following:

- Sample 1: typical lens element
- 2: same lens element with a sun shade (to discriminate solar UV effects)
- 3: quartz lens used for ultraviolet measurements
- 4: same lens element with a sun-shade
- 5: }
- 6: } typical optical filters and lens combinations
- 7: }
- 8: }
- 9: }
- 10: } optical filters with sun-shields
- 11: }
- 12: }

EXPERIMENT SPECIFICATION

Dimensions:	12 inches diameter 5 inches high
Weight:	15 pounds
Power:	8 watts during readout
Thermal:	-20°C to +60°C
Data:	900 bits/readout
Mounting:	sun oriented
Preferred Orbit:	any

## SECTION VII

### SUPPORTING SCIENCE

#### INTRODUCTION

The supporting science has been included as a portion of the engineering experiments, since they play an important part in the data analysis, separation of effects and correlation of the engineering experiments. The environment encountered in space has been monitored in some fashion by all U. S. satellites to date, and reasonable data is available, yet the biggest unknown in engineering experiments is the "cause and effect" due to space conditions.

The supporting science experiments included in this section have flown on previous spacecraft or their design is based on proven hardware concepts. The primary intent of these experiments is to furnish data on the environment as seen by the engineering experiments on a "real-time" basis. A secondary benefit will be the additional knowledge of the environment.

#### Supporting Science Classification

The areas covered by the supporting science experiments have been divided into the following classifications:

1. Solar Ultraviolet
2. Solar Lyman Alpha
3. Proton-Electron Particles
4. Solar Gamma Ray
5. Solar X-Ray
6. Micrometeoroids
7. Magnetic Field
8. Pressure

Since there is a variety of missions and experimental payloads possible the science experiments will vary accordingly. In each class a typical science experiment has been cataloged to give the experimenter some basic information in providing the supporting science payload. It should be noted these are representative supporting science experiments and not the only choices available, but are typical of the type already developed and flown.

EXPERIMENT VII-A  
SOLAR ULTRAVIOLET

1. BACKGROUND

The major portion of the ultraviolet radiation exposure to the spacecraft will be directly from the sun. This direct radiation will be the primary cause of any ultraviolet damage to the engineering experiments. The measurement of this direct radiation will concentrate in the 2000 to 3000<sup>o</sup>A region. The regions below 2000<sup>o</sup>A are monitored by the solar Lyman-Alpha and solar X-ray supporting science experiments. This division of regions will aid in separating the "cause and effects" on the engineering experiments.

2. EXPERIMENT DEFINITION

The solar ultraviolet will be monitored by a broadband instrument (2000<sup>o</sup>A to 3000<sup>o</sup>A). The instrument consists of an objective lens made of quartz, a filter, a Fabre lens, a photomultiplier detector and associated electronics.

On-board calibration of the instrument is provided by a mercury source which emits at 2537<sup>o</sup>A.

3. INSTRUMENT SPECIFICATION

Dimensions: 4 inches x 4 inches x 3 inches  
Weight: 1.0 pound  
Power: 1 watt  
Thermal: -20<sup>o</sup>C to +60<sup>o</sup>C  
Data: ~6 bits/min, continuously  
Mounting: Directly at the sun  
Preferred Orbit: Any



EXPERIMENT VII-B  
SOLAR LYMAN-ALPHA EXPERIMENT

1. BACKGROUND

The solar Lyman-Alpha ( $\lambda \approx 1216\text{\AA}$ ) line has been shown to exhibit an absorption feature when viewed with a high dispersion spectrograph flown above the Earth's atmosphere. This feature is composed of two components; a broad weak reversal, and a deep narrow central absorption core at  $1215.67\text{\AA}$ . The broad reversal is believed to originate in the solar atmosphere whereas the absorption core is attributed to neutral hydrogen lying between the ionized E-layer of the Earth's atmosphere and the sun, but outside the sun's atmosphere. The emission line itself arises in the chromosphere of the sun. The kinetic temperature required to form the line is of the order of  $T_e \approx 60,000$  to  $100,000^\circ\text{K}$ . However, the temperature characterizing the emergent radiation, averaged over the disk of the sun, is about  $7200^\circ\text{K}$ .

Measurements made to determine how much the net solar Lyman-Alpha flux increases during flares indicate that the Lyman-Alpha flux remains essentially unchanged during the occurrence of a flare. This does not imply that the intensity of the Lyman-Alpha may not increase greatly from a flare at the time of a flare, but only that this enhancement does not appreciably alter the total amount of Lyman-Alpha radiation emanating from the solar disk.

Although no spectra of Lyman-Alpha have been obtained for flares, it is probably that the central reversal will be absent, as it so often is in the Ca II lines. The weak reversal is caused by the partial absorption of the line by hydrogen in the chromosphere at lower temperature than the source of the line. During a flare, it is possible that the upward and outward surge of hot gases would blow the cooler gas away, thus tending to preserve the original line shape. It may be that a flare or a series of flares, whether detected optically or not, will distribute sufficient hydrogen into the region between the sun and earth

to measurably affect the depth of the absorption core. While it is known that the rise time of flares is most generally less than 10 minutes, it is not known how long flares may take to cause a change in the absorption core; if they do so at all.

## 2. EXPERIMENT DEFINITION

The objective of the experiment is to obtain a knowledge of how the density of neutral hydrogen clouds, between the earth and the sun, changes with time, to determine any correlation with solar activity and any effects on engineering experiments.

An ionization chamber is used for measuring the intensity of the hydrogen Lyman-Alpha radiation and comprises a nitric-oxide gas-filled tube, or cylinder, 1 inch long by 0.8 inch diameter, made of oxygen-free copper and fitted with a lithium fluoride window at one end (see Fig. 39). The lithium fluoride is opaque to radiation below about  $1100\text{\AA}$  and the photoionization threshold of nitric-oxide is  $1340\text{\AA}$ , thus the spectral response of the ion chamber is limited to radiation in this  $240\text{\AA}$ -wide wavelength region. Since more than 95 percent of solar radiation between  $1100\text{\AA}$  and  $1340\text{\AA}$  is concentrated in the Lyman-Alpha line near  $1215\text{\AA}$  the output signal from this ion-chamber detector is a good measure of the Lyman-Alpha radiation.

## 3. INSTRUMENT SPECIFICATIONS

Dimensions:	Sensor: 1-1/2 inch x 1 inch diameter
	Electronics: 7 inches x 2 inches x 6 inches
Weight:	Sensor: 1 pound
	Electronics: 3 pounds
Power:	2 watts at 28 volts
Thermal:	$-20^{\circ}\text{C}$ to $+60^{\circ}\text{C}$
Data:	1 voltage (0-5 v) 6 bits/sample
Mounting:	Sensor directly toward sun continuously
Orbit:	Any

# Instrument Specification Sheet

LYMAN-ALPHA ION CHAMBER

Inst. 1  
Vanguard SLV-1  
27 May 1958

Page 2 of 2

DEPOSITORY FOR DATA  
NRL

## REFERENCES

Annals of the International Geophysical Year, VI, Parts I-V, "Rockets and Satellites," pp. 318 ff, ed. by L.V. Berkner, Pergamon Press, New York, 1958.

## PHOTOGRAPHS AND DRAWINGS

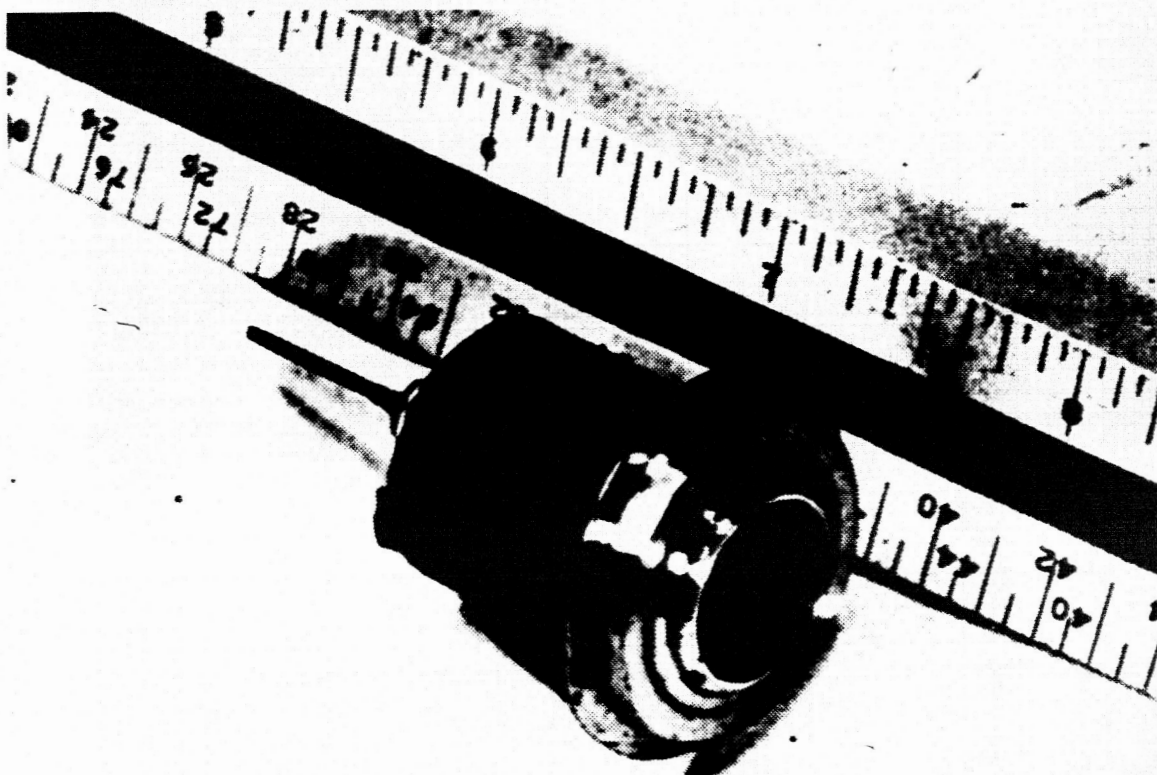


FIG. 39 LYMAN-ALPHA DETECTOR (Annals of the International Geophysical Year, VI, Parts I-V, "Rockets and Satellites," ed. by L.V. Berkner, Pergamon Press, New York, 1958, facing page 320.)

**ELECTRO-OPTICAL SYSTEMS, INC.** Pasadena, California

EXPERIMENT VII-C  
PROTON AND ELECTRON SPECTRA AND DIRECTION

1. BACKGROUND

Despite the large number of experiments which have been carried out to determine the space radiation environment, there still exists a need for additional information in order to assess the effects of this environment for specific satellite missions. There are several reasons for the uncertainties which remain despite the measurements carried out to date, one being the lack of adequate particle discrimination in the early experiments which were performed.

Another is the large perturbation in the environment which was introduced into the natural radiation environment by the detonation of high altitude nuclear devices during the latter half of 1962. Besides the complex time decay pattern followed by the artificially injected electrons, recent experiments indicate that the intensity of the proton belt at the low altitudes is increasing with time, but data is sparse.

The objectives are to obtain measurements of proton and electron spectra in well-defined energy intervals as a function of direction. The energy intervals chosen will depend upon the particular orbit of the satellite upon which the experiment is conducted.

2. EXPERIMENT DEFINITION

The proposed experiment is designed to measure proton and electron spectra in the following ranges:

<u>Protons</u>	<u>Electrons</u>
30 - 50 Mev	0.5 - 1.5 Mev
50 - 100 Mev	1.5 - 2.8 Mev
100 - 200 Mev	> 2.8 Mev

Three directions would be measured. These ranges are most suitable for a circular orbit at approximately 325 nautical miles. The ranges may be tailored to fit other orbits as required.

Solid state detectors are used in a telescope configuration backed by electronic amplifiers, coincidence circuits, discriminator gates, and a data conditioning section. The data conditioning section converts raw pulses from the coincidence circuits to a form ready for telemetering. At present, the conditioning circuit accepts pulses from five pulses  $\text{sec}^{-1}$  to  $1.5 \times 10^5$  pulses  $\text{sec}^{-1}$  and produce logarithmically a d-c voltage varying from 0 to 5 volts, where each volt corresponds approximately to a decade.

### 3. EXPERIMENT/SPACECRAFT INTERFACE REQUIREMENTS

The interface requirements for the proton and electron spectra and direction experiment are:

Special Instrument	3 Charged Particle Telescopes
Volume	300 in <sup>3</sup> (total package including electronics)
Weight	24 pounds (total package including electronics)
Power	9 watts
Output signal	20 voltages (0-5v)
Telemetry Accuracy Required	1 percent of full scale reading

Three telescopes are to be mounted on mutually perpendicular axes with one of the axis pointed to the sun. The telescopes are to be mounted so that they have an unobstructed view of space. In order to evaluate the measured data, it is also necessary to know the spacecraft's position and orientation in space.

The primary experiment does not require that the spacecraft be oriented about the roll axis. If this is the case, only one telescope (instead of three) pointing to the sun would be used. This would alter the interface requirements summarized above to the following:

Special Instrument	1 Charged Particle Telescope
Volume	100 in <sup>3</sup> (total package including electronics)
Weight	8 pounds (total package including electronics)

Power

3 watts

Output Signal

6 voltages (0-5v)

As before the telescope requires an unobstructed view.

## EXPERIMENT VII-D

### SOLAR GAMMA RAYS

#### 1. BACKGROUND

Low energy gamma-rays, from 0.1 to 5 Mev, result from radioactive decay of excited nuclei, fusion of light elements, and perhaps electron-positron annihilations. High energy gamma-rays, from 50 to 200 Mev, should result from the decay of neutral  $\pi$ -mesons produced in nuclear interactions with high-energy particles and from the annihilation of matter and antimatter. The high energy range is of greater interest because the expectation of finding something is more definite.

As far as the low end of the energy spectrum of gamma radiation is concerned, there has been an observation of a flash of 0.5 Mev gamma-rays 0.5 minutes before a solar flare. Thus continuous monitoring of solar gamma rays is important.

In order to provide answers to some of the solar problems, e.g., flare mechanisms and particle acceleration, and possible effects on the engineering experiments, continuous monitoring of the solar gamma radiation would be helpful.

#### 2. EXPERIMENT DEFINITION

The proposed experiment is designed to measure the solar gamma-ray flux in the energy range of 0.1 to 200 Mev and correlate with any effects on the engineering experiments.

The solar gamma-rays will be measured with scintillation detectors. The signal pulses will go into a pulse height analyzer and will be sorted into six energy ranges. The pulses from each channel will be fed into a counting rate circuit whose output will be a d-c voltage in the range of 0 to 5 volts suitable for the telemetry system.

#### 3. EXPERIMENT/SPACECRAFT INTERFACE REQUIREMENTS

The interface requirements for the solar gamma-ray experiment are:

Special Instruments	Scintillation Detectors
Size	150 in <sup>3</sup>
Weight	8 pounds
Power	4 watts
Output Signal	6 voltages (0-5v)
Telemetry Accuracy Required	1 percent of full scale reading

Each of the six channels would be sampled approximately once per minute in order to detect any correlation between increased gamma-ray activity and solar flares. The scintillation detectors must be oriented to the sun and be mounted on the spacecraft so that they have an unobstructed view of space.



## EXPERIMENT VII-E

### SOLAR X-RAY

#### 1. BACKGROUND

The X-ray intensity varies with time and has a large variation from sunspot minimum to sunspot maximum. The solar cycle increase is about a factor of 200 in the 2 to  $8\text{\AA}$  band and about a factor of 50 in the 8 to  $20\text{\AA}$  band. The increases in the intensities in the 2 to  $8\text{\AA}$  and 8 to  $20\text{\AA}$  bands are even greater at times of solar flares and the characteristic flare-produced X-ray spectrum is considerably harder than that from the quiet sun. The radiation of the sun in the wavelength range of X-rays is a consequence of the high temperature of the emitting layers, namely the corona and the region of transition to the chromosphere.

#### 2. EXPERIMENT OBJECTIVE

In order to provide answers to some of the solar problems; e.g., flare mechanisms, temperature gradient in corona, coronal structure, and effects on engineering experiments, continuous monitoring of solar X-rays is necessary. The solar X-ray flux should be monitored continuously or at least sampled as often as is practical.

#### 3. EXPERIMENT DEFINITION

The proposed experiment is designed to measure the solar X-ray flux in the 2 to  $8\text{\AA}$  and 8 to  $20\text{\AA}$  bands. Measurements are to be made once a minute in order to detect any correlation between increased X-ray activity and solar flares.

The solar X-ray fluxes would be measured with Geiger counters. The spectral sensitivity of the counters would be defined by the transmission of the window and by the absorption and photoionization properties of the filling gas (Ref. 1). The Geiger counter covering the 2 to  $5\text{\AA}$  band would have an aluminum window having a thickness of  $1.534 \text{ mg cm}^{-2}$ , and the counter covering the 8 to  $20\text{\AA}$  would have a beryllium window having a thickness

---

<sup>1</sup>R. W. Kreplin, "Solar X-Rays," Annales de Geophysique, Vol. 67, 1962

of  $24.4 \text{ mg cm}^{-2}$ . Both counters would be filled with 8.6 millimeters of ethyl formate and 702.6 millimeters of neon. The signal pulses would be amplified, conditioned, and fed into a counting rate circuit. The output would then be a d-c voltage in the range 0 to 5 volts suitable for the telemetry system. The size of each counter would be determined by the expected counting rate range and would be adjusted for the specific orbit finally chosen.

#### 4. EXPERIMENT/SPACECRAFT INTERFACE REQUIREMENTS

The interface requirements for the solar X-ray experiment are summarized below:

Special Instruments	Geiger Counters
Size	100 in <sup>3</sup>
Weight	3 pounds
Power	1 watt
Output Signal	2 voltages (0-5v)
Telemetry Accuracy Required	1 percent of full scale reading

The Geiger counters must be oriented to the sun and be mounted on the spacecraft so that they have an unobstructed view of space.

## EXPERIMENT VII-F

### MICROMETEORIDS

#### 1. BACKGROUND

The micrometeoroid supporting science experiment is designed to monitor the micrometeoroid population around the earth and the relative number of hits an engineering experiment may have encountered.

#### 2. EXPERIMENT DEFINITION

A crystal microphone detector is used for its simplicity and its reliability. A crystal microphone is mounted against a sounding plate which is acoustically isolated from the remainder of the vehicle by isolating mounts. Additional isolation can be achieved by tuning the microphones to frequencies above any spacecraft vibrational frequencies. (Valuable information could be obtained if instrumentation of the secondary panels directly was provided).

#### 3. INSTRUMENT SPECIFICATIONS

##### Dimensions:

Detector Plate	5 inches x 10 inches x 1/4 inch (each)
Electronics	6 inches x 6 inches x 1 inch (total)

##### Weight:

Detector Plate	6 pounds (total)
Electronics	2 pounds (total)

Power: 1 watt

Thermal: - 20°C to +60°C

Data: ~ 100 bits/orbit

Mounting: Perpendicular to vehicle motion and directly on secondary panels

Preferred Orbit: Any

## EXPERIMENT VII-G

### MAGNETIC FIELD

#### 1. BACKGROUND

The magnetic field experiment is designed to measure the local magnetic field of the spacecraft and record any variations with time or events. The local magnetic field of the spacecraft is important in correlating several of the supporting science instruments readings and explaining any large deviations.

#### 2. EXPERIMENT DEFINITION

The magnetometer is a three-core device. Each of the three orthogonal sensors will produce an output voltage proportional to the magnitude of the component of the combined magnetic field along the axis of that sensor. The output voltages of the three sensors will each occupy a separate channel and will be combined after reception to form the total magnetic field vector. The field strength range of this instrument is from 100 to 50,000 gammas.

#### 3. INSTRUMENT SPECIFICATION

Dimensions:	5 inches x 4 inches x 4 inches
Weight:	4 pounds
Power:	0.5 watt
Thermal:	-30°C to +60°C
Data:	~ 50 bits/minute
Mounting:	Directly on a secondary panel near supporting science measurements
Preferred Orbit:	Any

## EXPERIMENT VII-H

### LOCAL PRESSURE

#### 1. BACKGROUND

The local pressure supporting science experiment is designed to monitor the pressure in the spacecraft. Information on outgassing rates and its variation with time and events will supply valuable information on the amount and types of material being given off by the spacecraft. Experiments such as the Sublimation of Materials require some knowledge of the hardness of the vacuum to make meaningful calculations.

#### 2. EXPERIMENT DEFINITION

Pressure in a chamber exposed to the atmosphere through a knife-edged orifice is measured as a function of orifice orientation (with respect to direction of motion) and payload velocity. If the gas composition is known, or can be assumed with fair accuracy, the pressure in the chamber can be used to determine the total gas density. The gauge is sealed before flight and is opened automatically at desired altitude.

Two modified magnetron-type "Redhead" pressure gauges for measurement of pressure over the range of  $10^{-11}$  to  $10^{-5}$  mm Hg. The ion traps are cylindrical electrodes painted on the gauge walls between the ionization region and the orifice. In operation, 4800 volts are applied between the anode and the cathode which was grounded through the electrometer. Magnetic field strength is 1000 Gauss. During each 4 minute operating cycle, 30 volts is applied between the ion traps for  $\sim 90$  seconds to determine the effect of charged ambient particles.

In the pressure range,  $10^{-9}$  to  $10^{-6}$  torr, the gauges usually strike a discharge in less than 30 seconds. The electrons are trapped axially by the potential of the cathode end-plates, and radially by the magnetic field. Ions are formed from collisions between electrons and incoming neutral particles and are collected at the cathode to create the cathode current which is fed into a logarithmic electrometer. Gauge sensitivity in amps/torr varies with pressure and particle species.

### 3. INSTRUMENT INTERFACE

#### Dimensions:

Sensor 4 inches x 5 inches x 5 inches

Electronics 6 inches x 6 inches x 1 inch

Weight: 5 lbs (total)

Power: 3 watts

Thermal: -20°C to +50°C

Data: ~ 100 bits/minute

Mounting: Inside spacecraft in area of interest

Preferred Orbit: Any